ADAPTABLE SLOPE ESTIMATION MODULE AND ITS APPLICATION IN A COOLANT MONITORING SYSTEM FOR PREDICTIVE OBSERVATION

A Thesis
Presented to
The Academic Faculty

By

Roman A. Burkart

In Partial Fulfillment
of the Requirements for the Degree
Master of Science in the
George W. Woodruff School of Mechanical Engineering and the University of Stuttgart

Georgia Institute of Technology

August 2018

ADAPTABLE SLOPE ESTIMATION MODULE AND ITS APPLICATION IN A COOLANT MONITORING SYSTEM FOR PREDICTIVE OBSERVATION

Approved by:

Dr. Kurfess, Advisor
School of Mechniacal Engineering
Georgia Institute of Technology

Dr. Saldana
School of Mechanical Engineering
Georgia Institute of Technology

Dr. Sawodny
Institute of System Dynamics
University of Stuttgart

Dr. Tarin
Institute of System Dynamics
University of Stuttgart

Date Approved: July 20, 2018

ACKNOWLEDGEMENTS

First of all, I would like to thank my advisor Dr. Thomas Kurfess. He helped me in various discussions developing ideas and understanding correlations of different circumstances. He also provided me with input on different topics which are discussed in this thesis.

I would also like to thank Andrew Dugenske. He supported me on several questions on the digital architecture used in this thesis.

A great thanks is also dedicated to a various number of my colleagues. Without their help and support on different topics my research would have been less successful.

Finally, I would like to thank my parents for providing me with support and encouragement through my years of study which led to this point. Without their help and support I would not have been able to accomplish this piece of work.

Roman A. Burkart

TABLE OF CONTENTS

LIST OF TABLES

LIST OF FIGURES

SUMMARY

In the following thesis, a slope estimation module for predictive maintenance of manufacturing based variables is developed. Based on the output of a state estimation filter (also referred as filter), the slope of the data is calculated and used for predictive maintenance of a system. This helps to indicate possible failure of a system or a component of a system ahead of time. For achieving this goal, two common sensors are examined in particular: an ultrasonic distance sensor and a pH meter. The output of these two sensors is used to determine the requirements for such a slope estimation module.

The thesis puts its emphasis on 4 different main points. In the first one (3.1), the applied sensors are investigated on their output behavior regarding noise, resolution, hysteresis and so forth. This step is done to define the requirements for the slope estimation module. In the second step (3.2), a set of example signals is designed based on the output of the sensor testing. These example signals contain all the characteristics which are required to be detected by the slope estimation module. Afterwards, four different state estimation filter algorithms are developed, tuned and tested on the example signals (3.3). Based on the output of the final state estimation filter, the slope is computed and a warning is shown if the variable is approaching a minimum or maximum value (3.5). At the end, the developed algorithm is validated with the help of an original signal from both sensors (3.6).

Based on the developed slope estimation algorithm, a warning can be given to the operator if a system variable is approaching a critical range close to its maximum or minimum. Furthermore, a prediction about the failure can be made. This prediction is only accurate if the conditions do not change. The algorithm is very robust against high frequency noise, interruptions in sampling data as well as wrong measurements. However, low frequency noise with a high amplitude can lead to false predictions.

CHAPTER 1

INTRODUCTION AND BACKGROUND

The Fourth Industrial Revolution is seen to a have a major impact on the globalization of manufacturing [1]. The digitalization of production processes is one main part of this revolution. By digitalizing the production, new ways of collaborations between internationally located factories and even different companies arise. But opportunities are not restricted to manufacturing. By making machines digital and providing a connection to the Internet, the Internet of Things (IoT) has been created. This IoT can be used in every aspect of our daily lives, such as organizing our home, monitoring our health and so forth [2]. Finally, people are also part of the IoT, controlling it and making use of it [3].

The Fourth Industrial Revolution contains three main technology drivers [4]:

- Digital
- Physical
- Biological

The first two aspects already have been discussed. Especially by connecting them together, major contributions can be made. The biological aspect deals with Genetic Engineering as well as Neurotechnology.

All these fields are strongly data driven, either by collecting (Physical machines, sensors, ...), evaluating (Big data and cloud computing, IoT, ...) or applying them (Genetic Engineering or Neurotechnology). There are different ways of evaluating these data, depending on their source as well as their purpose. One major interest is certainly the predictive maintenance of systems such as machines or subsystems of these machines. For this reason,

predictive maintenance is a crucial application of the Internet of Things and the digitalization of manufacturing. By using predictive maintenance, manufacturers could save a total of $240 to $630 billion in 2025 [5]. One main part about the accuracy of a predictive maintenance system is the information about how fast the value of a specific manufacturing system variable changes. These changes can be described mathematically as the derivative of the examined variable. An example for such a variable is shown in fig. 1.1. The change of this variable is displayed over time. The right part (Test series 2) shows a linear gradual change of the variable superimposed with a high amount of random Gaussian noise. The graph on the left side shows the same test series over a greater period of time. By a closer examination, one can see a non-linear pattern of the variable. The slope of the variable is slowly decreasing.

Two major problems can be identified in fig. 1.1

- Noise (measurement noise and system noise) is always present in a periodic or non-periodic pattern.
- Macrotrends are dependent on the period of examination of the test run.

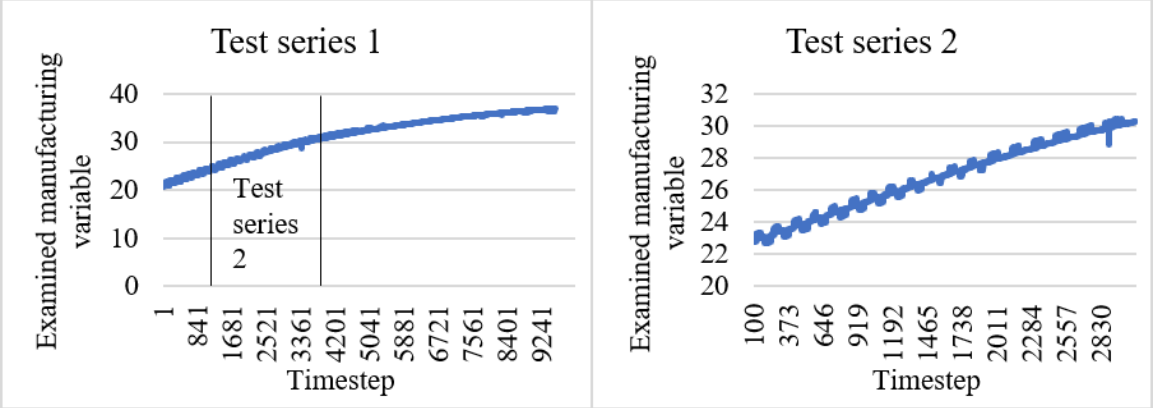

Figure 1.1: Raw data for estimated speed of change

To solve these problems, a set of different slope estimation algorithms (also referred as slope module), including a Kalman Filter and a Least Square Mean Filter, is developed

and tested for different use cases. The slope estimation module is capable of handling the superimposed noise on a broad variety of signals as well as detecting macrotrends in data series. It can deal with different (manufacturing based) variables and it handles diverse timesteps, frequencies of noise, timescales of macrotrends and more.

CHAPTER 2

STATE OF THE ART

The following chapter lays the framework for the whole thesis. The theoretical background for the different topics is discussed.

This theoretical background includes all topics which are important for the development of the slope estimation module. For this reason, at the very beginning the noise and the signal itself are discussed. Different kinds of noise are investigated to give a better understanding of the task. Afterwards, different approaches for filtering the noise are examined. This is one of the main parts in this thesis as it lays the framework for the future slope estimation module. In section 2.4, the deployed sensors are investigated and the sensing principles are explained. This is important to understand the output of the sensor which acts as input for the slope estimation module. In section 2.4, a compendium of different topics which are required to support the framework are explained. It contains the sensors itself, the power supply of sensors with a focus on Lithium Ion batteries as well as several transmission protocols. All the different chapters and their interactions with each other are shown in fig. 2.1.

The different boxes show different ways of combining the tasks. The signal conditioning can either be done locally combined with the process of data collection or cloud based directly before the data are written to a database.

2.1 Signal Noise

Nearly every signal is somehow corrupted by noise. This noise changes the signal so there is a discrepancy between the actual value and the displayed one. In general, there is process

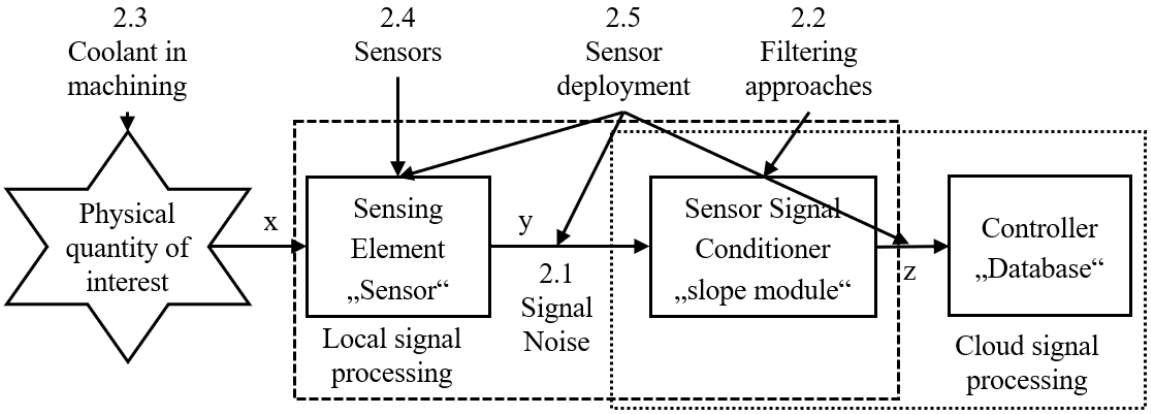

Figure 2.1: Structure chapter 2

noise, which influences the signal itself, as well as measuring noise, which is added to the signal during the measuring process.

2.1.1 Analog Signals

Analog signals need to be read by an Analog to Digital Converter (ADC) first before they can get processed and worked on. The ADC converts the analog signal (Voltage level) to a digital signal (readable number). The selection of an adequate ADC has a high influence on the signal itself.

There are different architectures for ADCs; the main important ones are [6]:

- Successive Approximation (SAR)
- Sigma-Delta
- Pipeline

To choose between those three, the following abilities have to be considered [7]:

- Conversion rate
- Conversion resolution
- Latency

- Power Consumption and Power Supply
- Costs

Since the ADC is only used as a tool to complete the task, the actual mode of operation is not explained in this thesis. Nevertheless, the abilities of the different architectures are explained and discussed to choose the suitable ADC.

Conversion Rate

The conversion rate or sampling rate is given as the number of updates per second [Hz]. To determine the required sampling rate of an ADC, two major factors have to be considered: the bandwidth of the signal as well as the required update rate.

Beside these two requirements, the sampling rate needs to fulfill the Nyquist criteria. The Nyquist criteria states, that the sampling rate f_S has to be well above twice the frequency of the signal f:

$$f_S > 2 * f \tag{2.1}$$

The Nyquist frequency is shown in fig. 2.2. The sampling rate in this example is 4 times the frequency of the signal. In the case of oversampling, the available memory cannot be used efficiently. [8]

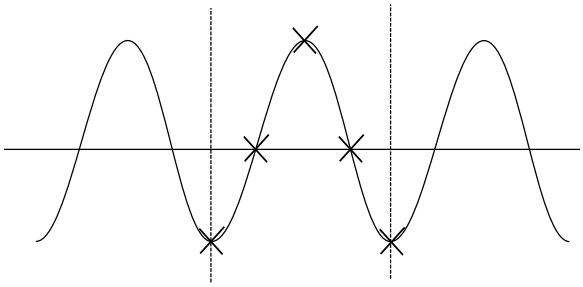

Figure 2.2: Nyquist Frequency

Conversion Resolution

The resolution of a system is directly connected to the accuracy which can be achieved. The resolution describes the number of bits used by an ADC, whereas the Least Significant Bit (LSB) is the minimum change of the input signal which changes the output signal [9]. An n-Bit ADC can convert a continuous input into $2^n - 1$ digital steps. The integer number n is the resolution of the ADC. Table 2.1 shows the number of steps which is dependent on the number of bits.

Table 2.1: Resolution of ADC

Bits	Steps	20 V Range	3 V Range
8	256	78.1 mV	11.72 mV
10	1024	19.5 mV	2.93 mV
12	4096	4.88 mV	0.73 mV
16	65536	0.305 mV	0.05 mV

To improve the accuracy of a system, not only the resolution of the ADC has to be considered. There are other electrical components, such as amplifiers, which influence the overall accuracy. It can be obtained by taking the root-sum-square of the errors for the specific parts. An example for such errors can be found in table 2.2. [7]

Table 2.2: Typical Errors in a 12-Bit data acquisition system [7]

Error Source	Typical Part	Typical Error
Instrumentation Amp	INA114	0.003%
Multiplexer	MPC508	0.0025%
Drive Amp	OPA602	0.01%
A/D Converter	ADS7806	0.01%

In fig. 2.3, a comparison of the three main architectures of ADCs regarding sampling frequency and conversion rate is shown. It can be observed, that for high conversion rates Pipeline ADCs are more adequate, whereas for lower conversion rates with higher resolution, Delta Sigma ADCs are more suitable.

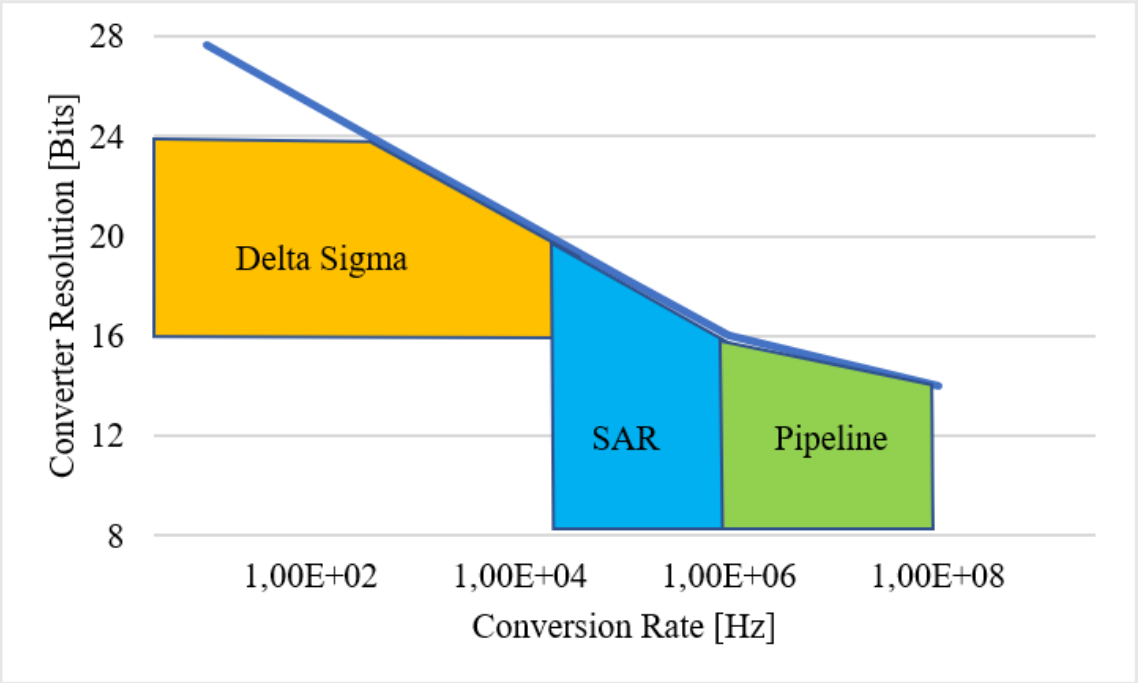

Figure 2.3: Different ADC architectures [10]

2.1.2 Different Origins of Signal Noise

Signal noise is a very important topic for signal processing. Every signal is corrupted with noise in various ways. There are a lot of different ways noise can penetrate into signals. Some of them are shown in fig. 2.4 which is one possible way of classifying signal noise. The different types of noise are classified into three main groups. The environmental noise includes the noise acting on the signal from the environment. The thermal one includes noise acting on the process of converting the signal. The last source of noise is the one from inside the receiver.

In the group of the environmental noise, man-made noise can be radiated by electrical wires passing by, the ignition from car engines, etc. In many cases, man-made noise can be avoided by shielding of the source of the noise or the receiver. Sky noise, however, is a bigger problem, since it cannot be shielded, and it contains wideband noise from the sun, radio stars as well as radiations of galactic origin. This noise is automatically picked

up if an antenna is used as receiver. The second big group is the thermal noise acting on the potential resistor in a sensor. The thermal noise is based on the Brownian movement discovered in 1828 by Robert Brown. Since the movement the electrons increases with temperature, the number of collisions also increases. These collisions of the electrons generate a proportional voltage. This voltage is overlaying the signal in the wire.

The third group is the noise within the receiver. There are several influences acting on the receiver. Not all of them are discussed in particular.

The Intermodulation and crosstalk noise is induced by nonlinearities in the signal processing. This can be seen at diodes, poorly conducting or corroded joints etc. The nonlinearities lead to higher harmonics if there is one signal, or a combination of higher harmonics ($mf_1 \pm nf_2$) if there are two signals. They act as noise since they interfere with the actual signal.

Quantization noise is induced into the signal by the quantization of the signal itself. This happens if for example an ADC is applied somewhere in the system. The signal gets quantized into a predefined number of levels, which makes it a replica of the original signal. The difference between the original signal and the quantized signal can be seen as error and represents the quantization noise.

Phase noise is very similar to thermal noise. It is induced by the Brownian movement of electrodes. Instead of changing the amplitude of the signal, it influences the phase of a signal. It can be seen at frequency measurements. Ideally a frequency measurement is represented by an infinitesimally narrow line. In reality, a spread of frequencies can be observed around the main frequency.

Popcorn noise is encountered in semiconductors and integrated circuits. It is named after the audible effect of loudspeakers and it can have a frequency of 1 beat per minute until 100 Hz. It is due to defects in semiconductor junctions and can be controlled up to a certain point in the process of manufacturing them.

Flicker or 1/f noise is low frequency noise. It is normally encountered in nonequilibrium systems, which is mostly if dc current is flowing [11]. In theory, the noise would be infinite if the frequency approaches zero. Indeed, it was found that the pattern in the Flicker noise of 1/f is followed until a signal frequency of several cycles per day [12].

Shot noise is spontaneous current fluctuations superimposed on a DC current. It is due to the particle character of the current itself [11]. Since the electrons are emitted from the cathode at a random rate, the current can be observed as granular. This granular behavior leads to the fluctuation around the average.

Quantum noise has its origin in the quantum physics, and Heisenberg's uncertainty principle. It is negligible in frequencies used in engineering but has a high importance for optical frequencies. [13]

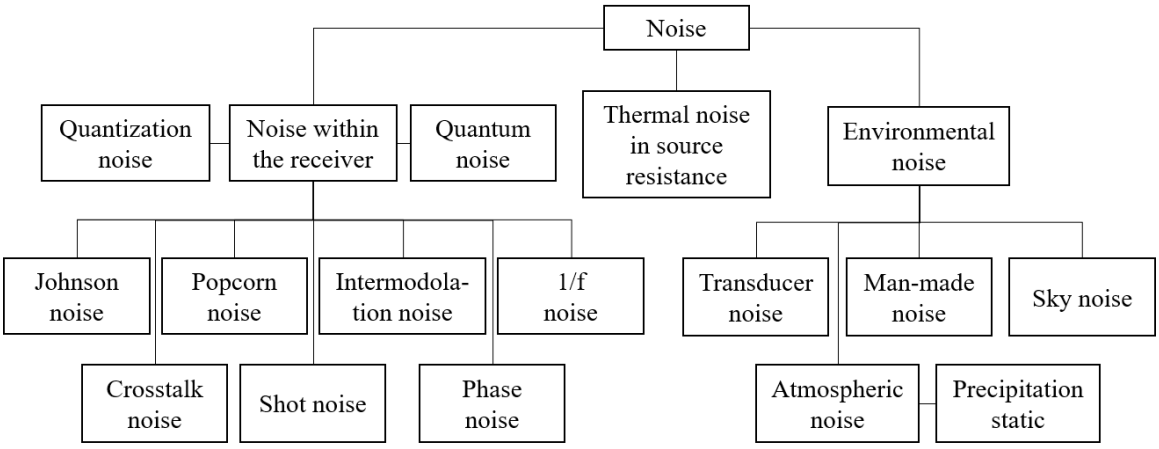

Figure 2.4: Different kinds of noise [13]

2.1.3 Gaussian Noise

Gaussian noise is defined as noise with a probability distribution function (PDF) of a normal distribution, also known as Gaussian distribution [14]. It can be expressed by eq. (2.2).

$$p(n) = \frac{1}{\sqrt{2\pi\sigma^2}} \exp\Big[-\frac{(x-\mu)^2}{2\sigma^2}\Big] \tag{2.2}$$

The distribution of Gaussian noise is totally defined by the standard deviation σ as well as the mean value of the distribution μ. An example for a Gaussian noise distribution with $\mu = 4$ and $\sigma = 2$ is shown in fig. 2.5.

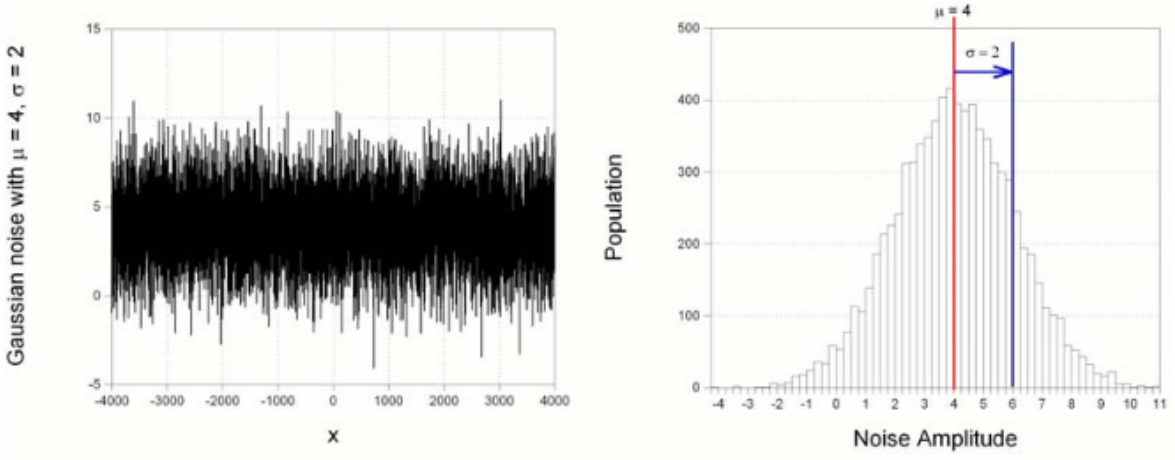

Figure 2.5: Gaussian noise distribution [15]

There are several ways of smoothing Gaussian noise, such as averaging or using a median filter. The problem about these filters is the smoothing of sharp edges and peaks in signals. [16]

There are several reasons why the Gaussian noise is widely used to simulate signal noise:

- Most variables have a normal distribution. Even the ones without a normal distribution mostly can be approximated with a normal distribution.
- Based on the central limit theorem, the distribution of the mean values of sample batches converge to a normal distribution as long as the sample size approaches infinity [17]. This theorem is valid if the samples are independent of each other, if the number of samples is high enough and if the variance is finite. Even if the distribution by itself is not Gaussian, the distribution of the mean values in general is Gaussian.
- A lot of statistical tests are based on normal distributions. Even though the variables are sometimes more or less normally distributed, most of them still work.

Additive White Gaussian Noise

Additive White Gaussian Noise (AWGN) is a frequently used model for all communication channels. It is very similar to Gaussian noise but has some specific abilities:

Additive The word additive describes the fact that it is added to the signal itself. This can happen while transmitting it. The received signal r includes the original, noise free signal s as well as the White Gaussian Noise w, see eq. (2.3).

$$r = s + w \tag{2.3}$$

White The color white refers to the characteristics of white light to have a uniform power across its frequency band. Independent of the frequency of the signal itself, the intensity of the noise is constant.

Gaussian The added noise signal (w in eq. (2.3)) has a Gaussian distribution. [18]

Qantile-Qantile Plot

The Quantile-Quantile plot (q-q plot) can be used as graphical method for checking if different sets of data have a normal distribution. By plotting the first data set against the second one, for an optimal normal distribution the values form a 45° line. This can be seen in fig. 2.6. As the difference between values and the 45° reference line increases, the accuracy of the normal distribution's approximation decreases. The q-q plot is created by sorting both batches and plotting them. If the batch sizes are different, the missing values for the smaller batch are interpolated. Compared to other methods, the sample size of both batches does not have to be equal, and several distributional aspects can be tested at once. [19]

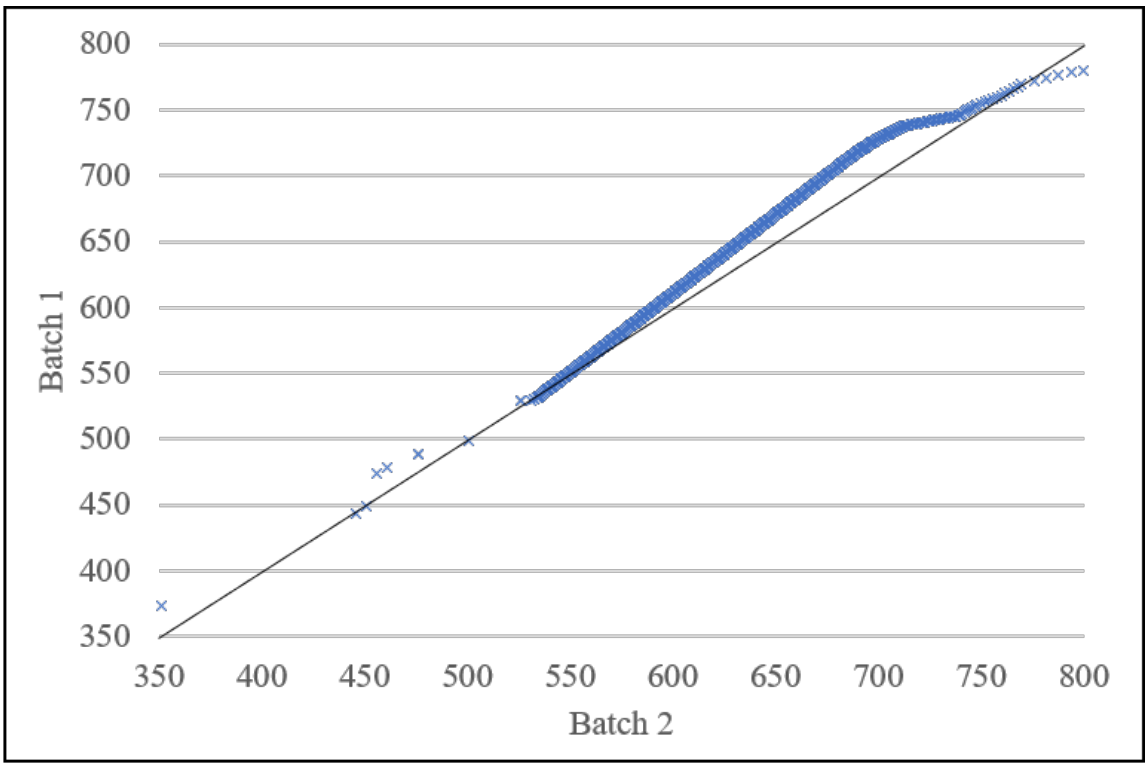

Figure 2.6: Illustration of Quantile-Quantile plot [19]

2.1.4 Non Gaussian Noise

As discussed in section 2.1.3, most kinds of noise can be approximated by using a Gaussian noise model with a normal distribution of the signal. Nevertheless, in this chapter other types of non Gaussian noise are investigated.

There are several non Gaussian noise models. In the following, a Gaussian sum approach is discussed. [20, 21]

In general, any signal with an arbitrary probability density function can be expressed as the summation of Gaussian signals; this relation can be seen in eq. (2.4). With the factor a_i as $\sum_{i=1}^{l} a_i = 1$ and $N(\mu_i, B_i)$ as a Gaussian density with the mean value μ_i and the

covariance matrix B_i.

$$f_A(x) = \sum_{i=1}^{l} a_i N(\mu_i, B_i) \tag{2.4}$$

A special case of this Gaussian sum approximation is the $\epsilon - mixture$. It can be used to describe several non-Gaussian noise environments and is shown in eq. (2.5). The parameter ϵ can be chosen as $\epsilon \in (0, 1)$, f_G is the probability density function of the Gaussian signal and F_{nG} is the probability of the non-Gaussian signal. [22]

$$f(x) = (1 - \epsilon) f_G(x) + \epsilon f_{nG}(x) \tag{2.5}$$

There are several approaches for filtering this Gaussian noise. Sorenson and Alspach [23, 24] developed a mean-squared state estimator for the case of non Gaussian noise. A possible filter based on the Gaussian sum is developed by Plataniotis [22]. Since both approaches are not applied in this work, their content is not discussed in here. For further interest one can read into the stated sources.

2.1.5 Signal-to-Noise Ratio

The signal-to-noise (SRN) ratio defines the ratio of the signal power compared to the noise power. To evaluate this ratio, the power has to be defined first. For this reason, the signal power is shown in eq. (2.6)

$$P_s = \frac{1}{T} \int_0^T s^2(t) dt \tag{2.6}$$

where T is an arbitrary observation interval and s is the signal itself.

If the signal is periodic ($A \sin 2\pi f_0 t$), the power of the signal can be described with the

correlation function $R_s(\tau)$. This is shown in eq. (2.7).

$$R_s(\tau) \equiv E\left[s(t)s(t+\tau)\right]; \quad P_s = R_s(0) \tag{2.7}$$

The power of the noise P_N can be evaluated in a similar way.

$$P_N = R_s(0) \tag{2.8}$$

The ratio can be directly calculated from the power

$$SNR = \frac{P_s}{P_N} \tag{2.9}$$

The SNR is a very important measure for defining the quality of a signal. In engineering, it is often expressed in decibels:

$$SNR(dB) = 10log_{10}\frac{P_s}{P_N} \tag{2.10}$$

Alternatively, the SNR can be computed with the Voltage of the signal [25]. For this reason, the Root Mean Square Value of the signal as well as the noise has to be computed.

$$SNR_V = \frac{\text{RMS Signal Voltage}}{\text{RMS Noise Voltage}} = \frac{V_s}{V_N} \tag{2.11}$$

To find the decibel value of the Voltage SNR, a similar approach can be chosen. The results of both are equal and not effected by the way they are computed.

$$SNR(dB) = 20log_{10}\frac{V_s}{V_N} \tag{2.12}$$

2.2 Filtering Approaches

Filters in general try to fulfill two different goals:

- separation of two combined signals
- restoration of a manipulated signal

Both points are further investigated since they are essential for the implementation of the task. For this reason, several approaches are discussed in this chapter and their application is investigated in chapter 3.

In the following, only digital filters are examined since their application and adaption on different situations is easier. Nevertheless, it has to be mentioned that there is also a wide variety of analog ones. [26]

Since the example applications (see section 2.4) have non-periodical signals, the following filter approaches are restricted to filter all periodic fractions out of the signal.

2.2.1 Moving Average

A very simple filter is the moving average filter. There are several possibilities to implement this filter; therefore, it should be explained in its most general form with x as the input into the filter and y as the output. a_p is a weighting factor which follows the restriction $\sum_{p=i}^{h} a_p = 1$.

$$y_k = \sum_{p=i}^{h} a_p x_{k-p} \tag{2.13}$$

The parameters i and h describe the number of x values which define the moving average. Depending if i is positive, zero or negative, only values from the past and/or the future of the current timestep k are used to calculate the average. This is shown in fig. 2.7. Input and output values are plotted on the same time axes and should symbolize the samples taken in

the time domain.

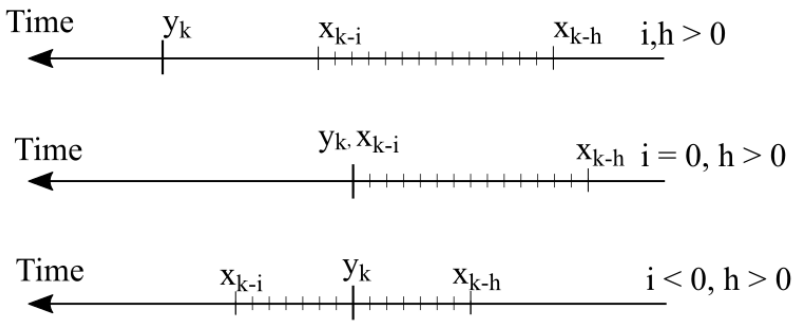

Figure 2.7: Illustration of moving average based on set of input data

Although the moving average is a very simple filter, it is very effective in reducing Gaussian noise. Based on the central limit theorem in combination with the law of large numbers, the amount of values taken ($h >> i$) has to be big enough to reduce the Gaussian noise while maintaining the signal. A graphical representation can be seen in fig. 2.8 and fig. 2.9. The first plot shows the signal, which is constant at a value of 0.5 and corrupted by white noise. The second plot is the average taken of fig. 2.8. The axis of abscissae represents the number of samples for taking the average. [26]

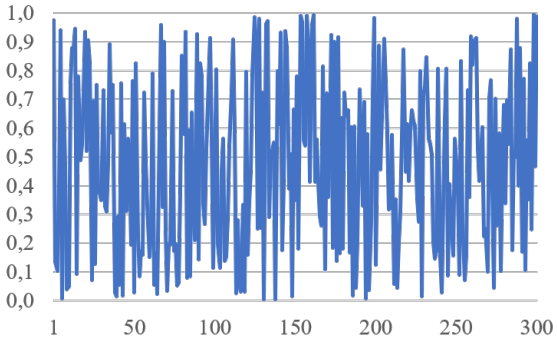

Figure 2.8: White noise signal

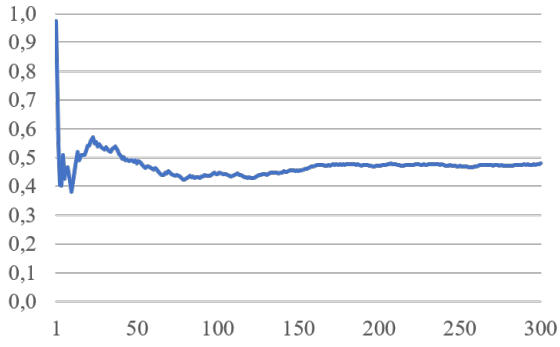

Figure 2.9: Averaged white noise signal

From fig. 2.9 one can see the need for as many values as possible to make the moving average filter working reliable. For this dataset, 300 values still have an offset.

2.2.2 Least Mean Square Filter

The Least Mean Square Filter (LMS) is one of the most common adaptive filters introduced by Widrow and Hoff in 1960 [27]. One of the reasons for this wide usage of the filter is its simplicity compared to other adaptive filters. In fig. 2.10, the general scheme of an LMS filter is shown. The adaptive part of the filter is represented by the "Adaptive Algorithm", which recalculates the filter weights after every update.

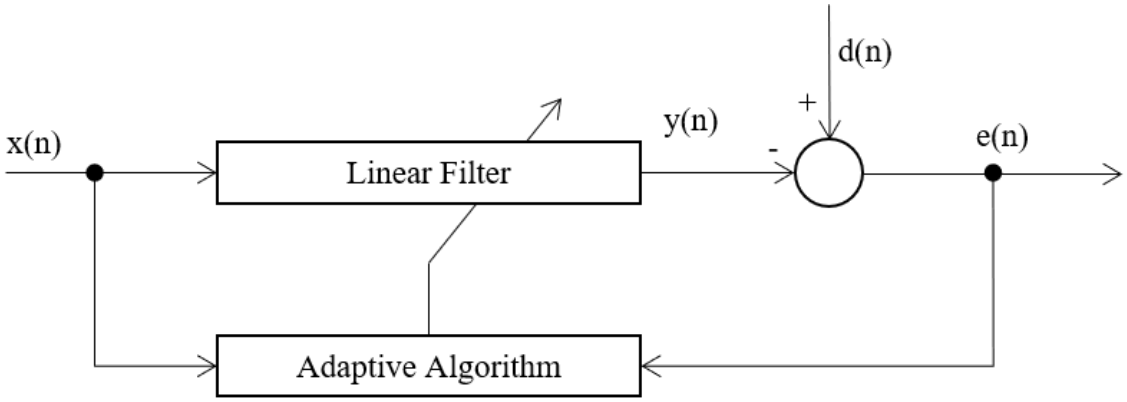

Figure 2.10: Graphical illustration of Least Square Mean filter [28]

Filtering

The filtering itself is done by the weighting factor $w(n)$ and the input $x(n)$. The output of the filter can be calculated as followed:

$$y(n) = w^T(n)x(n) \tag{2.14}$$

Error estimation

For estimating the error, the output $y(n)$ is subtracted from the desired output $d(n)$. This results in the error estimation signal $e(n)$.

$$e(n) = d(n) - y(n) \tag{2.15}$$

Tap-weight Vector Adaptation

To update the weighting factor $w(n)$, the previous factors, the step size μ as well as the error estimation are used. The step size in general is critical for fast convergence and low misalignment [29]. For this reason, in a lot of cases a variable step size is used.

$$w(n+1) = w(n) + 2\mu e(n)x(n) \tag{2.16}$$

There are several variations of the LMS filter as for example an LMS filter with variable step size [30]. Due to the application, only the standard LMS algorithm is examined in this section.

2.2.3 Standard Deviation

Standard deviation as a measure is widely used in different areas of science. It is primarily not directly correlated to filters but it can describe the distribution of several measures. The standard deviation was influenced by several researchers; one of the most famous ones is Carl Friedrich Gauss [31].

The standard deviation is used to quantify the amount of variation in a set of data. To fully describe a normally distributed population for example, the mean value μ as well as the Standard Deviation σ are sufficient. For a normally distributed set of data, one σ contains

$68.2\ \%$ of the data and two σ contains $95.5\ \%$ of the data of the distribution. The range is defined by adding and subtracting σ from μ. This can be seen in fig. 2.11.

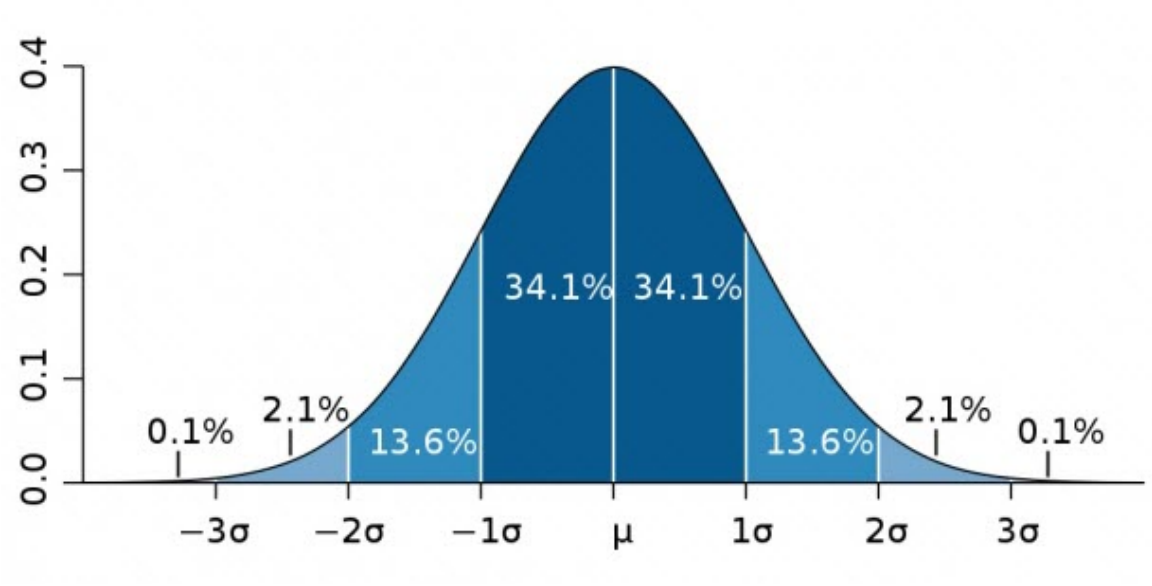

Figure 2.11: Illustration of the Standard Deviation [32]

The standard deviation (s) can be calculated in case it is just a fraction of the whole batch as described in eq. (2.17). With n as the number of samples used to calculate the Standard Deviation, X as the values themselves and $\overline{X}$ as the average value.

$$s = \sqrt{\frac{\sum \left(X - \overline{X}\right)^2}{n-1}} \tag{2.17}$$

2.2.4 Kalman Filter

The Kalman Filter is used for estimating the state of a system. Based on previous measurements and a model of the system, the current state is estimated according to the current measurement and the previous state of the system [33].

History of the Kalman Filter

The first attempt to implement a Kalman Filter was made by Thorvald Nicolai Thiele in 1880. He established a method for predicting a state of a system by estimating the regression component. With this first version of the Kalman filter he was trying to make a prediction of the Brownian motion [34]. In the 1940s, Norbert Wiener and Andrei N. Kolmogorov developed a state-space form for optimal estimation in the frequency domain. First in the 1960s, Rudolf E. Kálmán and Richard S. Bucy created the discrete time step Kalman Filter. The Kalman-Bucy Filter is a continuous time version of the Kalman Filter. [35]

After the first publication of Kalman in 1960 [36], the filter was mainly applied in aerospace, for example for the Apollo mission. The main advantage of the Kalman Filter was to provide guidance, although sensor outputs could take hours. Another approach by Stanley F. Schmidt and his team, of which Kalman was a member, was to use a nonlinear version of the original Kalman Filter. By estimating the current mean and covariance of a state, the extended Kalman Filter was introduced.[37] This filter is used in most applications for navigation systems and GPS.[38]

Explanation of Kalman Filter

To use a Kalman Filter, the system needs to be modeled first. For the basic Kalman filter, a linear system is required. The system can be modeled in a basic form as seen in eq. (2.18). In this case, A, B and C are matrices and describe the system. x is the state of the system which changes for every timestep k. u is the known input to the system while w and z are both noise signals. In this case the noise is separated into system noise w as well as

measurement noise z. The measured output is represented by y. [33]

$$\begin{aligned} &\text{State equation:} \\ &x_{k+1} = Ax_k + Bu_k + w_k \\ &\text{Output equation:} \\ &y_k = Hx_k + z_k \end{aligned} \tag{2.18}$$

The basic idea of the Kalman filter can be seen in fig. 2.12. The filter is updated for every new sample. Based on this, previous measurements do not have to be stored, which saves storage. This is important especially for Microprocessors and Microcontrollers. On the other hand, the Kalman filter requires matrix calculations, which are very costly from a computational perspective.

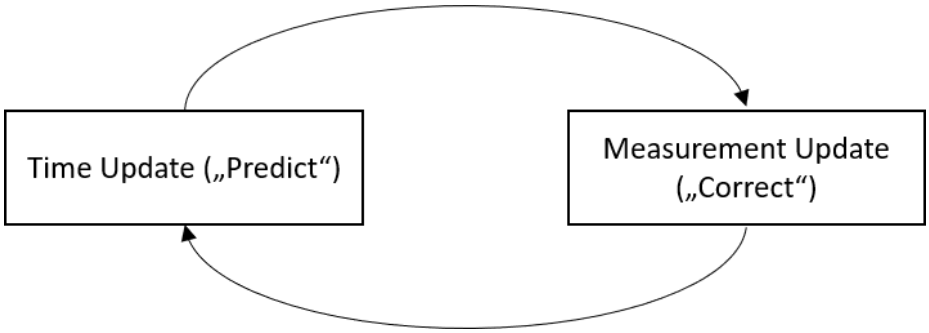

Figure 2.12: Kalman filter scheme [39]

The Time Update step is a predictive step. The new state of the system is predicted based on the known input u and the modeled systems A and B. In the same step, an update of the covariance matrix is made. The covariance matrix P correlates the input into the system z and the theoretically predicted state from the update step. Therefore, the previous covariance matrix is used as well as the process noise covariance matrix Q. The Equations

can be found in eq. (2.19).

$$\begin{aligned} &\text{Time Update [39]} \\ &\text{First step:} \qquad \widehat{x}_k^- = A\widehat{x}_{k-1}^- + Bu_{k-1}^- \\ &\text{Second step:} \qquad P_k^- = AP_{k-1}A^T + Q \end{aligned} \tag{2.19}$$

Afterwards, the measurement update describes the corruption of the output of the system. In the first step, the so called Kalman gain K is computed based on the covariance error matrix P^- and the measurement noise covariance R. Afterwards, the state of the system x is computed based on the Kalman gain as well as the measurement z. At the end, the error covariance matrix P is updated.

$$\begin{aligned} &\text{Measurement Update [39]} \\ &\text{First step:} \qquad K_k = P_k^- H^T (HP_k^- H^T + R)^{-1} \\ &\text{Second step:} \qquad \widehat{x}_k = \widehat{x}_k^- + K_k(z_k - H\widehat{x}_k^-) \\ &\text{Third step:} \qquad P_k = (I - K_k H)P_k^- \end{aligned} \tag{2.20}$$

Before applying the filter, the measurement (R) as well as the process noise covariance matrix (Q) have to be calculated. They both can be expressed as the expected values of the noise applied to the system w_k and the measurement z_k. [33]

$$\begin{aligned} Q &= E(w_k w_k^T) \\ R &= E(z_k z_k^T) \end{aligned} \tag{2.21}$$

In practice, the measurement covariance can be obtained by measuring a constant signal. By subtracting the original signal, the measurement noise z_k can be obtained, and by this the covariance of the measurement. However, the system noise is harder to determine. Some approaches focus on calculating the standard deviation of the signal to obtain the

system noise covariance.

2.3 Cutting Fluids

In modern machining, cutting fluids (also known as machining coolant) have several tasks. These tasks can be described by the 4 basic functions of cutting fluids [40]:

- Cooling
- Lubrication
- Corrosion protection
- Cleaning

By addressing these tasks, the tool wear is decreased, and the surface quality of the finished part is improved [41]. To fulfill these tasks, four different types of cutting fluids can be used.

Straight Oil

Straight oils are mainly made of mineral or vegetable oil. The oil is not mixed with water and has viscous properties. Due to the high viscosity and the lack of water, it is mostly used for lubrication and less for cooling of the cutting process. Lower cutting speeds and high metal-to-metal contact is the primarily use case for straight oil.

Soluble Oil

Soluble oil or emulsifiable oil consists of 30 - 85 % lubricant based oil and emulsifiers to maintain the solubility in water. The cooling properties of soluble oil are better compared to straight oil, although the corrosion protection is worse due to the amount of water. Furthermore, they have a smaller sump life and a critical mix stability.

Semisynthetics

Semisynthetic fluids contain a fraction of 5 - 30 % less severely refined base oil. Their corrosion protection is improved as well as their sump life. The ingredients are very similar to soluble oil but have a more complex mixture of emulsifiers.

Synthetics

Synthetics do not contain any petroleum oil. They are based on detergent-like components to "wet" the part and other additives for the required performance. They provide the best cooling of the part as well as an improved corrosion control and have a longer sump life.

2.3.1 Mechanisms of Cutting Fluids

To understand the mechanisms of cutting fluids, the cutting process itself has to be understood. This cutting process is shown in fig. 2.13. The primary deformation zone is also known as the shear deformation zone, the secondary as the contact zone of the tool and the chip and the tertiary as the tool-workpiece zone. In all of these zones heat generation can be seen. The cutting fluid has access to all three of these zones, as shown by the arrows A, B, C. The heat reduction can be achieved by conduction, convection and evaporation. By cooling the cutting process, several risks can be avoided:

- chemical reaction
- heat damage of the material and the tool
- material adhesion between the workpiece and the tool
- thermal expansion, which leads to inaccuracies

For the lubrication of the cutting process, the ability of the cutting fluid to penetrate into the three cutting zones is important (see fig. 2.13). To maintain a proper penetration of the

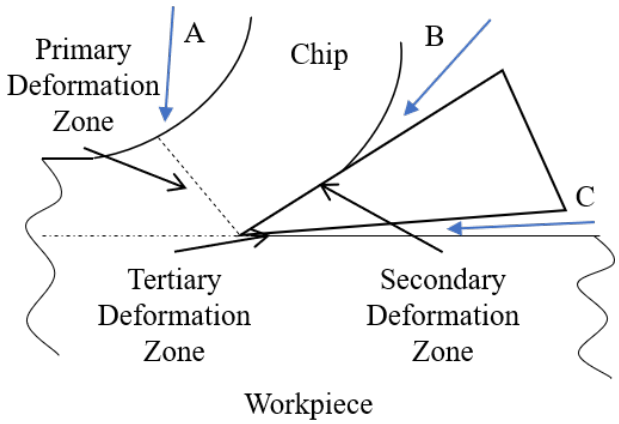

Figure 2.13: Areas affected by cutting fluid [40]

cutting zones, the selection of the cutting fluid plays an important role (also the matching of the cutting fluid and the workpiece material). In certain cases, minimum quantity lubrication (MQL, see section 2.3.3) can help to achieve this goal. There are several models to explain the penetration of the cutting fluid into the cutting zones; some assume a liquid cutting fluid, others assume an aerosol to penetrate into the gap of the workpiece and the tool as well as the tool and the chip. Besides the used model, it is well known that the penetration of the cutting fluid has an important influence on the quality of the cut; therefore a proper adjustment of the cutting fluid nozzles plays an important role for machining.

The corrosion protection of the created surface is another important task of the cutting fluid. The abilities of cutting fluid concerning this task are mainly dependent on the chemical composition of the cutting fluid as well as on the material of the workpiece. The interactions between these two are most important and influence a proper selection of the cutting fluid. [40]

2.3.2 pH Value of Cutting Fluids

The pH value is one property of the cutting fluid which needs to be monitored to maintain a high quality in the tank. There are different influences on the pH level. An example could be acids which are inserted by glass and floor cleaners [42]. Besides alien substances,

microbial activities can decrease the pH value. The bacteria digest the fluid which makes it ineffective as lubricant. Furthermore, a big number of bacteria makes it dangerous for operators who are exposed to cutting fluid on a daily basis, especially if they suffer from hypersensitive pneumonitis or asthma. [43]

To maintain the amount of bacteria at a proper level, it is required to monitor them. This can be done by a pH value measurement since it has a big influence on the bacteria growth rate [44] [45]. If the pH level is above 9, the bacteria growth rate is inherently smaller compared to pH values of 7 to 9. There are different ways of measuring the pH level, for example with pH strips or electrical pH meter, see section 2.4.3. [46] Another way to directly detect the amount of bacteria per milliliter is to count the number of bacterial strains in a diluted solution of machining fluid in a petri dish. This is shown in fig. 2.14. The values represent the amount of dilution.

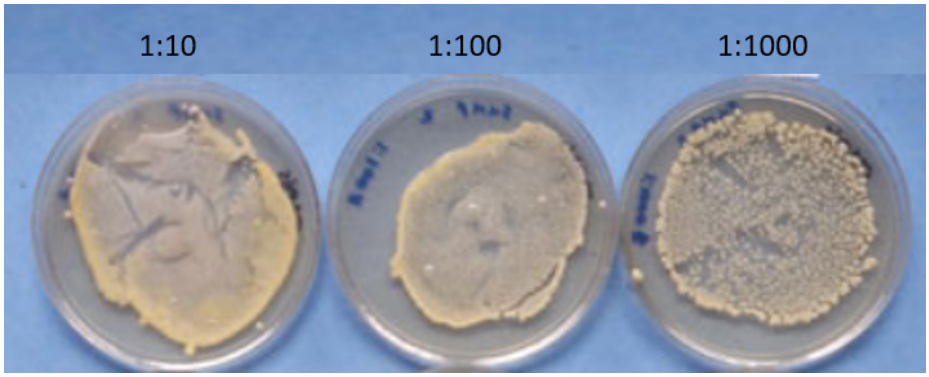

Figure 2.14: Growth of bacteria in diluted machining fluid [43]

2.3.3 Trends in Cutting Fluids

Cutting fluid is known to be a major factor for the costs of machining. An evaluation of Klocke and Eisenblätter [47] shows, that $10 - 17$ % of the machining costs are due to cutting fluids (cooling and lubrication). This is a very high amount compared to the tool costs of $2 - 4$ %. Based on these numbers, a lot of research is done on cutting fluids.

Dry Cutting

Dry cutting avoids the usage of cutting fluids. A main requirement is to keep the same cutting parameters (cutting time, tool wear, quality of parts, ...) compared to cutting with cutting fluids. This requirement can hardly be fulfilled. Even for grey cast iron, although it is well suited for cutting at a low cutting temperature, one cannot switch from cutting with cutting fluid to cutting without cutting fluid. For this reason, a minimal quantity of lubricant is used and injected directly into the cutting zone. By this, the amount of cutting lubricant can be reduced to $50\ ml$ per hour. [47]

Adjustment of Cutting Fluid Nozzles

The process of adjusting the nozzles to directly feed the cutting zone is connected to the minimum quantity of lubricant. If the amount of lubricant is decreased, the adjustment of the nozzles gets more important for the cutting fluid to reach the actual cutting zone. [40]

Cutting Fluid Quality Management Program

Since the quality requirements on cutting fluids are directly linked to the part quality, they are getting more important. For this reason, monitoring of the cutting fluids becomes more and more interesting, as money can be saved and the quality of the machined parts can be increased. For this reason, cutting fluid monitoring systems are becoming more popular. [48]

2.4 Sensors

Sensors have a long history. It is connected to the history of material science. In the early 1800s the difference in electrical resistance of material at different temperatures was

discovered, which helped W. von Siemens in the 1860s to develop a temperature sensor. [49]

But this is only an example for one sensor type and one measurand. A classification is made by R. White [50] and can be seen in table 2.3. Besides classifying them by their measurands one can also use the field of application, the material of the sensor etc.

Table 2.3: Sensor classification [50]

Measurands	Examples
Acoustic	Wave amplitude, Phase, Spectrum, ...
Biological	Biomass (concentration, states, ...)
Chemical	Components (identities, concentrations, ...)
Electrical	Charge, Current, Potential, ...
Magnetic	Amplitude, Phase, ...
Mechanical	Acceleration, Position, Pressure, ...
Optical	Wave Amplitude, -Phase, ...
Radiation	Type, Energy, Intensity, ...
Thermal	Temperature, Flux, ...

2.4.1 Distance Sensors

Location in general and distance in particular can be detected with different types of sensors and sensing principles.

Most common principles are Infrared sensors as well as Ultrasonic sensors. They are widely used in robotics for detecting obstacles. In many cases they are both used and their readings can be meshed [51]. While Infrared (IR) sensors are strongly dependent on the surface of the detected obstacle, Ultrasonic (US) sensors are rather dependent on the angle "a" between sensor and obstacle, see fig. 2.15. Both sensor types work on different measurement principles: while IR sensors detect the intensity of light at a specific wave length, US sensors measure the time from sending to receiving an ultrasonic soundwave [52]. Due to the principle of measurement, US sensors are dependent on temperature, humidity and appearance of ambient noise while IR sensors are nonlinear [53].

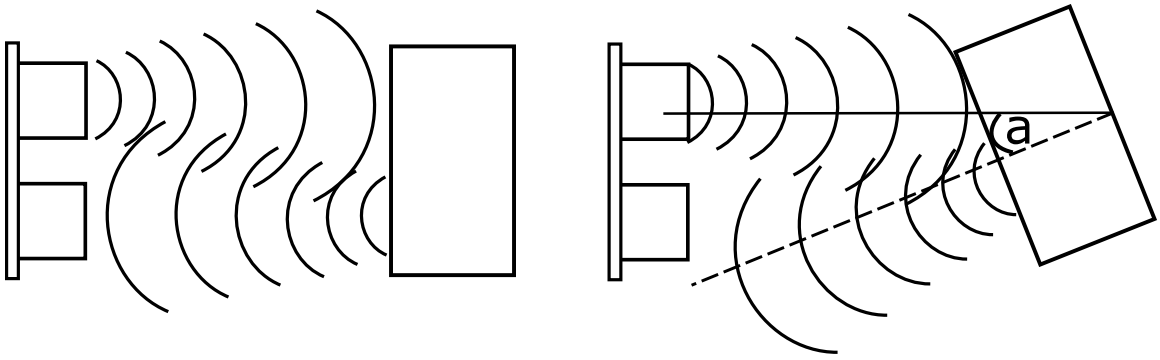

Figure 2.15: Ultrasonic sensor with obstacle at an angle

2.4.2 HC-SR04

The HC-SR04 US sensor is used for non contact measurement and has a range of 20 mm - 4000 mm. It includes a transmitter (left), a receiver (right) and the required control circuit (backside). It is shown in fig. 2.16. [54]

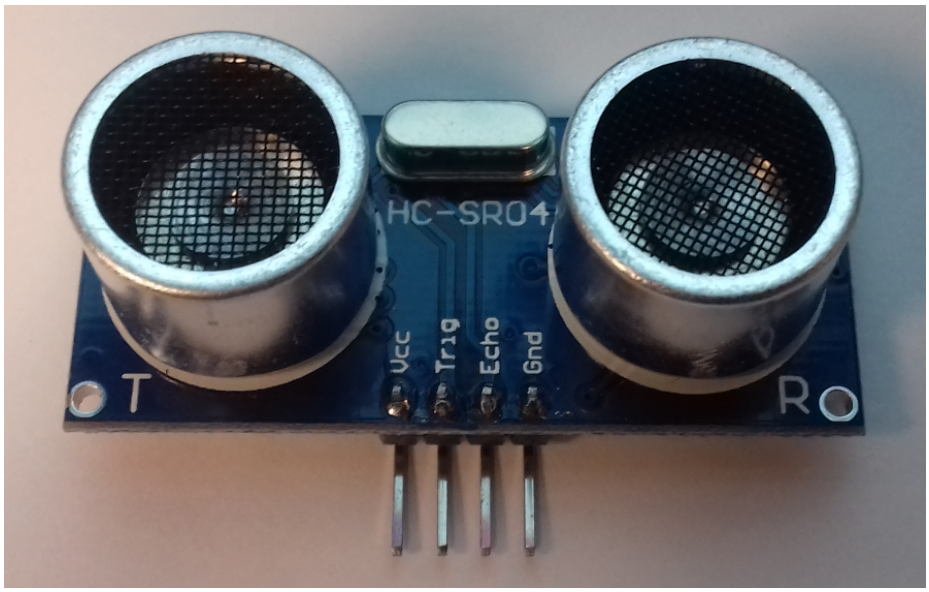

Figure 2.16: HC-SR04 Ultrasonic sensor

For taking a distance measurement, a $10\ \mu s$ pulse is sent to the "Trig" Pin (second Pin from left side). This triggers the US module to send 8 pulses of a frequency of $40\ kHz$ via the

transmitter. The time from sending to receiving the echo with the receiver is accumulated and with this time, the distance can be calculated. The timing diagram is shown in fig. 2.17.

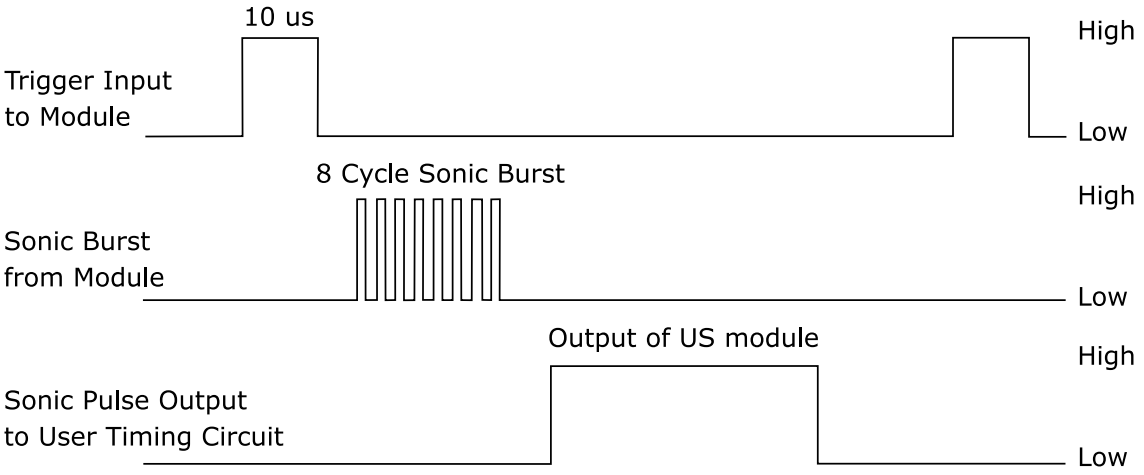

Figure 2.17: Timing diagram of HC-SR04 ultrasonic sensor [54]

For the calculation only half of the time can be used since the soundwaves travel the distance twice. The calculation can be seen in eq. (2.22)

$$\text{Range} = \text{high level time} * \frac{\text{velocity of sound}}{2} \tag{2.22}$$

2.4.3 pH Sensor

To measure the pH value of a solution, pH meters are used. Similar to the previously discussed distance sensors, pH meters cannot directly measure the pH value. Instead the number of hydrogen (H^+) ions is used. For aqueous solutions, the product (K_w) of hydrogen (H^+) and hydroxide (OH^-) ions stays the same. This leads to eq. (2.23). The K^- value is dependent among other things on the temperature of the aqueous solution.

$$K_w = [H^+] * [OH^-] \tag{2.23}$$

PH meters measure the concentration of H^+ ions and convert it to a pH value, see eq. (2.24)

$$\text{pH} = -\log H^+ \tag{2.24}$$

The concentration of H^+ in pure water for example is 10^{-7} $\frac{moles}{liter}$. By adding acid, this value increases. The increase leads to a drop in pH value. An aqueous solution with a concentration of 10^{-4} $\frac{moles}{liter}$ has a pH value of 4.00. [55]

There are more H^+ ions in acid solutions than in neutral solutions. This imbalance makes H^+ ions diffuse into the outer layer of the glass membrane. By this imbalance, a current is generated. The current is proportional to the amount of H^+ ions in the testing solution. This mechanism is shown in fig. 2.18.

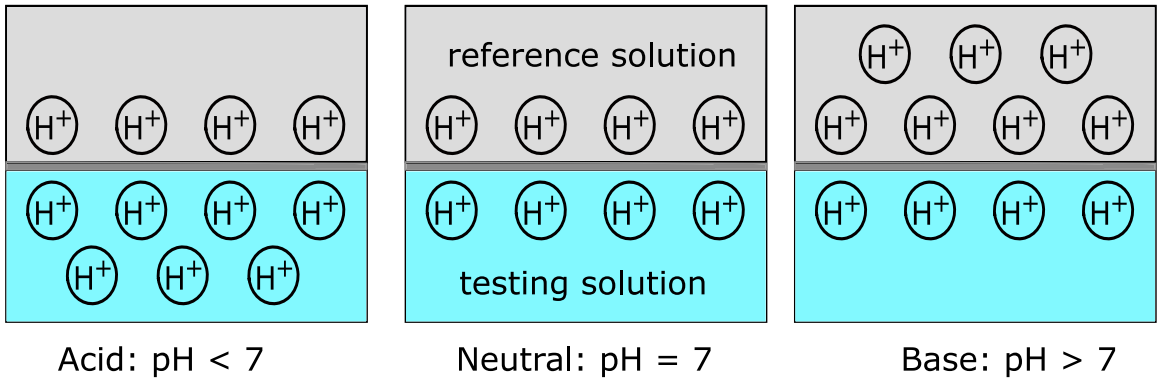

Figure 2.18: Measurement of pH value with glass electrode [56]

2.4.4 Signal Processing

The signal processing is done by a Microcontroller, also known as MCU (Microcontroller Unit). In this case, a Particle Photon is used. In comparison to a Programmable Logic Controller (PLC), an MCU is running at a lower voltage level and therefore requires less power. Due to their wide variety in frequency and their compatibility with different communication protocols, they represent a suitable platform for computing the required data as

well as transmitting them to a storage hub. A cloud based database can be used as storage hub. [57]

2.4.5 Transmission Protocols

There is a great variety of different communication protocols and formats. They are not discussed in detail in here. Nevertheless, the applied protocol is explained.

Message Queuing Telemetry Transport MQTT

Message Queuing Telemetry Transport (MQTT) is designed to transfer data to several receivers at the same time. It is a publish/subscribe protocol where several clients can publish to a topic (Sensors, MCUs, ...) and others can subscribe to it (Mobile devices, Laptops, Databases). This infrastructure represents an easy and simple way of communication between different devices. Furthermore, due to its low power consumption, it is suitable for IoT and its applications in embedded systems. [58]

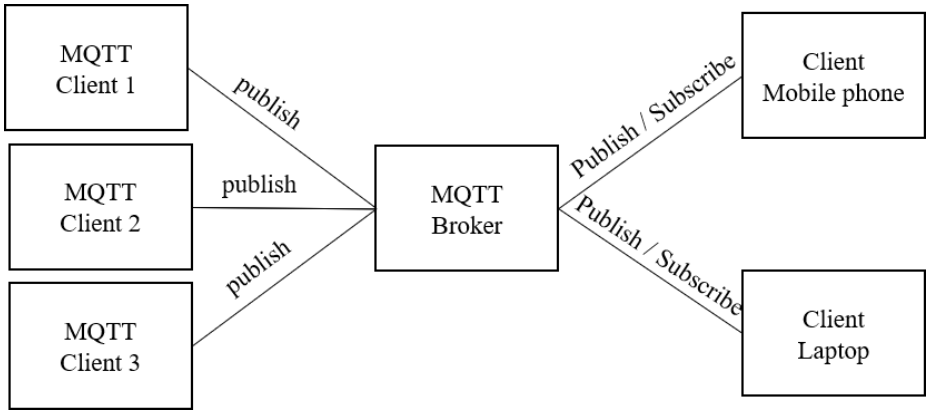

Figure 2.19: Scheme of MQTT [58]

2.4.6 Online Power Supply

The online power supply is the simplest way to run electronic devices. In an ideal case (reliable power network) the supply voltage is constant and can be adjusted by a converter. With a constant voltage of the power supply the sensor and other electronic parts such as Microcontrollers and/or Microprocessors can source as much energy as they require.

However, in many cases an online power supply is not available or cannot be accessed. Some systems also have to be designed to be independent of their location. For these cases alternative power sources have to be found.

2.4.7 Battery Powered

To be independent of online power supplies, electronic devices run on batteries. There is a great variety of different kinds of batteries. In the following, one type of battery is investigated to prove its suitability for this project.

Batteries have to be distinguished in three different types:

- Primary cells which are based on an irreversible electrochemical reaction. They are also known as nonrechargeable batteries.
- Secondary cells which are based on a reversible electrochemical reaction. They are also called rechargeable batteries.
- Fuel cells which are run continuously by for example hydrogen and oxygen. The reaction of the two reactants is irreversible which makes fuel cells nonrechargeable.[59]

The focus in this thesis is held on rechargeable batteries because they can be reused which makes them more cost efficient. To justify this assumption, the number of recharge cycles is investigated.

Lithium Ion Battery

To source power from Lithium Ion batteries, positively charged Lithium ions move from the Anode to the Cathode. To keep an equilibrium in the solution, negatively charged ions (anions) move through a wire from the Cathode to the Anode. This current can be used by sensors, actuators, etc. The anode is made of carbon material whereas the cathode is made of oxide material containing lithium. The whole process as well as the process of charging is shown in fig. 2.20. [60]

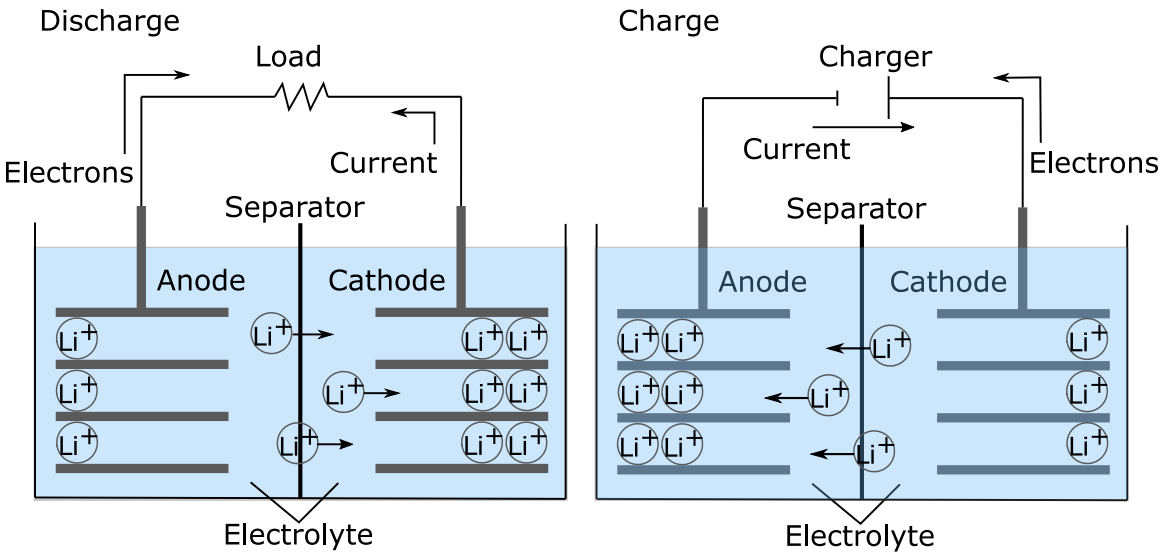

Figure 2.20: Charging and discharging of a Lithium Ion battery [60]

Another interesting aspect of a battery supply is its voltage level. This level needs to be hold constant to maintain a proper deployment of electronic devices. The voltage level is in general dependent on several factors:

- Discharge capacity
- Discharge current
- Temperature
- Life cycle

Discharge capacity The discharge capacity describes the amount of energy left in the battery. It can be expressed as a percentage or as the amount of discharged power in mAh. This is critical in particular as the discharge capacity changes very rapidly in every life cycle and so does the voltage level. Furthermore, this behavior is independent of the number of recharge cycles and can be seen at new as well as used batteries. This behavior is shown in fig. 2.21. The figure shows a high decrease at the beginning before this decrease is getting smaller until it hits an almost constant voltage level. Shortly before there is no power left in the battery, the voltage drops significantly. The observed battery is charged at a level of 4.2 V. Only if the battery is fully charged (0 % discharged power) can this voltage level be reached. Otherwise the voltage level is always below the charge voltage.

An explanation for this behavior can be found in the internal resistance of the battery. This resistance is increasing with increasing discharge of the battery due to polarization. Polarization describes the development of isolating interfaces between the electrode and the electrolyte [61]. The loss in voltage V_{loss} is the difference between the theoretical voltage $V_{theoretical}$ of the battery compared to the working voltage $V_{working}$, see eq. (2.26). [62]

$$V_{loss} = I * R_{Polarization} \tag{2.25}$$

$$V_{working} = V_{theoretical} - V_{loss} \tag{2.26}$$

Discharge current In fig. 2.21 one can also see the influence of the discharge current on the cell voltage. For this reason, discharge currents of $400\ mA$ to $4000\ mA$ are presented. The cell voltage drops with increasing discharge current. This can also be explained with eq. (2.25). With an increasing current I, V_{loss} is also increasing, which decreases the cell voltage.

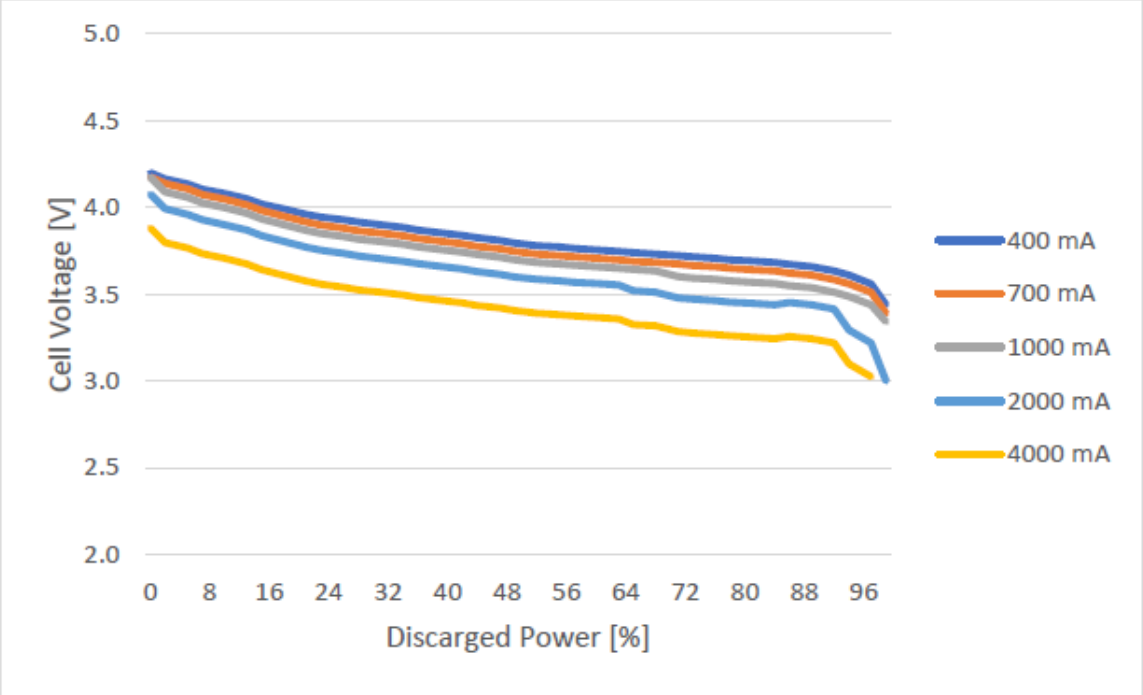

Figure 2.21: Discharge load characteristics of a Lithium Ion battery [60]

Temperature The cell voltage is furthermore strongly dependent on the temperature. A lower temperature reduces the cell voltage. The reduction of cell voltage can be up to $20\ \%$ for a drop of $70\ °K$ ($+\ 45\ °C$ to $-\ 25\ °C$). [60]

The reason for this behavior is based on the reduction in chemical activity as well as the increase of internal resistance at lower temperatures. But not only is the absolute value of the cell voltage decreased, the slope of the cell voltage over the discharged power is decreased as well. This slope is mainly influenced by the internal resistance, which is increased for lower temperatures. [62]

Life Cycle As seen in fig. 2.22, the available capacity of a battery decreases over time, especially over the number of charging and discharging cycles. This aging process can have several reasons:

- Formation of passivated surface layer

- Increasing anode impedance
- Degradation due to the loss of recyclable Lithium Ions
- Metallic Lithium plating on the anode

All these points contribute to an aging process of a battery [63]. They are not discussed in detail since the aging process is unavoidable and can be resolved by removing the battery as soon as its Discharge capacity hits a threshold of $80\ \%$.

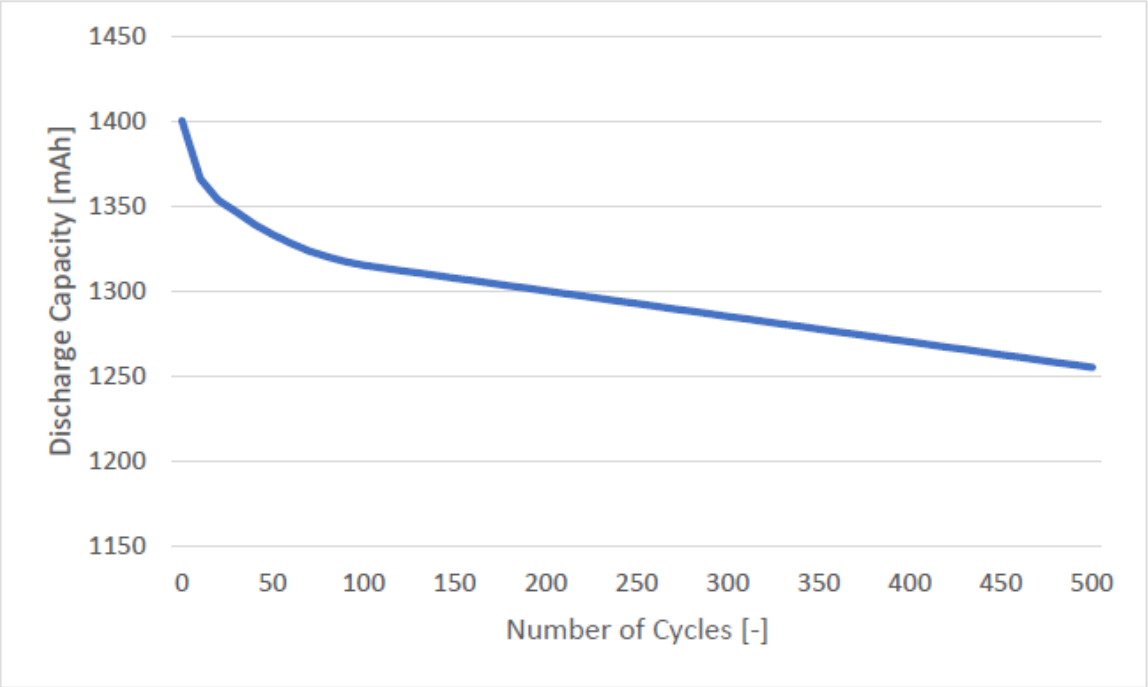

Figure 2.22: Life cycle characteristics of a Lithium Ion battery [60]

Beside these points, there are more influences on the battery performance, such as the duty cycle of the applied load on the battery. It can be either continuous or pulsed. The influence is not discussed in this report in detail.

Other Power Supplies

Besides a power supply by a power network and a battery supply, there are more possible ways to power an electronic device. They can be summarized as power harvesting from the environment of the device. There are different possible ways to harvest energy:

- Photovoltaic
- Motion and Vibration
- Temperature Difference
- Wireless Power Transmission [64]

They are often used in connection with batteries, as their power output is not constant and is dependent on their environment (day and night, summer or winter, ...). For specific interest in any of these, further literature can be found in [65].

Power Consumption

To give a complete picture of the power stream, not only the power supply but also the power consumption has to be investigated. In this chapter, the theoretical power consumption is discussed based on a model of a sensor in connection with a transmitting and receiving unit. To give a general idea about power consumption, fig. 2.23 shows the used power for several everyday life devices.

Figure 2.23: Power consumption of everyday life devices [65, 66, 67, 68]

To be able to have a closer look at the power consumption of a sensor and the respective data signal conditioning unit, the power consumption is separated in the fields of:

- Sensing of physical abilities
- Processing of sensor data
- Sending of data

Sensing of physical abilities is done by the sensor. The actual process of sensing, which is in our case a conversion into an electrical signal (analog or digital) is in most cases useless without a respective reading unit. For this reason, the sensing itself is the process of the converting a physical ability into an electrical signal and the reading process of this signal. The processing of the data is the computational part, where sensor data are interpreted, done by a processing unit (microcontroller).

To analyze the energy efficiency of a sensor and the respective reading unit, a definition has to be found of what is waste energy and what is useful. A possible way of categorizing is shown in table 2.4.

Table 2.4: Categorization of energy usage [69]

Useful energy consumption	Transmitting/receiving data Processing query requests Converting physical abilities to electrical signals
Wasteful energy consumption	Idle listening to the channel Retransmitting due to packet collisions Overhearing Generating/handling control packets

Sensing of data To determine the power used for sensing a duty cycle, "D" has to be defined. This duty cycle describes the fraction of time when the sensor is active.

$$D = \frac{t_{on}}{T} \tag{2.27}$$

In this case, T describes the period for one measurement with the sensor and t_{on} is the part of this period while the sensor is running. The period consists of the time while the sensor is running t_{on} and while it is not running t_{off}. In both conditions, they require a different amount of power, P_{on} and P_{off}.

$$T = t_{on} + t_{off}$$
$$P_{avg} = \frac{P_{on} * t_{on} + P_{off} * t_{off}}{T}$$

Since the $P_{on} >> P_{off}$, we get:

$$P_{avg} = \frac{P_{on} * t_{on}}{T} = P_{on} * D \tag{2.28}$$

To decrease the required power, either the power in the active mode can be decreased or the time of the sensor running in it can be decreased. Since the sensor needs to run for a specific amount of time to get acceptable data, in many cases only the power required while it is running can be diminished.

Processing of data The power consumption for processing the data can hardly be estimated since it is very much dependent on the processing unit and the program running on it. Nevertheless, by taking the number of clock cycles and the architecture of the processing unit into account, Wang [70] proposes a theoretical model to calculate the power consumption, see eq. (2.29).

$$P_{total} = P_{comp} + P_{leak} = N * C * V_{dd}^2 + V_{dd} * \left(I_0 * e^{\frac{V_{dd}}{nV_T}}\right)\left(\frac{N}{f}\right) \tag{2.29}$$

Table 2.5: Parameters of power consumption in data processing [70]

Parameter	Definition
P_{total}	Total Power consumption
P_{comp}	Active Power dissipation
P_{leak}	Power loss
N	Number of clock cycles
C	Average Capacitance switched per cycle
V_dd	Supply Voltage
V_T	Thermal Voltage
n	Constant, depending on architecture
I_0	Leakage Current
f	Maximum performance / Switching frequency

This model is developed based on the StrongARM SA-1100, an Intel Microprocessor.

Based on this model, several measures can be taken to reduce the power consumption. By varying the processor speed (VPS), the clock frequency can be decreased which leads to a smaller required supply voltage [71]. By this, a smaller power consumption can be achieved. Another measure is the Dynamic Power Management (DPM) where components of the computing device can be switched off dynamically if not needed [72].

Sending of data The Wireless Communication is the most power consuming part of a sensor network [73]. For this reason, a decreased power consumption of the communication of the sensor network has a high influence on the overall network. For this reason, Shih

[74] proposes the model in eq. (2.30)

$$P_{radio} = N_{tx}\Big[P_{tx}\big(T_{on-tx} + T_{st}\big) + P_{out}T_{on-tx}\Big] + N_{rx}\Big[P_{rx}\big(T_{on-rx} + T_{st}\big)\Big] \tag{2.30}$$

Since the receiving part is in most cases fixed and has an online power supply, only the sending part needs to be investigated. By this restriction, eq. (2.30) simplifies to:

$$P_{radio} = N_{tx}\Big[P_{tx}\big(T_{on-tx} + T_{st}\big) + P_{out}T_{on-tx}\Big] \tag{2.31}$$

All the Parameters used are explained in table 2.6.

Table 2.6: Parameters of power consumption in data communication [74]

Parameter	Definition
N_{tx} / N_{rx}	Number of times transmitter/ receiver is used
P_{tx} / P_{rx}	Power consumption of transmitter/ receiver
T_{on-tx} / T_{on-rx}	Transmit/ Receive on-time
T_{st}	Startup time Transmitter
P_{out}	Output Transmitter power

Since the Power consumption of the transmitter can hardly be influenced while sending data, the time while the transmitter is running can be decreased. This can be done by compressed data (change of data type). Furthermore, the amount of transmitted data can be reduced to lower the power consumption. As a third point, the startup power time can be reduced. This can be done by a better availability of the signal of the receiver.

For eq. (2.30) and eq. (2.31), the assumption has been made that the transmitting unit is only running when there is data for transmission. In every other case it is not running.

CHAPTER 3

RESULTS

In the following section, the results of the thesis are presented. The order of the presented results represents the order of the separate tasks which leads to the overall result. At the beginning, the sensors are tested on their abilities. From these tests, a representative signal is derived which is applied on several developed filters. Based on the results an optimal filter is developed.

3.1 Sensor Testing

First, the characteristics of the used Ultrasonic sensor as well as the pH sensors are examined. This step is important to know the influence of the sensor on the signal, which also defines the requirements to calculate a reliable slope of the examined parameter. Furthermore, this testing leads to an example signal in section 3.2.

3.1.1 HC-SR04 Ultrasonic Sensor

To evaluate the Ultrasonic (US) sensor, two sets of tests are required. The first one is a laboratory test where the sensor output under optimal conditions is tested. This is done with a specified distance and target which the sensor has to identify. The second test runs on the coolant level itself. The unfiltered output of the sensor is evaluated and used as input for the creation of an example signal.

Laboratory tests Ultrasonic Sensor

While testing the US sensor, certain abilities of the sensor have to be evaluated. At first, the accuracy and precision are examined. Afterwards a test on hysteresis is executed.
For all these experiments, the set-up can be seen in fig. 3.1. The US sensor is mounted in a case to maintain a constant height as well as direction. A measuring tape is used to adjust a given length which is measured by the sensor. The target is a hollow aluminum block. The sonic reflecting abilities of aluminum as compared to other materials is relatively good.

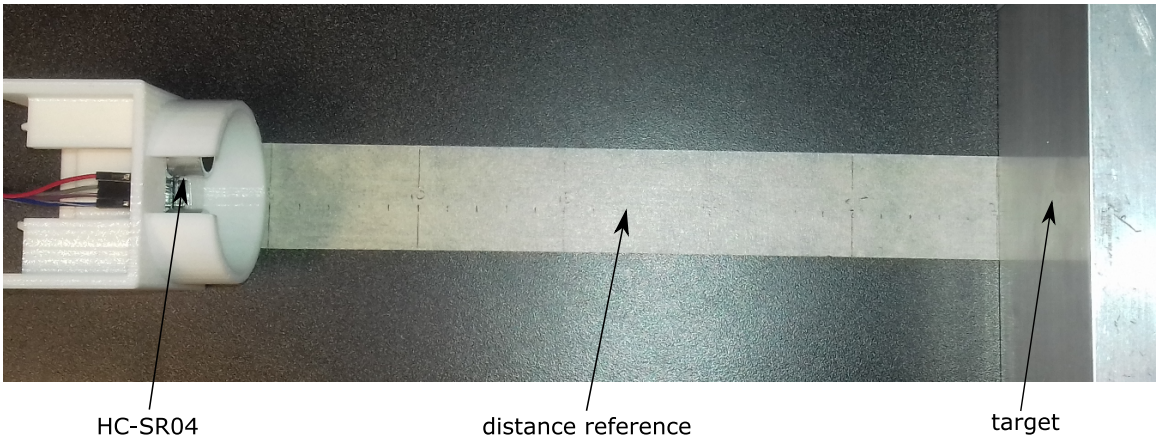

Figure 3.1: HC-SR04 sensor laboratory testing

Accuracy The accuracy of the sensor is measured by incrementally increasing the distance from the sensor to the target. The readings of the sensor are plotted in fig. 3.2. Every $10\ mm$ 300 readings are taken and averaged. This is done 4 times (test run 1 - 4).
The grey line represents a reference line with a fictional perfect measurement. One can see that all 4 test runs are very similar when compared to each other. This shows a good repeatability of the readings. However, the accuracy is in the range of $50\ mm$ to $250\ mm$, which is not as good as expected. The linearity of the signal in this region is not totally fulfilled. Above a distance of $250\ mm$, however, the signal is very much linear. Beside this linearity one can see a deviation of the signal and the actual length. This deviation is

identical for all four test runs.

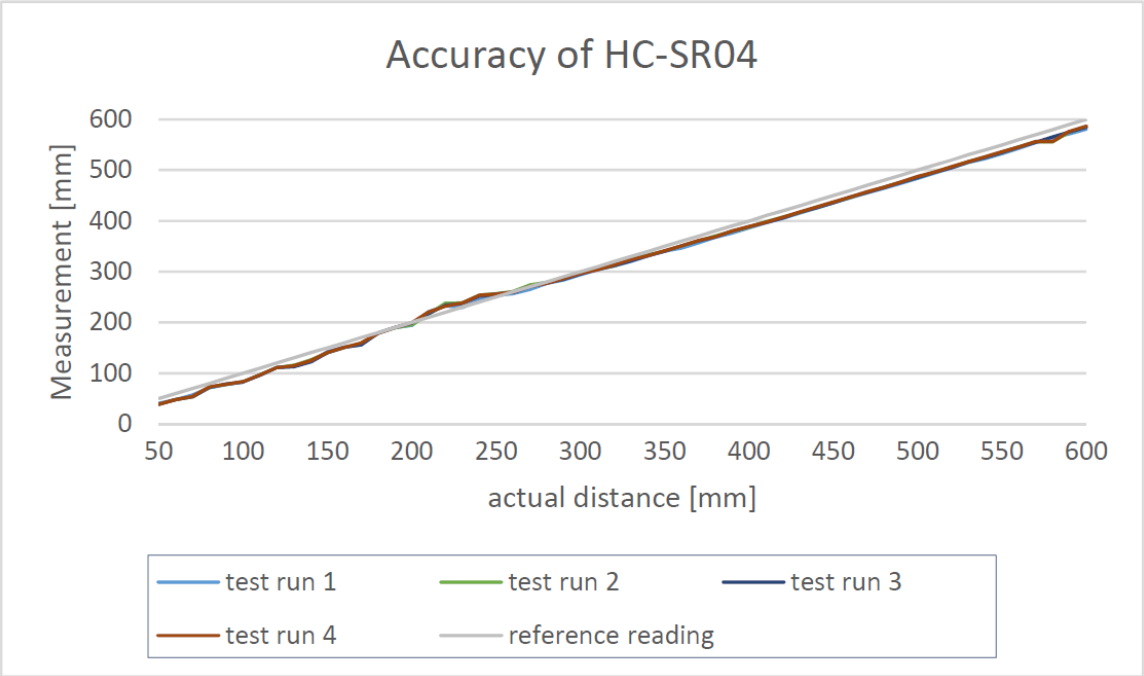

Figure 3.2: HC-SR04 accuracy test laboratory

For further examination, the absolute error of the signal is shown in fig. 3.3. The strong repeatability of the signal can be seen again among the different test series. Test runs two to four overlay, while test run 1 follows the trend but is not directly overlaying. One can see the increasing deviation with greater reference distances. This may be due to a systematic error. The distance is calculated by the time the sonic waves are traveling. This time is mostly dependent on the temperature. A small deviation in temperature can lead to a mistake in the calculated distance. This mistake gets greater with an increasing reference distance. The influence of a 1 K deviation of temperature at a reference distance

of $500\ mm$ can be seen in eq. (3.1).

$$\begin{aligned}
&\text{speed of sound at } 21\ ^{\circ}C : u_{21\,^{\circ}C} = 344.0\ \frac{m}{s} \\
&\text{speed of sound at } 22\ ^{\circ}C : u_{22\,^{\circ}C} = 344.6\ \frac{m}{s} \\
&\text{distance } \Delta l\ =\ 2\ *\ 500\ mm\ *\ \frac{\Delta u}{u_{21\,^{\circ}C}}\ =\ 1000\ mm\ *\ \frac{600\ \frac{mm}{s}}{344000 \frac{mm}{s}}\ =\ 1.744\ mm
\end{aligned} \tag{3.1}$$

This error is small compared to the error one sees in fig. 3.3 with a value of $13\ mm$ for a distance of $500\ mm$. By this we can see that there may be an accumulation of errors influencing the absolute error. The temperature measurements for the test runs have an accuracy of $1\ ^{\circ}C$ which is the assumption for eq. (3.1). All in all, the signal of the HC-SR04 has an error of $0.45\ \%$ based on the maximum range of $4000\ mm$, which is strongly dependent on the distance at which the measurement is taken. This error has to be considered when evaluating the output of the sensor.

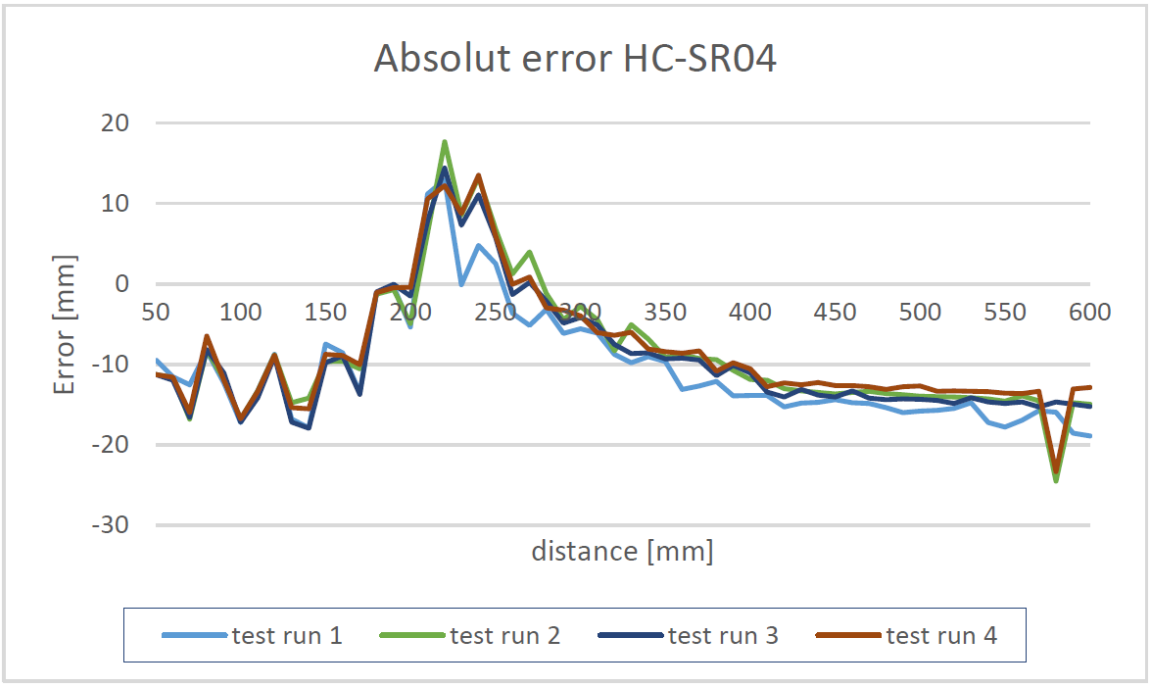

Figure 3.3: HC-SR04 absolute error

Hysteresis Another common error is the Hysteresis error. It is defined as the difference of a signal at the same measurement point for an increasing value compared to a decreasing value. A typical Hysteresis error is shown in fig. 3.4.

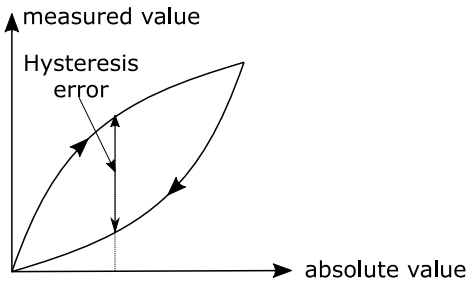

Figure 3.4: Example for a Hysteresis error

To measure the Hysteresis error, the measured value is increased until its maximum and afterwards decreased again till it reaches its initial value.

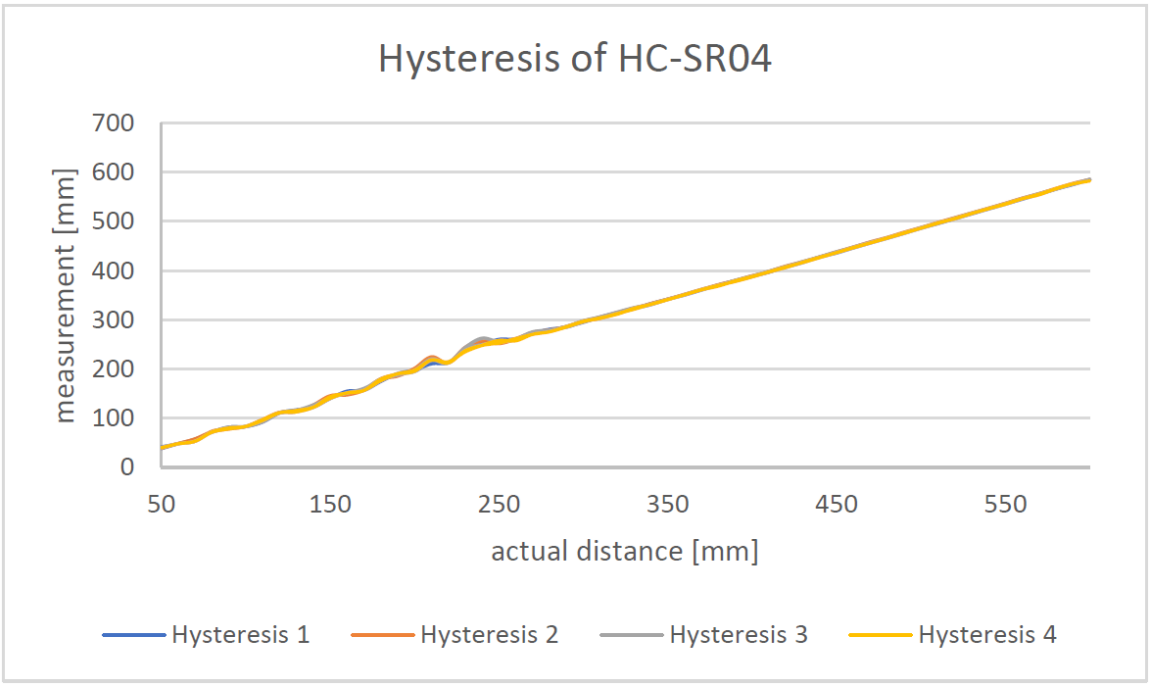

Figure 3.5: Hysteresis error HC-SR04

In fig. 3.5 the actual measurement is shown. One can see the inaccuracy of the readings in the range of 230 mm to 250 mm, which is also shown in fig. 3.3. A significant Hysteresis

error cannot be seen in these tests.

All in all, the HC-SR04 sensor shows a high repeatability, as seen in the several tests performed. The accuracy within the range of $50\ mm$ to $600\ mm$ is at $0.45\ \%$ of the maximum range $(4000\ mm)$. A Hysteresis error cannot be observed.

3.1.2 pH Sensor

A pH sensor (potential of hydrogen) is used to determine the level of acidity in a solution, see section 2.4.3. In the following, two different pH sensors are compared. An industrial solution (Industrial pH probe by AtlasScientific; $\$209$) as well as a low cost pH sensor by Gravity ($\$57$). By this comparison the need for high-end products should be identified. Furthermore, the results of both tests are used to create the example signal which is the input to design the filters.

Industrial pH Probe

To test the pH sensor, only a limited amount of test solutions is available. They have to be at a specific pH level to be able to test the sensor. Solutions with a pH value of 4, 7 and 10 are used for testing. The result of this test is shown in fig. 3.6. Every second, one measurement is taken. The testing solutions in the shown figure are changed after a different amount of measurements to make it more visible. All three test series behave similarly for a change of pH value. The time required to get to the new pH level is for all three tests around 12 to 15 seconds. Compared to the Ultrasonic sensor, this is a very slow response. Compared to the state estimation filter (see table 3.4) the rise time for a step of pH 3 is very fast.

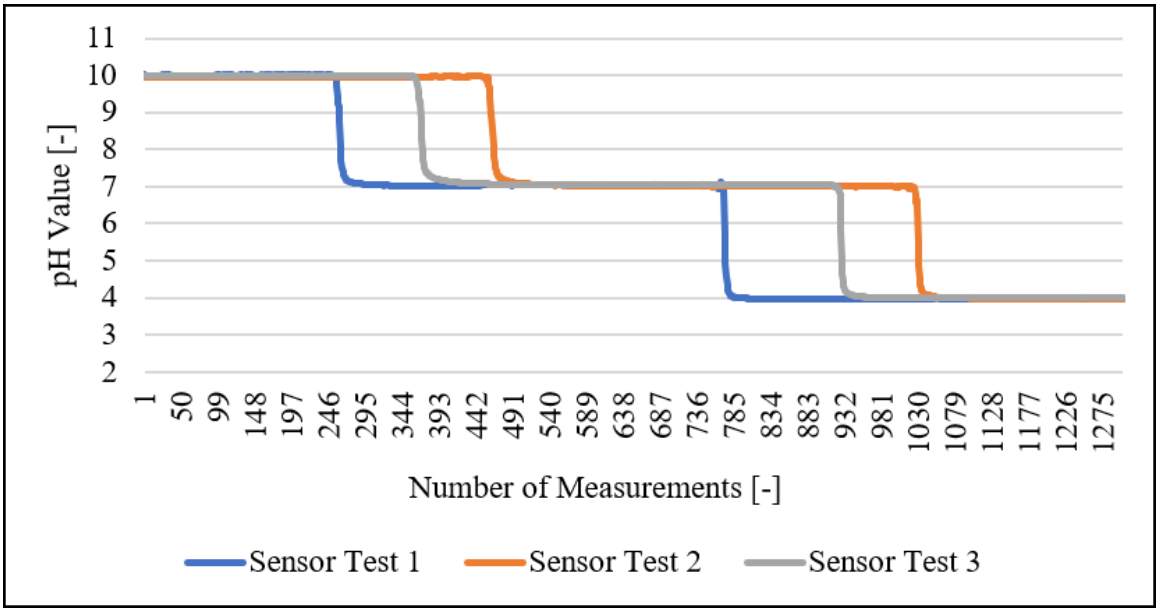

Figure 3.6: Sensor testing of industrial pH probe

Another point of interest is the Hysteresis of the sensor. Tests on this can be seen in fig. 3.7 and fig. 3.8. For both tests, a Hysteresis cannot be seen.

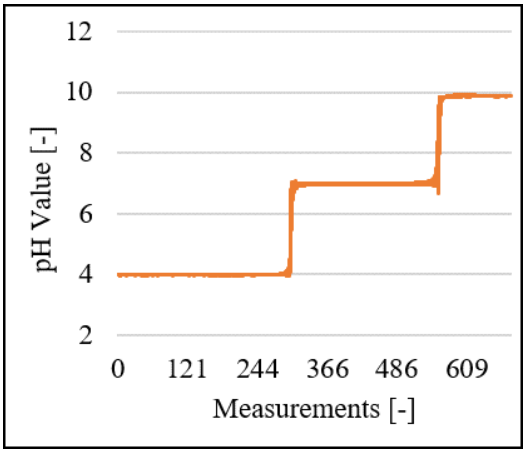

Figure 3.7: Hysteresis of industrial pH sensor 1

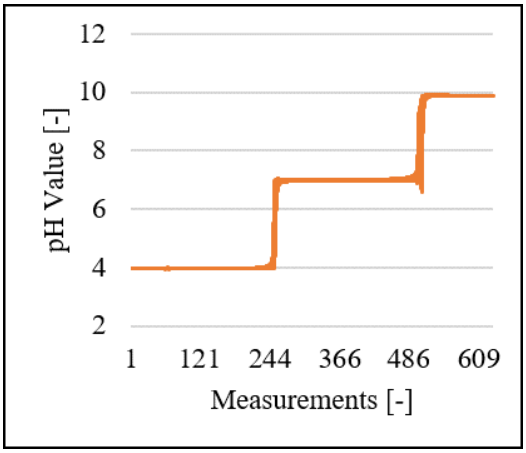

Figure 3.8: Hysteresis of industrial pH sensor 1

Low Cost pH Meter

The low cost pH meter compared to the industrial one shows a very similar performance. The SNR for both pH Meters is varying between $40\ dB$ and $50\ dB$. The industrial pH meter

has higher values for some test runs but cannot maintain these values (SNR of 69 dB) for all tests.

The final pH level of the low cost version is changing over time. Furthermore, the offset due to calibration for the low cost version is worse compared to the industrial pH meter. This is due to the automatic calibration of the industrial one versus a manual calibration of the low cost one.

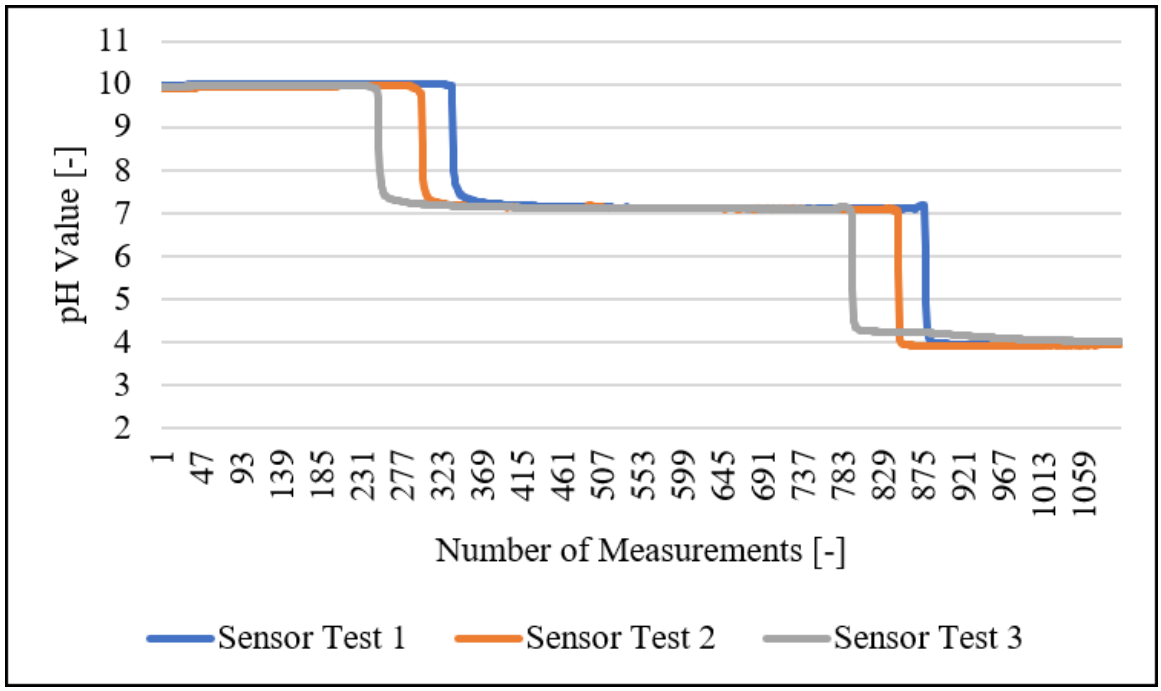

Figure 3.9: Sensor testing of low cost pH probe

None of the pH meters shows a Hysteresis, as seen in fig. 3.10 and fig. 3.10. For this reason, both sensors have a very similar behavior. The industrial one performs better concerning long term trends, which is a very obvious advantage for the slope estimation. For this reason, the industrial pH meter is chosen.

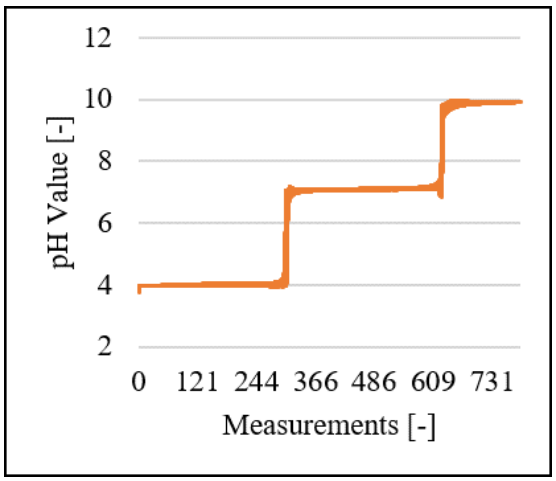

Figure 3.10: Hysteresis low cost pH sensor 1

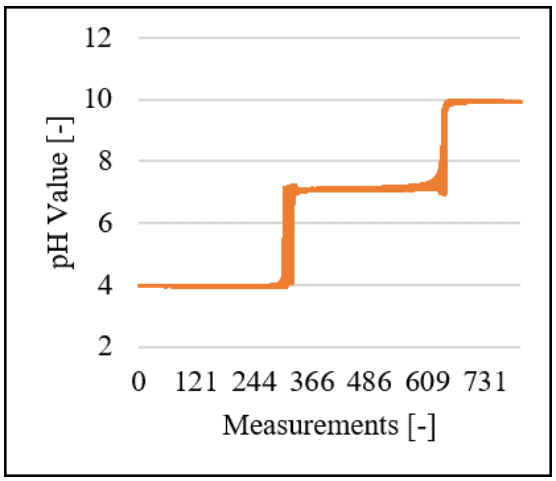

Figure 3.11: Hysteresis low cost pH sensor 2

3.2 Example Signal

To compare the performance of the different slope calculation modules a standard example signal is developed in the following section. This example signal includes the following characteristics:

- High frequency noise
- Low frequency noise
- Long term trends
- Wrong readings

The example signal is based on the measurements taken of the different pH meters as well as the height sensor HC-SR04 (see section 3.1). Based on these measurements, a set of artificial measurements is developed to evaluate the quality of the algorithms.

3.2.1 High Frequency Noise

High Frequency noise can be induced into the signal due to different mechanisms while transmitting or also while collecting the data. To evaluate the importance of the high frequency noise in our example, the pH measurement is further investigated. This choice is made due to the analog measurement of the pH value compared to the US sensor, see section 2.4.3.

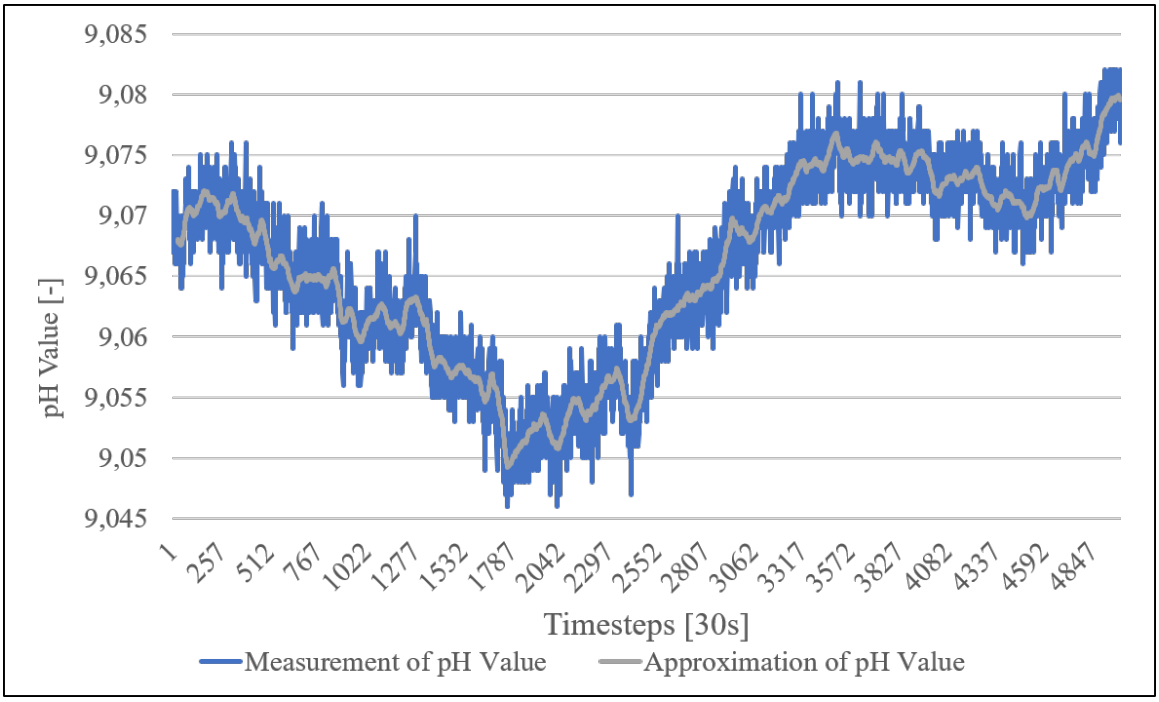

Figure 3.12: Signal of the pH meter corrupted by High Frequency noise

In fig. 3.12 a possible pH measurement is presented. Furthermore, the approximated real value of the pH value is shown. This approximation is done by a moving average over a large enough number of values (see section 2.2.1). By comparison of these both values, the noise can be identified.

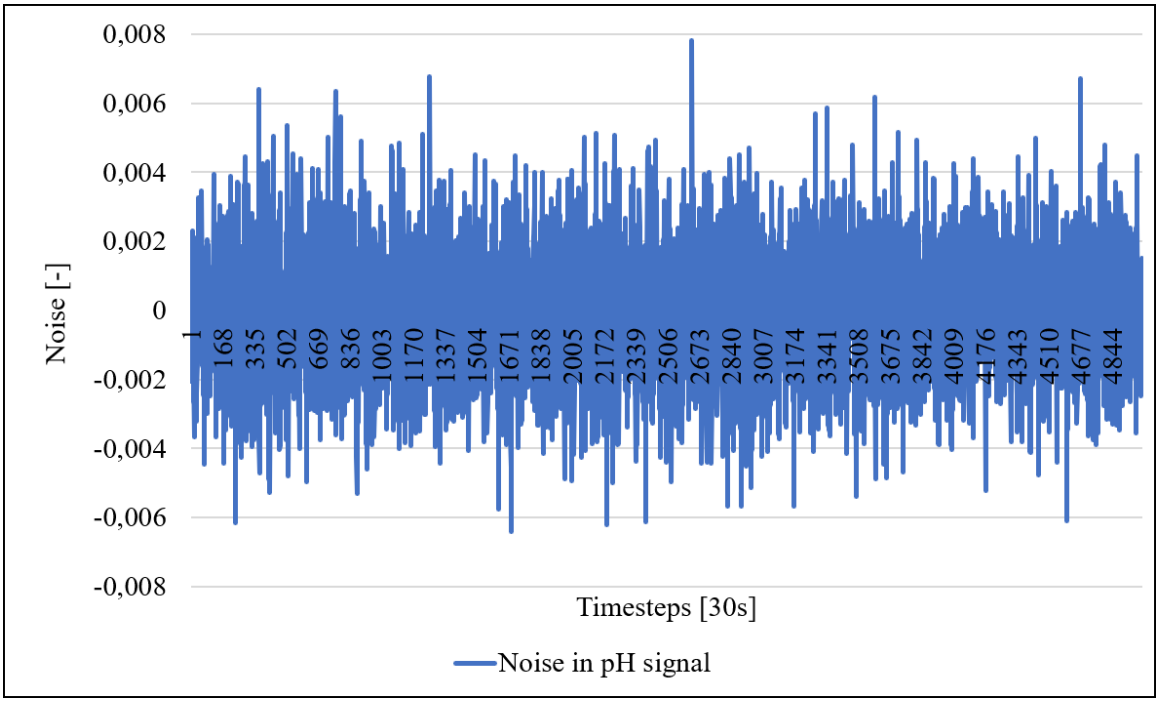

Figure 3.13: Separated noise on signal from pH measurement

A plot of the separated noise can be found in fig. 3.13. This separated noise can be presented as a Histogram where the different amplitudes are classified. With this classification, the noise can be tested to determine whether it is Gaussian noise. The plot of the Histogram is shown in fig. 3.14. In this plot, the Gaussian distribution shows that the signal noise is Gaussian. The zero value is represented by the red line in the plot. To further show that the noise is white Gaussian noise, a Fast Fourier Transformation had to be done. Since this is not necessary for a lot of filtering algorithms, this step is not done here.

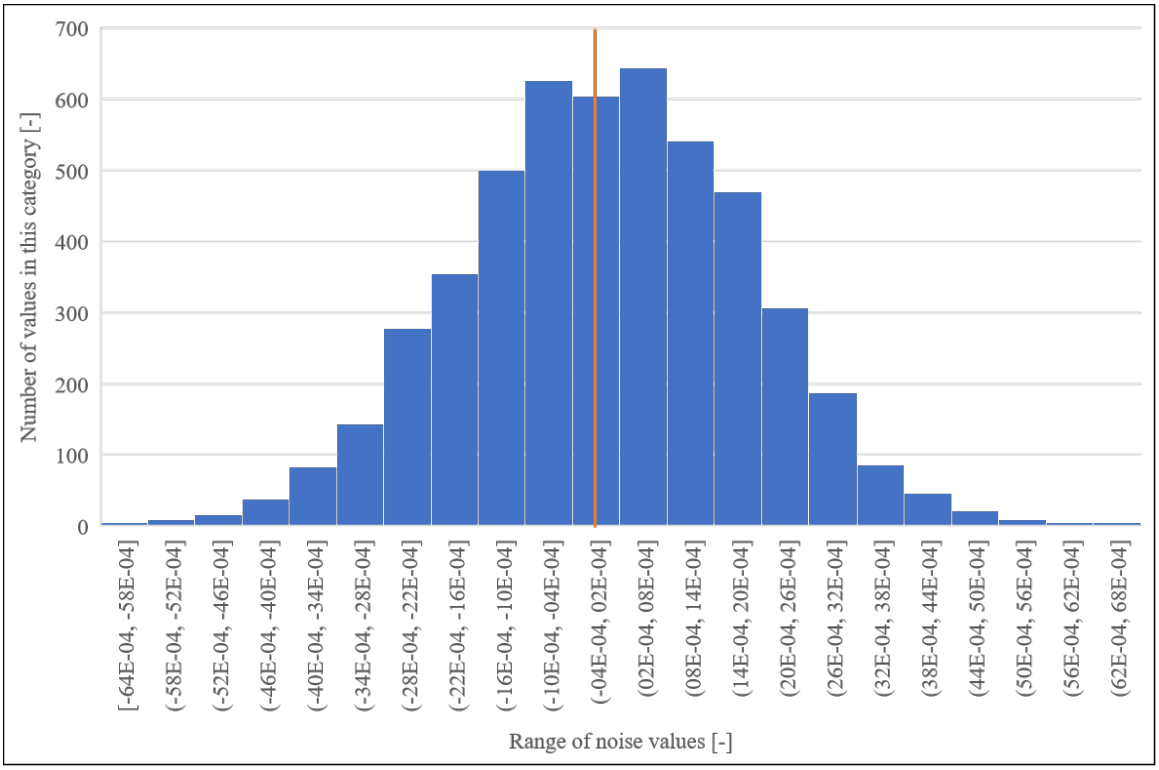

Figure 3.14: Histogram of the amplitudes of the noise in the pH signal

To conclude the influence of high frequency noise on the example signal, the Gaussian distribution can be assumed. The degree of the noise (see Signal-to-Noise Ratio (SNR) section 2.1.5) differs. In this plot the SNR can be calculated as followed:

$$SNR_V = \frac{\text{RMS Signal Voltage}}{\text{RMS Noise Voltage}} = \frac{2.59}{0.000517} = 5009.6$$

$$SNR_{dB} = 20 \log_{10} 5009.6 \approx 74$$

A SNR of 74 can be seen as a very good signal, since the critical limit is at $15\ dB$. To show the influence of different SNRs, 3 different variations are applied as shown in table 3.1.

Table 3.1: Set of noise for example signal

Set	Degree of noise
# 1	High noise; $SNR_{dB} = 15$
# 2	Medium noise; $SNR_{dB} = 32$
# 3	Low noise; $SNR_{dB} = 74$

3.2.2 Low Frequency Noise

Beside the high Frequency noise, there is also a low frequency pattern or low frequency noise added on the signal. This pattern can be seen in fig. 3.15. It has a period of approximately 8200 s, which can be assumed as one day. A decision on how to handle this noise compared to the high frequency noise is hard since the reason for this behavior is unclear. It can be either due to measurement errors or it is the true pH value of the fluid, which changes during a day. This assumption has to be proven. Furthermore, the periodic behavior stops for a certain amount of time (approximately 2 days) before it restarts.

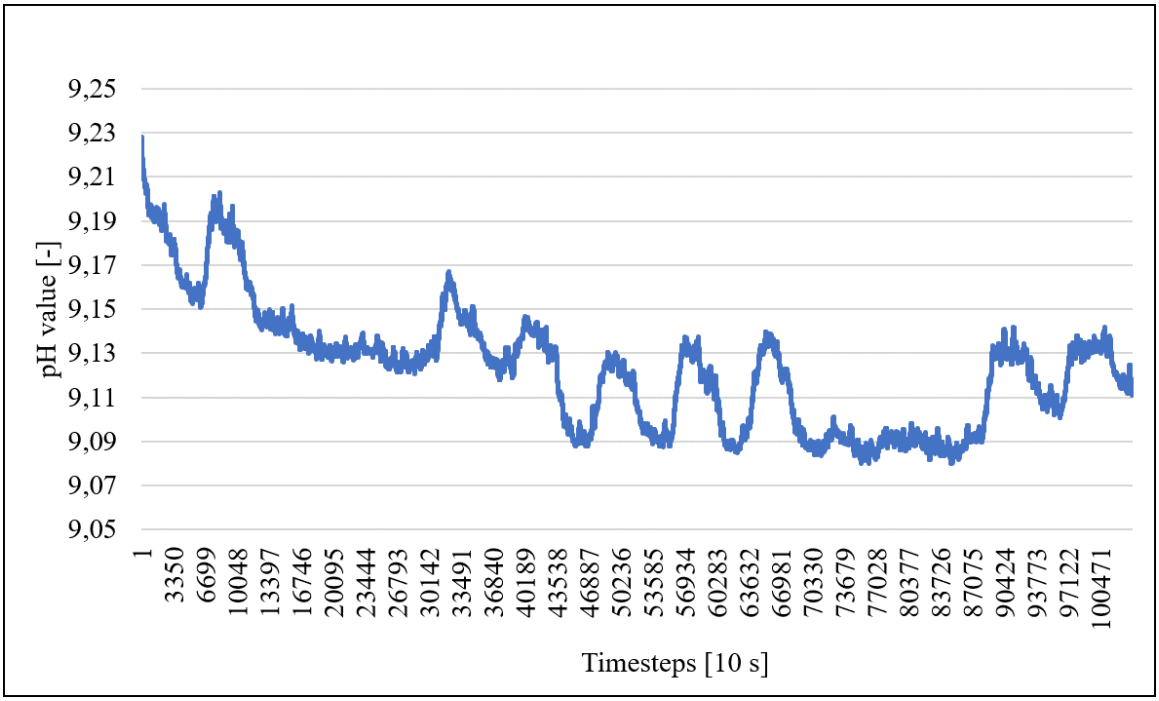

Figure 3.15: Low Frequency periodic pattern in pH measurement over a time period of 2 weeks

The shown behavior can be interpreted as the cycle of a week (5 working days, 2 days of weekend). Although the probe is not directly exposed to any environmental influences (sun, weather, heat, ...), the air conditioning is running only on working days. Due to this, the temperature is slightly increased on weekends and at night. A varying temperature can either change the pH value of the probe or influence the measurement. Since the pH value is connected to the amount of bacteria in the cutting fluid (see section 2.3), the increase of temperature could be a reason for the change of the pH value.

The second possibility, namely the influence of the temperature on the measurement method can be explained as follows:

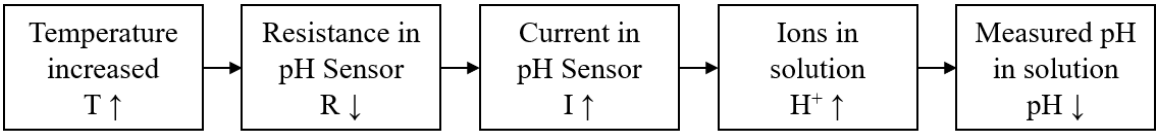

Figure 3.16: Chain of causation for influence of temperature on pH measurement

To decide about the main influence another test is performed. The same measurement is done with water instead of cutting fluid. The pH value of water should be independent of the temperature. The result shows the same pattern in the measurement. Due to this behavior, the low frequency noise is based on measurement errors induced by environmental changes (probably temperature) and not by a change of the pH value in the fluid itself.

This is only one example of how the environment of the measurement probe can influence the measurement itself. The possibilities can either be man-made (machines, habits of running the measurement, ...) or natural (sunlight, temperature, humidity, ...). The influences are hard to determine since the reason is mostly hidden. To still take it into account, the example signal has low frequency noise added onto it. This low frequency noise has to be filtered. The frequency of this noise is on the order of 1 period per day (as seen in the example).

3.2.3 Long term Trends

The goal of the slope estimation module is to determine the long term trend of a signal. Such a trend could be due to a leak in the cutting fluid tank or a constantly decreasing pH value because of bacteria growth. Since both of them are hard to capture (a leak is in general very rare and bacteria do not grow fast enough if coolant is used regularly), the parameters of a trend have to be designed. To give a realistic idea of these trends, an estimation has to be done.

Estimation of change of Cutting Fluid Level

There are two main reasons for the cutting fluid level to decrease:

- normal usage: evaporation and consumption
- leaks in tank and cutting fluid pipes

There are a lot of influences on the normal consumption of cutting fluids, such as evaporation, macro leaks (internally/ externally) and so forth. For this reason, an estimation is hard to make. There are several studies who evaluate the overall usage of coolant [75]. Nevertheless, an estimation of how fast cutting fluid is consumed in the machining process itself is very rare. For this reason, the evaporation of water is assumed. Since a lot of cutting fluids mostly consist of water and the tanks are not sealed, this assumption is a first step to create an example signal. To take consumption into account, one can assume every machined part taking a specific amount of cutting fluid out of the machine.

$$\text{Decrease in Volume} = \text{Evaporation} + \text{Consumption} \tag{3.2}$$

Since the amount of evaporation is relatively small, it can be neglected [76]. The amount of consumption can be estimated by the fluid taken out of the machine by sticking to the

machined parts. Depending on part size and complexity, an average of $1\ ml$ per part is assumed. With a process time of 2 minutes and a 2 shift working day, an amount of $0.48\ l$ is consumed. Based on the size of an average cutting fluid tank ($200\ l$ and $1\ m^2$ surface), a decrease of $0.48\ mm$ per day can be seen.

Compared to this, a leak causes a faster decrease in height level. Based on a leak of a diameter of $3\ mm$ at the bottom of the cutting fluid tank, a decrease in level of $12.09\ mm$ per day can be seen. Although leaks can have different diameters and locations, this value is used to create the example signal.

All in all, a decrease of $0.24\ \%$ or alternatively $6\ \%$ over a day can be seen.

Estimation of change of pH Level

There are very few literature sources available about change rates of the pH value in the case of an intense bacteria growth. Several sources propose to set it into relation with the change rate without increased bacteria growth [77, 46]. For this reason, the relative values from the previous section are used (section 3.2.3). Furthermore, a special focus is put on the detection of the transition from a constant behavior to a decrease or increase.

3.2.4 False Measurements

During several test runs for both sensors (pH sensor as well as height sensor) an amount of obviously false measurements could be detected. This is shown in fig. 3.18 where cutting fluid has been tested on its pH value in a separate container without any alien influences. Since these false measurements can be also seen in the height measurements, the slope estimation module has to be able to handle these influences. For this reason, the example signal has to have a number of obviously wrong measurements.

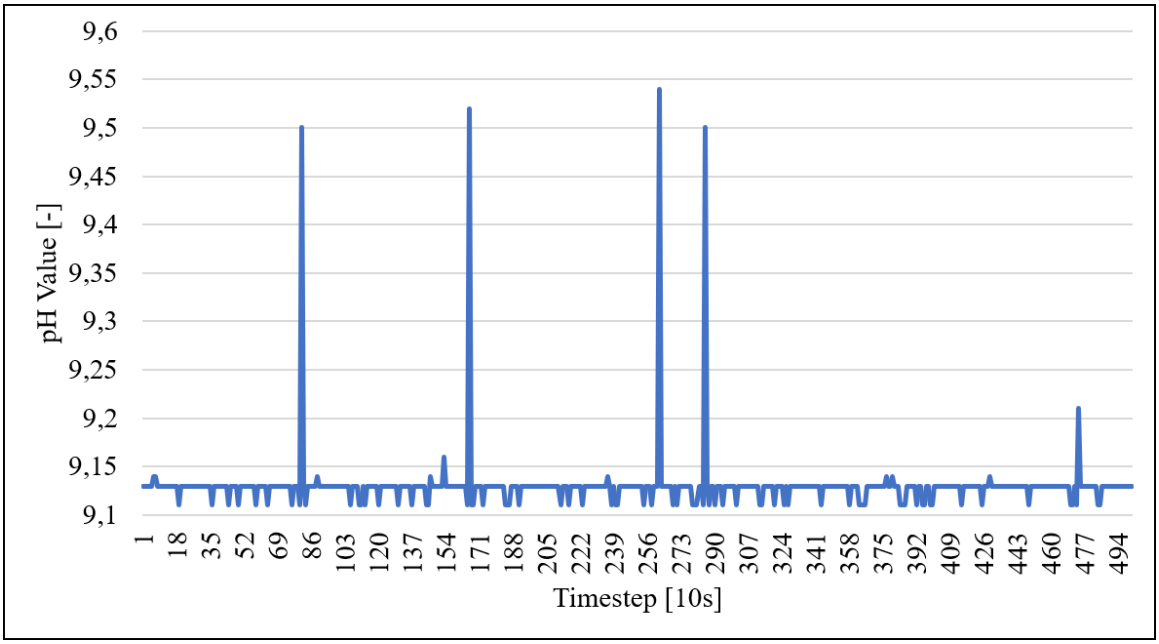

Figure 3.17: Wrong reading by pH meter in test fluid

A quantitative description is extremely hard to make, since a wrong reading could be above or below the average. Also, the actual value of such a reading cannot be described. For this reason, the standard deviation is used to describe failure in the measurement process, see table 3.2.

Table 3.2: Quantization of false measurement readings

Description	Quantization
Above or below	stochastically distributed
Standard deviation	in the range of 2σ to 20σ
Quantity of false measurements	irregular, average of 1 false measurement per 5000 readings

3.2.5 Interruption in sending Data

Since a wireless transmission is used to send up data to a cloud based storage hub, the reliability of the transmission is very much dependent on the strength of the Wi-Fi signal. In this case, the signal transmission is interrupted at several times, which prevented the storage hub of receiving data. To show the influence of these interruptions, fig. 3.18 plots the

interrupt times in between each measurement. It is significant that there are interruptions of one day or more.

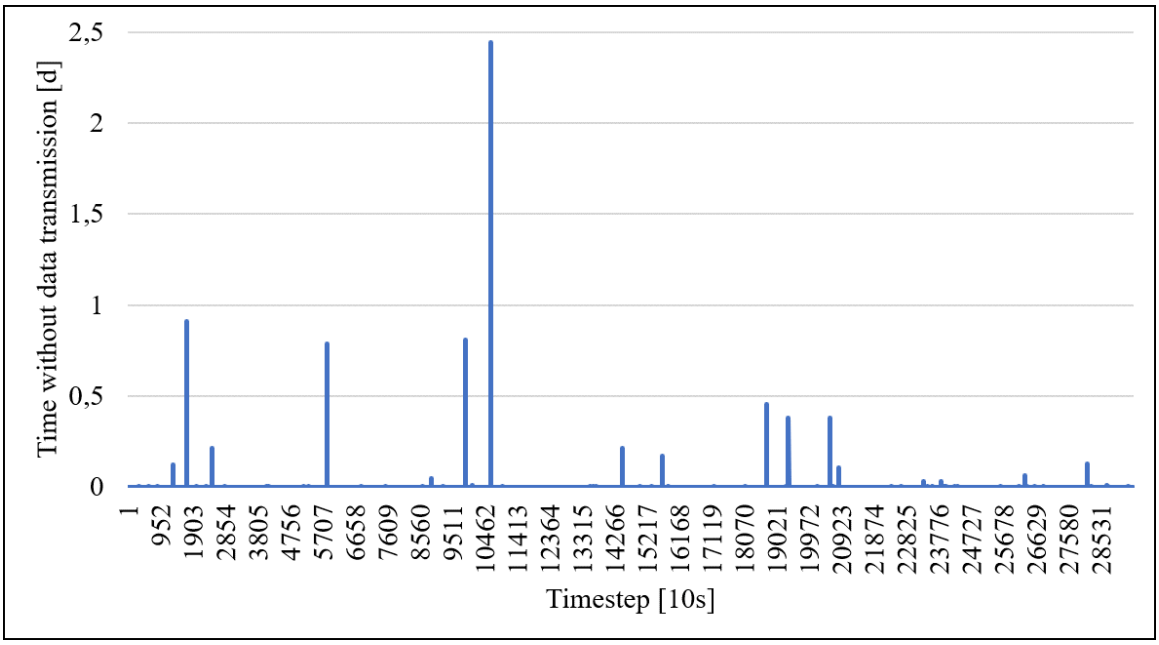

Figure 3.18: Interruption of sending data in wireless network

These interruptions can be due to a weak signal or connectivity problems in the network itself. Both problems can be solved by either proper maintenance of the network or better coverage of the Wi-Fi signal. Nevertheless, interruptions of the signal transmission have to be considered when creating the example signal. This can be done by including a jump into the signal which represents the missed values and transmission from one level to another. An example of the pH sensor values with an interruption can be seen in fig. 3.19. The shown jump in pH value is due to an interruption of 9 hours.

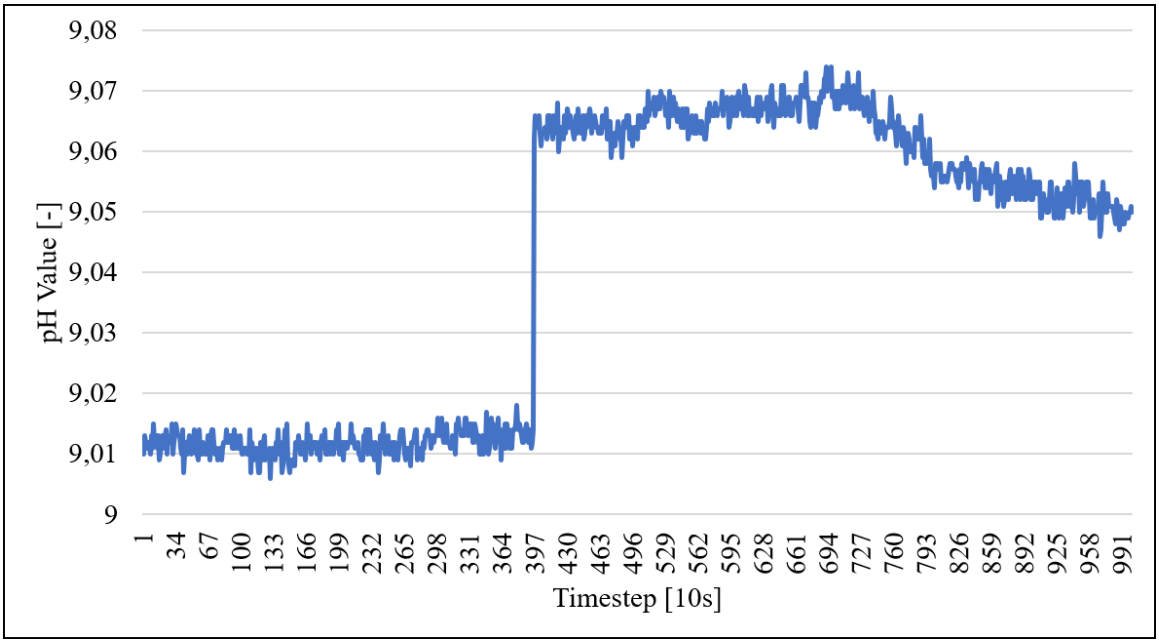

Figure 3.19: Jump in data due to interruption of sending data

3.2.6 Composition of Example Signal

The artificial example signal can be summarized by the aspects discussed in the previous chapters. The sampling rate for the example signal is of minor importance since the signal itself is continuous. Nevertheless, a created signal can only be a discrete one with a high number of data points. The only factor which has to be taken into account when addressing the sampling rate is an interruption in sending data, since this interruption has to be modeled in the example signal according to its sampling rate.

The timeframe of the example signal is modeled as a signal over one week, this can be seen by the low frequency noise, which is especially visible for high SNR ratios. Two configurations are shown in fig. 3.20 and fig. 3.21. For both configurations, a very high SNR (74) is used. One time with a slowly decreasing signal (fig. 3.20), the other time with a quickly decreasing signal (fig. 3.21). Further example signals can be looked up in the Appendix section B.1.

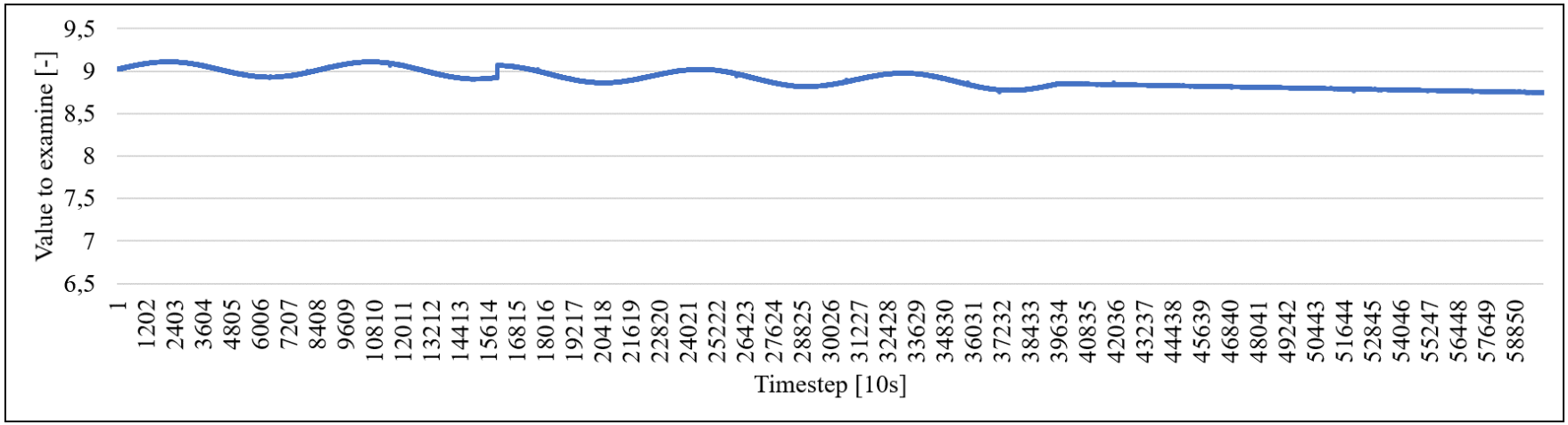

Figure 3.20: Example signal 1: SNR 74; 0.24% decrease per day

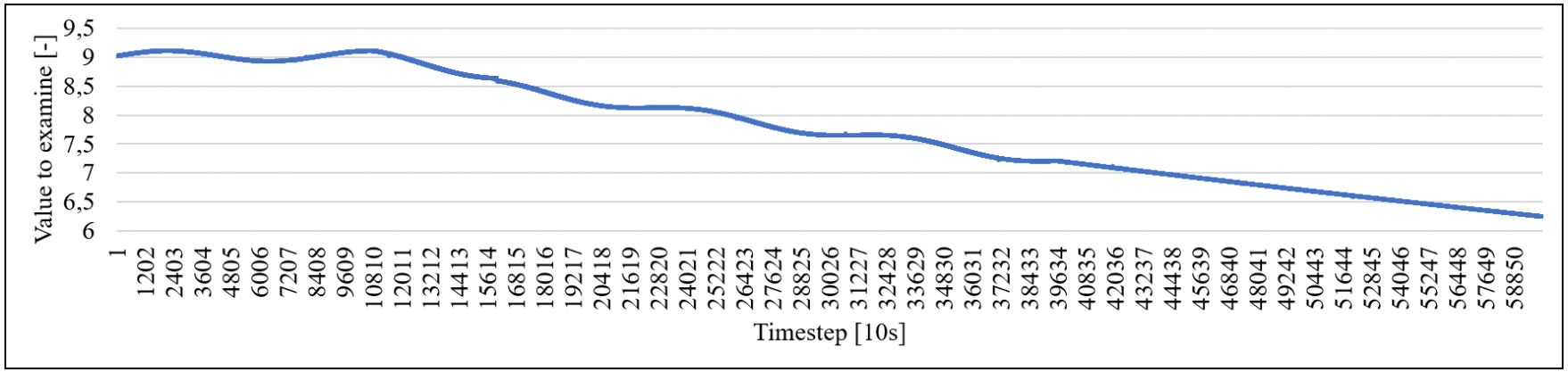

Figure 3.21: Example signal 2: SNR 74; 6% decrease per day

3.3 Application of Filter Algorithms

In the following chapter, the application of the previously presented filters is discussed. Several elements can be found repeatedly in the different chapters, as the optimal filtering algorithm has to be chosen and combined with a slope calculation module to achieve the optimum result.

In this first step, the main focus is put on filtering and not on the slope estimation. Based on an optimal state estimation filter, the slope estimation is done in the next subchapter.

3.3.1 Standard Deviation as preliminary Filter

As discussed, the standard deviation is not a filter by its nature. Nevertheless, with its ability to describe distributions, it is very powerful when it comes to probabilities. If one assumes a range of $\mu \pm 3 * \sigma$, which represents 99.7% of all samples included in a distribution, most values which are out of this range can be assumed to be not a part of the normal distribution. This ability helps to detect wrong measurements, see section 3.2.4. For this reason, there is a standard deviation filter implemented ahead of another filter. The result of this standard deviation filter can be seen by the comparison of fig. 3.22 and fig. 3.23.

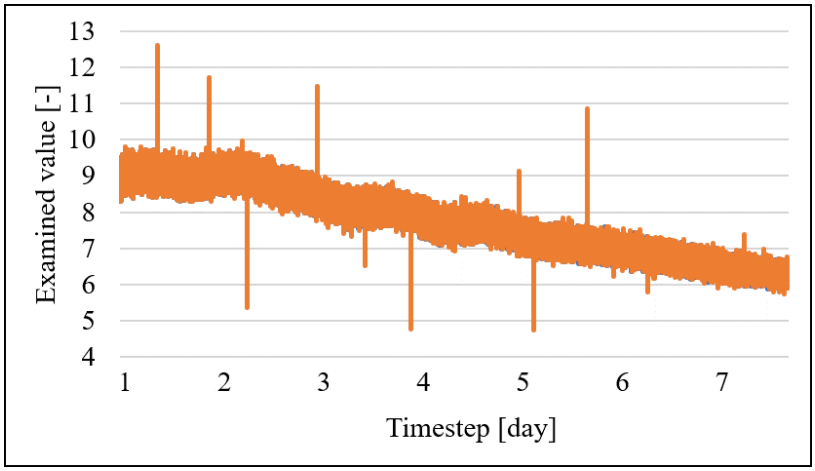

Figure 3.22: Unfiltered example signal; SNR of 32; decrease of 6 % per day from beginning of second day

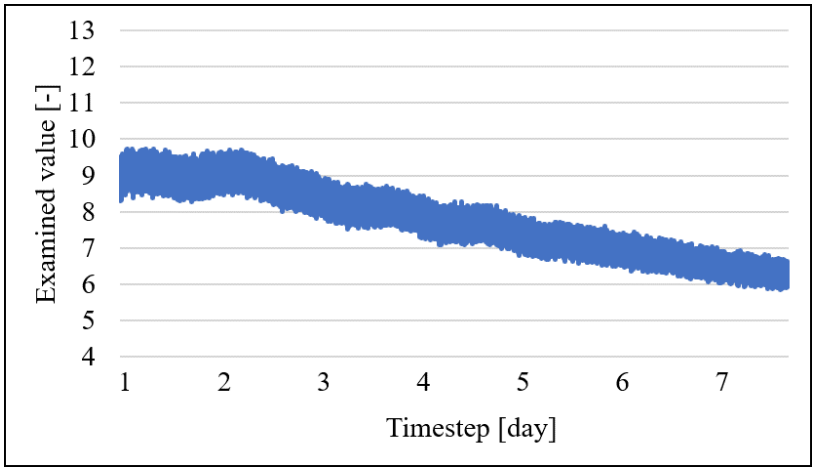

Figure 3.23: Standard deviation filter applied on original signal; SNR of 32; decrease of 6 % per day from beginning of second day

The signal has not been changed while only obviously wrong measurements have been filtered out. The standard deviation filter is only a valid tool as long as the amount of wrong measurements is restricted and is not affecting the signal and its standard deviation itself. As soon as the standard deviation value σ gets manipulated, wrong measurements cannot be detected anymore.

3.3.2 Application of the Least Mean Square Filter

The Least Mean Square filter consists of the three main steps as shown in section 2.2.2. They describe the basic procedure and can be added by further elements to adapt the filter. In fig. 3.24, the developed filter scheme is shown.

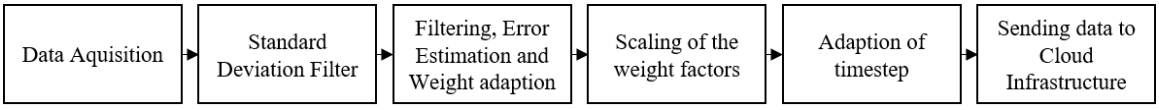

Figure 3.24: Scheme of developed Least Mean Square filter

To adapt the filter to the example signal, the update of the weight factor has to be adapted. For this reason, the update rate is divided by a factor of $50,000$, otherwise the filter would

be too sensitive for the noisy signal. The modified update of the weight factor is shown in eq. (3.3).

$$\text{weight} = \text{previous weight} + \frac{2 \times \text{timestep} \times \text{error estimation} \times \text{Input}}{\text{weight factor}} \tag{3.3}$$

In the shown equation, the error estimation is calculated by subtracting the current output from the previous output of the algorithm. This calculation assumes a constant signal which is not changing over time. Although this assumption is wrong for big timesteps (greater than one day), it is valid for small timesteps. The change of the true signal over different timesteps is shown in table 3.3. These numbers are based on the values defined in section 3.2.3. The decrease of the signal is especially for the slow decrease (0.24 % per day) small enough to be assumed as zero. If the fast decreasing signal (6 % per day) is used in combination with a big timestep ($\sim$ 3 minutes), the assumption gets worse since the signal is changing by 0.011 % for every sample.

Table 3.3: Change of signal (without noise) over different timesteps

Timestep	Change for slow decreasing signal	Change for fast decreasing signal
10 s	2.78×10^{-6} %	6.94×10^{-4} %
20 s	5.56×10^{-6} %	1.39×10^{-3} %
40 s	1.11×10^{-5} %	2.78×10^{-3} %
80 s	2.22×10^{-5} %	5.56×10^{-3} %
160 s	4.44×10^{-5} %	1.11×10^{-2} %
86400 s	0.24 %	6 %

Preliminary Tests

To evaluate the influence of the timestep, the number of values considered to be used for the LMS filter as well as the weighting factor is investigated. To rate their quality, they are compared to the original, noise free signal. An example of this setup is shown in fig. 3.25. In this case, a signal with a SNR of 32 and a decrease of the signal of 6 % is filtered and compared to the true, noise free signal.

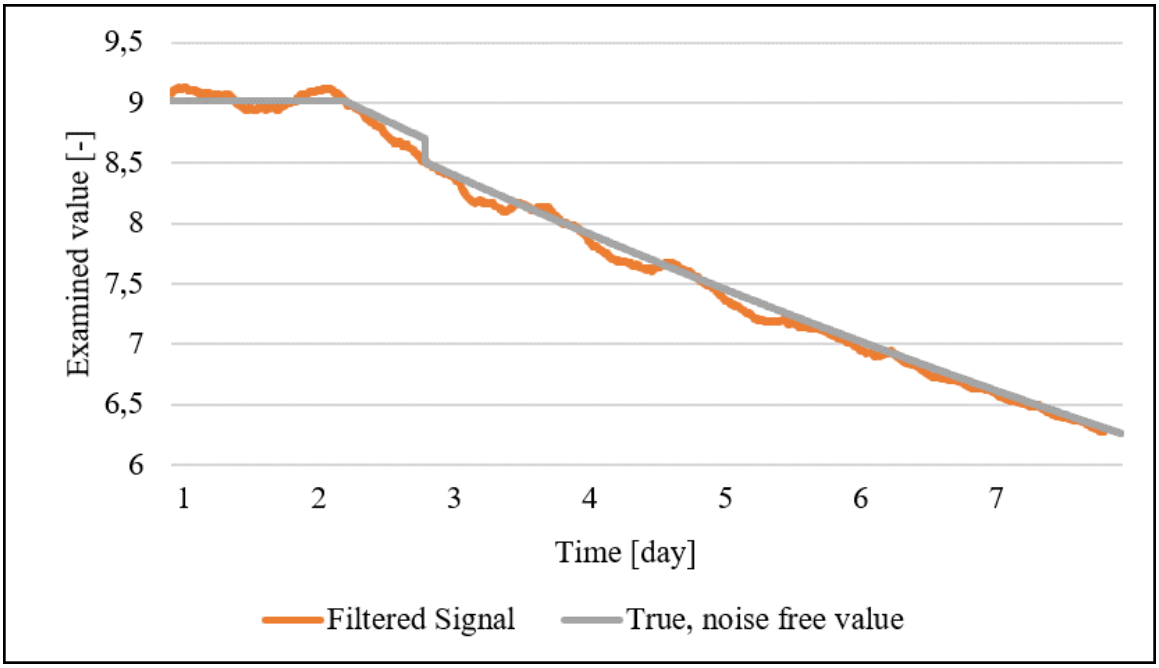

Figure 3.25: Comparison of noise free, true signal to filtered signal with SNR of 32 and a fast decrease

The error is mostly influenced by the low frequency noise which can be seen in fig. 3.25. The filtered signal follows the trend of this low frequency noise. Nevertheless, the performance of the filter can be improved by tuning the parameters as for example the timestep, the amount of values which are considered and the weighting factor. Since the filter is running continuously and the expected change of the signal is very low, classical approaches as rise time or overshoot are not used at this point. Instead, the average squared error of every point as well as the deviation around a local average is used to determine the performance.

For this reason, the example signal with a SNR of 32 and a fast decreasing value (see fig. 3.25) is used to evaluate the filter. The performance can be seen in fig. 3.26, fig. 3.27 and fig. 3.28.

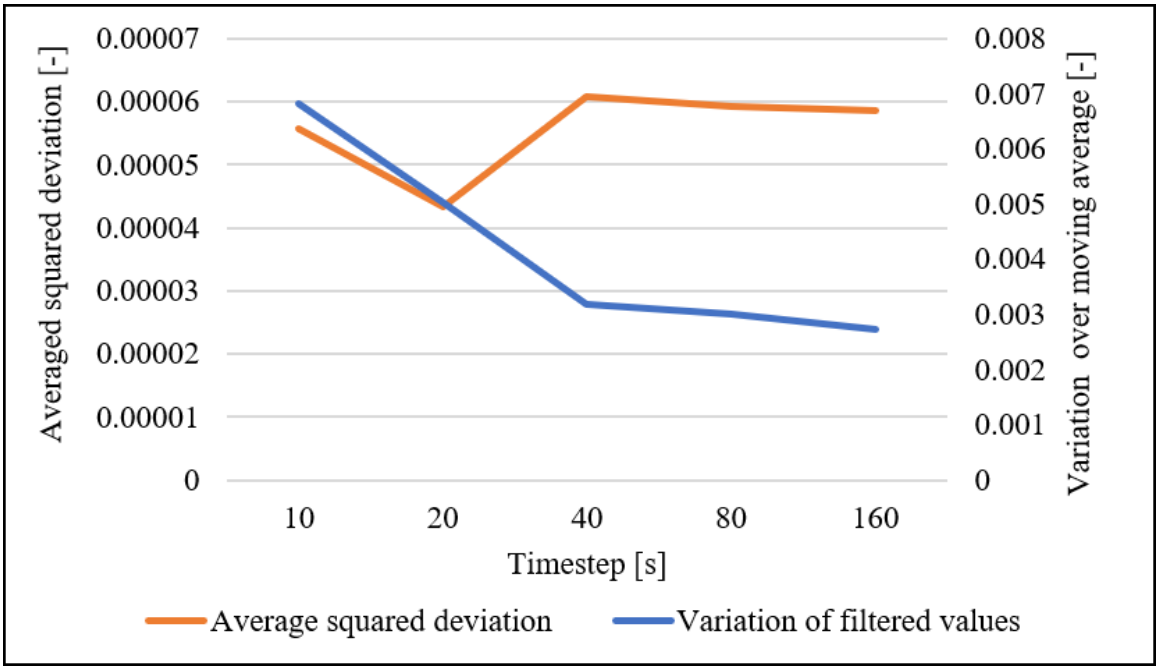

Figure 3.26: Performance of the LMS filter on varying timesteps

The timestep in between the measurements is influencing the number of measurements which have to be taken. By decreasing this number, the energy consumption is decreased, which has a positive influence on the battery life. In fig. 3.26, one can see a decrease of variation with increasing timestep, while the deviation of the filtered signal and the true signal is apart from a timestep of $20\ s$ constant. With the help of this diagram, the timestamp can be chosen to be approximately $40\ s$. If the timestep is increased, the assumption of a constant signal is not valid anymore.

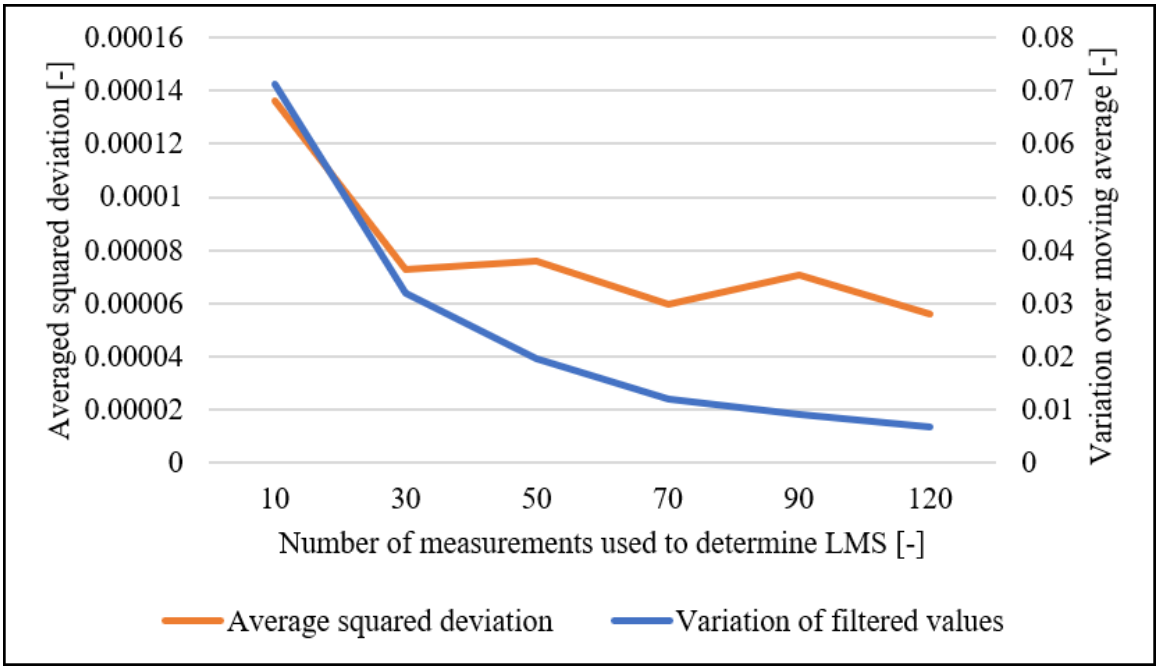

Figure 3.27: Performance of the LMS filter on varying number of measurements to calculate the filter output

The LMS filter is based on a number of previously taken measurements. This number is influencing the performance of the filter as shown in fig. 3.27. The averaged squared deviation as well as the variation over a moving average drop with an increasing number of values. Based on this, a high amount of measures would increase the performance of the filter. However, with an increasing number of measures, the influence of previously taken measurements is increased. If the signal changes over time and is still influenced by the measurements taken before the change in the signal, the output gets corrupted. For this reason, the number of measurements should be kept as small as possible. In this case, a number of 120 measurements can be chosen without taking the risk of the signal being influenced by historical data.

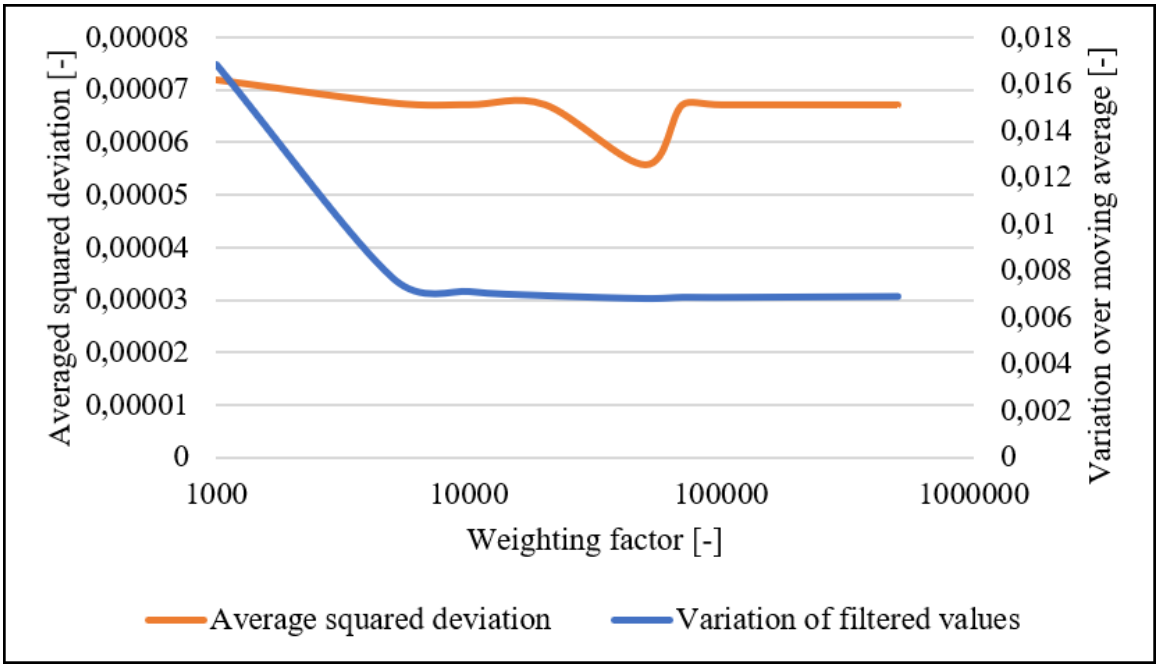

Figure 3.28: Performance of the LMS filter on a varying weight factor

The weighting factor defines the influence of previous measurements compared to the current one. The higher it is, the smaller is the influence of the current data. In fig. 3.28, a steep decline of the variation of the output of the filter can be seen for weighting factors until $10,000$. The average squared deviation is mostly constant apart for a weighting factor of $50,000$. For this reason, the value of $50,000$ is aligned to the weighting factor.

Performance on different Signals

After tuning the LMS filter, the performance on different types of signals is evaluated. For this reason, the filter is applied on the developed example signals (see section 3.2). The results for a fast decrease and a SNR of 74 (fig. 3.29) as well as a SNR of 15 (fig. 3.30) are shown.

It can be seen, that the low frequency noise with a period of 1 day is not filtered out. The SNR of the filtered signal is strongly dependent on the SNR of the unfiltered signal. Since the SNR of the pH meter is 74, this is not significant for the current application. Neverthe-

less, it might be a problem for other applications. Furthermore, the wrong measurements have no influence on the filtered signal. Based on this result, the standard deviation filter is working. The jump of the signal (at a value of 10840) got smoothed out by the filter but is still influencing the filtered signal.

3.3.3 Application of the Kalman Filter

There are several steps which have to be taken to deploy a Kalman filter. First of all, the system on which the filter is applied has to be modeled. Afterwards, the covariance matrices have to be computed and finally these values have to be tested and potentially adjusted.

Modeling of the System

To model the system, the coolant height is used as a representative. Many systems are very similar by means of their system behavior. The pH value as a system could be modeled identically for example.

To model the system, the system states are described as $x_1 =$ position p and $x_2 =$ slope s. By this, the simple correlation $\dot{x_1} = x_2$ is obtained. The input of the system Bu is the change by controlled removal of coolant from the system. Since this is not the case in the existing example, there is no input into the system. Furthermore, the same argument can be used as for the Least Mean Square filter: The expected change over time of the signal is negligible (see table 3.3). Based on this assumption, the system matrix A can be expressed as unit matrix.

$$A = \begin{bmatrix} 1 & \Delta T \\ 0 & 1 \end{bmatrix} \rightarrow A = \begin{bmatrix} 1 & 0 \\ 0 & 1 \end{bmatrix} \tag{3.4}$$

Another reason for using the manipulated system representation can be found in the noise. If a very low SNR such as $15\ dB$ is applied, the influence of the noise on the output of

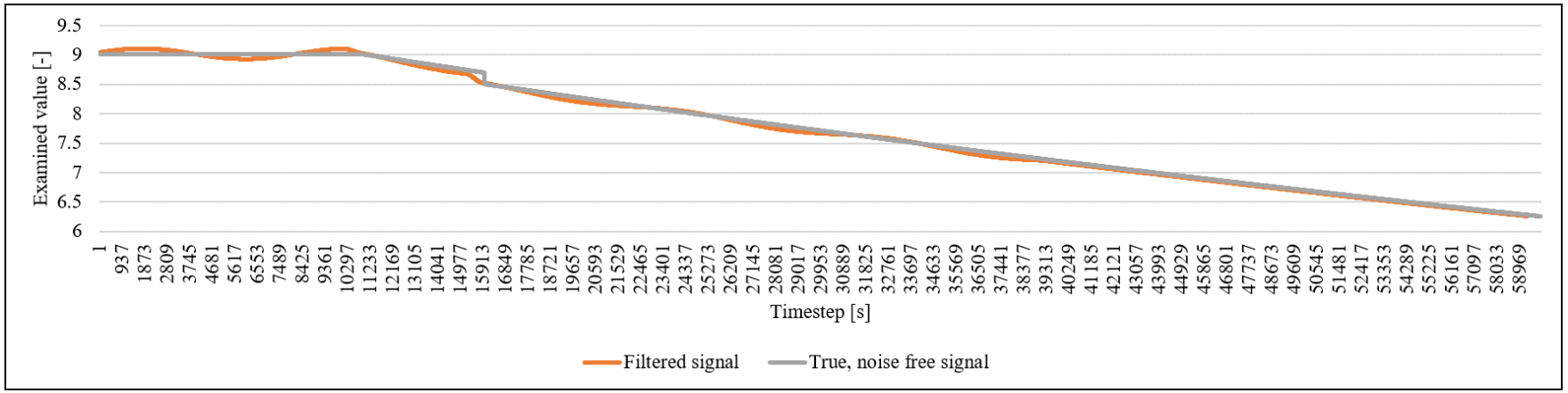

Figure 3.29: Filtered signal with a SNR of 74 and a fast decrease, filter parameter as described in section 3.3.2

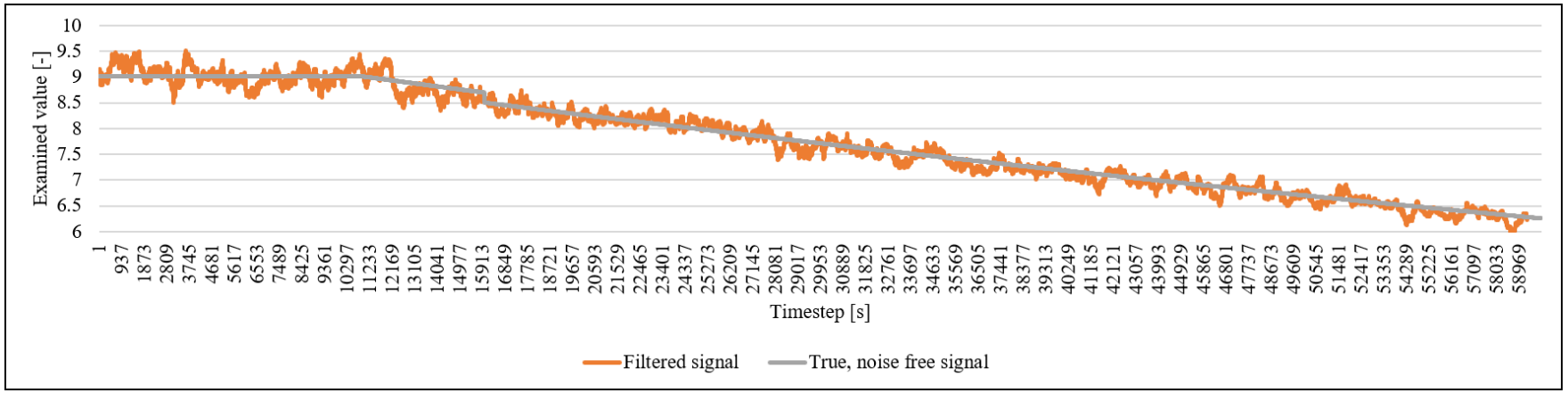

Figure 3.30: Filtered signal with a SNR of 15 and a fast decrease, filter parameter as described in section 3.3.2

the filter is higher compared to the actual change of the signal. The change of the signal is examined in section 3.2.3. For this reason, the filter can become unstable by just amplifying the noise. By using the manipulated system model, the filter can be tuned by the covariance matrices. Although they are also defined by the system itself, they offer a great possibility to act on the sensibility of the filter.

Covariance for Kalman Filter

The system covariance R is hard to determine and is used for tuning of the filter. For this reason, only a first guess is made in this chapter. However, the measurement covariance can be computed based on a known signal. The covariance of the measurement can be obtained by the standard deviation of the signal in combination with eq. (2.21).

$$R = E(z_k z_k^T) = \sigma^2 = 0.0915^2 = 0.00837 \tag{3.5}$$

The covariance of the system Q can also be examined based on eq. (2.21). For this reason, the state of the system x has to be evaluated.

$$Q = E(xx^T) = E\left(\begin{bmatrix} p \\ s \end{bmatrix} \begin{bmatrix} p & s \end{bmatrix}\right) = E\begin{bmatrix} p^2 & ps \\ sp & s^2 \end{bmatrix} \tag{3.6}$$

Based on this calculation, the noise values for the position p as well as for the slope s have to be determined and plugged into the equation. Other sources propose different approaches [78]. For small timesteps between the measurements ΔT, the process noise value is small, since the process noise has a smaller influence on the measurement. If systems are defined as in the present case $x = [x\ \dot{x}]$, the lower right element has the highest value. Its value can

be approximated by σ:

$$Q = \begin{bmatrix} 0 & 0 \\ 0 & \sigma^2 \end{bmatrix} \tag{3.7}$$

Tuning of the Filter

Since the simplified model of the system is used with a constant height / position, the timestep itself does not affect the process of filtering the noise. Nevertheless, it affects the calculation of the slope in the next step. For this reason, it is not part of the tuning process of the filter. For the purpose of tuning the filter, the same example signal as for the Kalman filter is used with a SNR of 32 and a decrease of $6\ \%$.

Constant approach Two sets of different combinations are used for testing reasons. First, all the entries of the system noise covariance matrix are identical. Based on this, the average squared error as well as the variation over a moving average are examined, see fig. 3.31. With smaller system covariance values, smaller errors as well as a smaller variation can be achieved. On the other hand, the rise time of the filter is increased. This can become a problem if the filter cannot follow the signal which leads to a delay, see fig. 3.32.

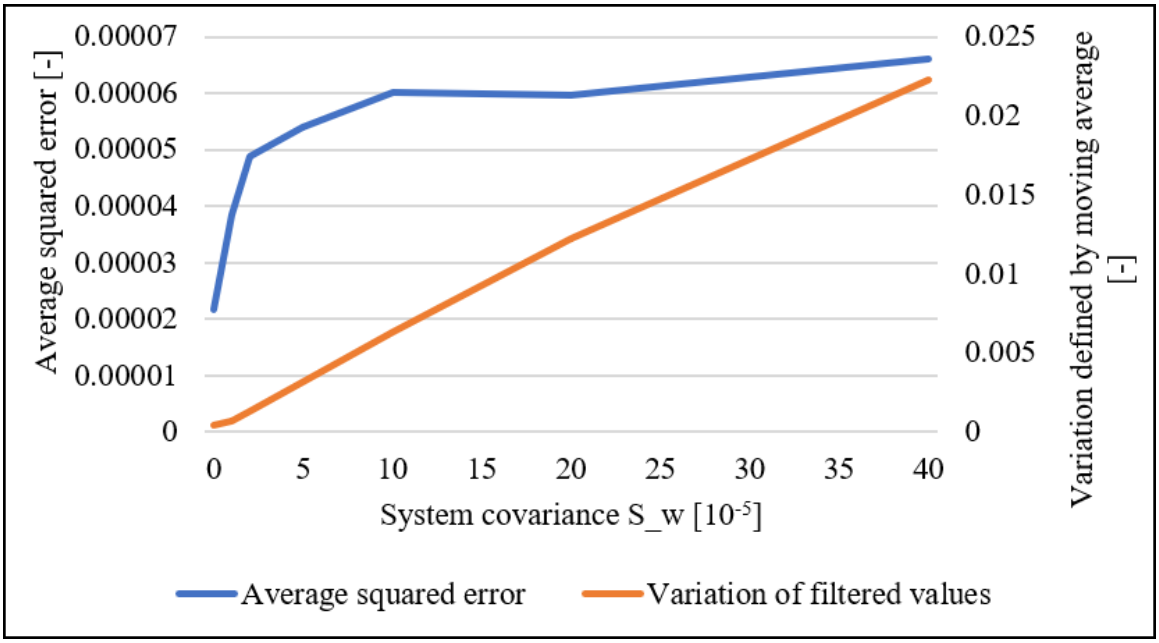

Figure 3.31: Variation of constant system covariance to tune Kalman Filter

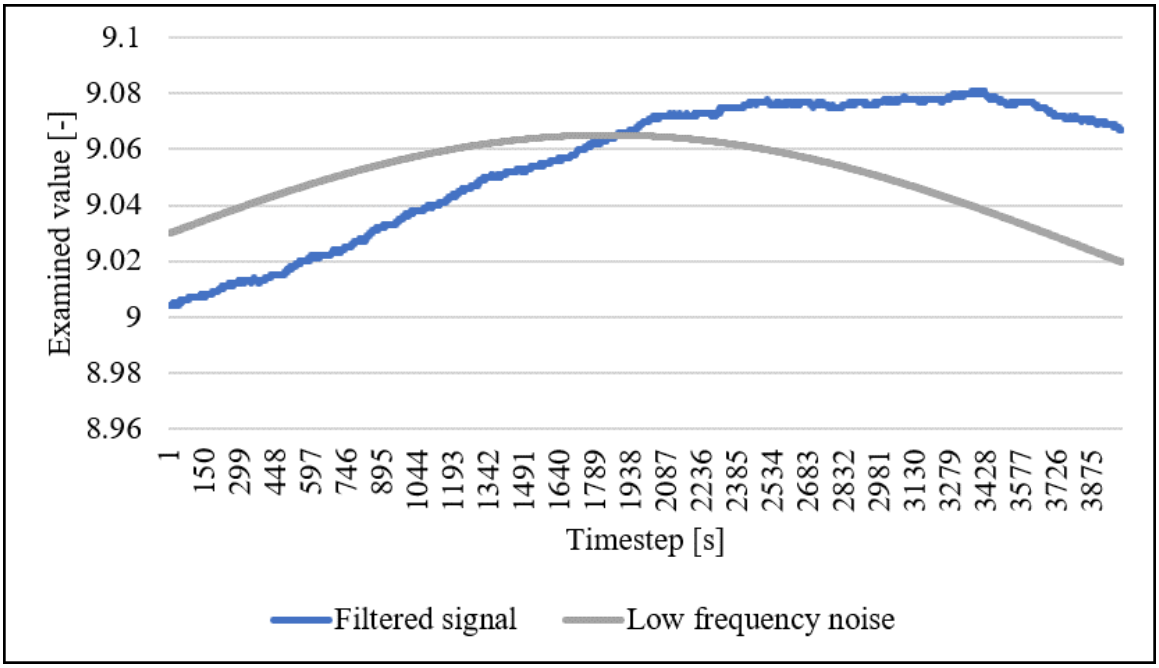

Figure 3.32: Delay for a chosen system covariance value of 0.000005 in the Kalman Filter

The low frequency noise in the example signal (see section 3.2.2) cannot be filtered out of the signal and remains in there, see fig. 3.31. The original signal is a constant at a value of 9.02 Furthermore, one can see a delay in the filtered signal. This delay is increasing with

smaller system covariance values. The trend of the delay is shown in fig. 3.33. It can be seen that system covariances smaller than $5 * 10^{-5}$ have an unacceptable delay and cannot be used.

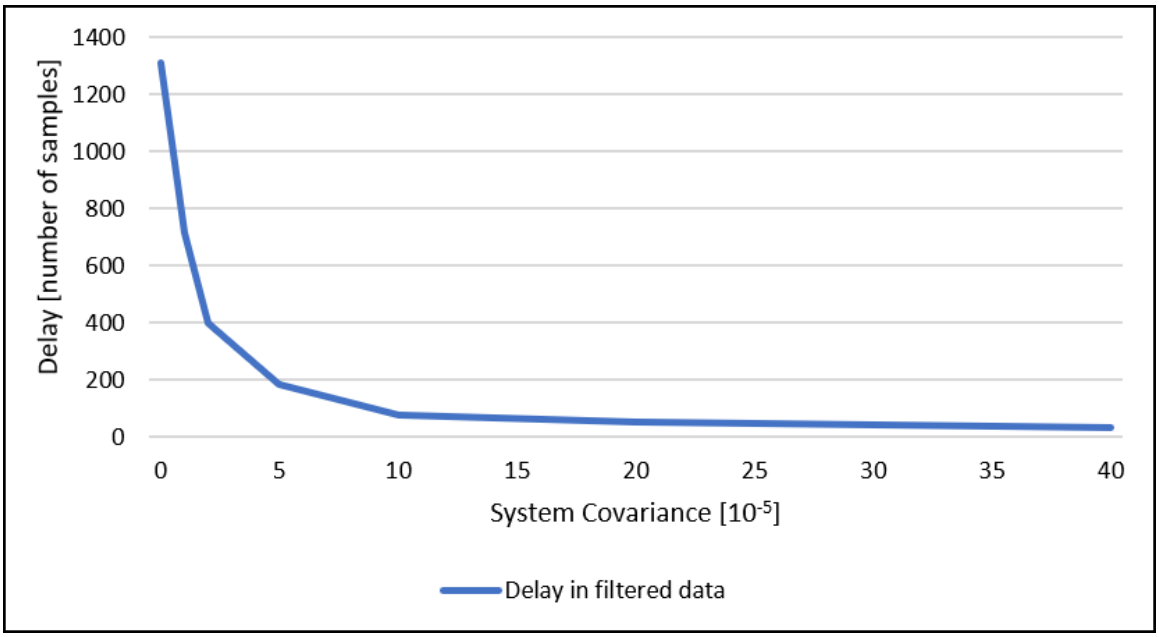

Figure 3.33: Delay of filtered data by Kalman filter over variation of constant system covariance

Classical Approach The system covariance based on eq. (3.6) has a different form. Since the noise on the slope value is in general higher, it can be described generically by eq. (3.8). In this case, κ is a varying factor.

$$Q = \begin{bmatrix} 1 * \kappa & 2 * \kappa \\ 2 * \kappa & 4 * \kappa \end{bmatrix} \tag{3.8}$$

For this composition, the same tests are carried out. The results for the average squared error as well as the variation defined over a moving average can be seen in fig. 3.34. The plot looks very similar to the results from fig. 3.31. Only the variation of the values is smaller in the classical approach of choosing the system covariance matrix. For this reason, the classical approach is chosen to continue with. The minimum value κ is selected from

fig. 3.33 as 0.000025. The delay diagrams for both approaches are nearly identical. Based on this, the system covariance matrix can be seen in eq. (3.9).

$$Q = \begin{bmatrix} 0.000025 & 0.00005 \\ 0.00005 & 0.0001 \end{bmatrix} \tag{3.9}$$

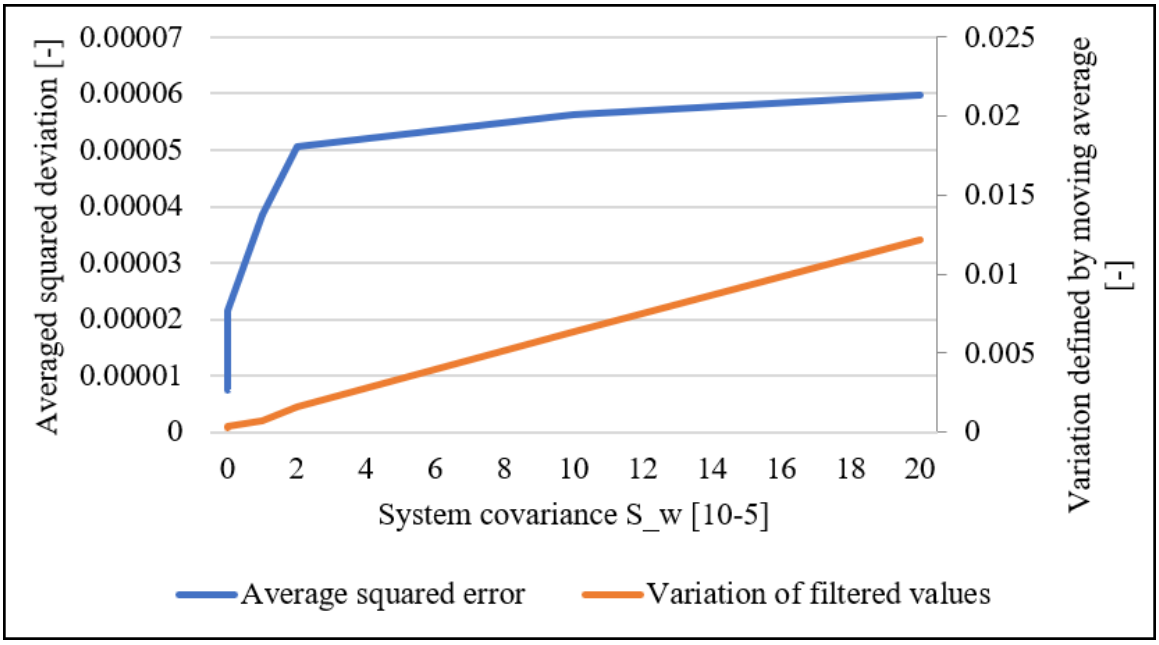

Figure 3.34: Variation of classical system covariance to tune Kalman filter

Performance on different Signals

One main aspect of the overall performance is in how far the signal can follow the long term trend (section 3.2.3). The performance on two of the example signals (SNR of 74 and 15, both fast decrease) can be seen in fig. 3.35 and fig. 3.36. Further tests of the Kalman filter on the other example signals can be found in the appendix section B.3.

All in all, the performance of the filter on the high frequency noise is better compared to the LMS filter. However, the low frequency noise could not be filtered out.

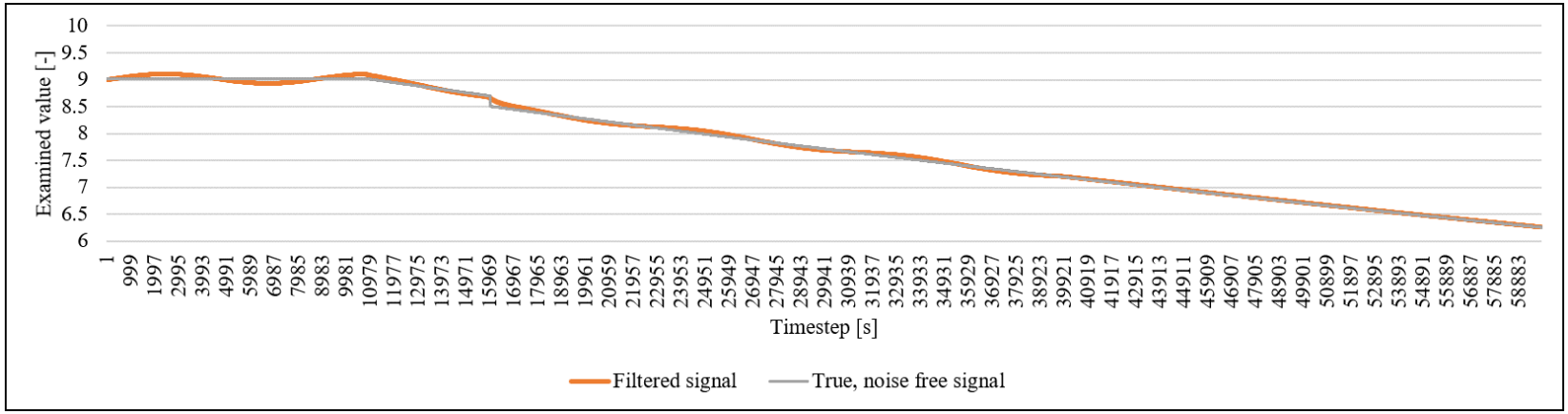

Figure 3.35: Kalman filtered signal with a SNR of 74 and a fast decrease, filter parameters as described in section 3.3.3

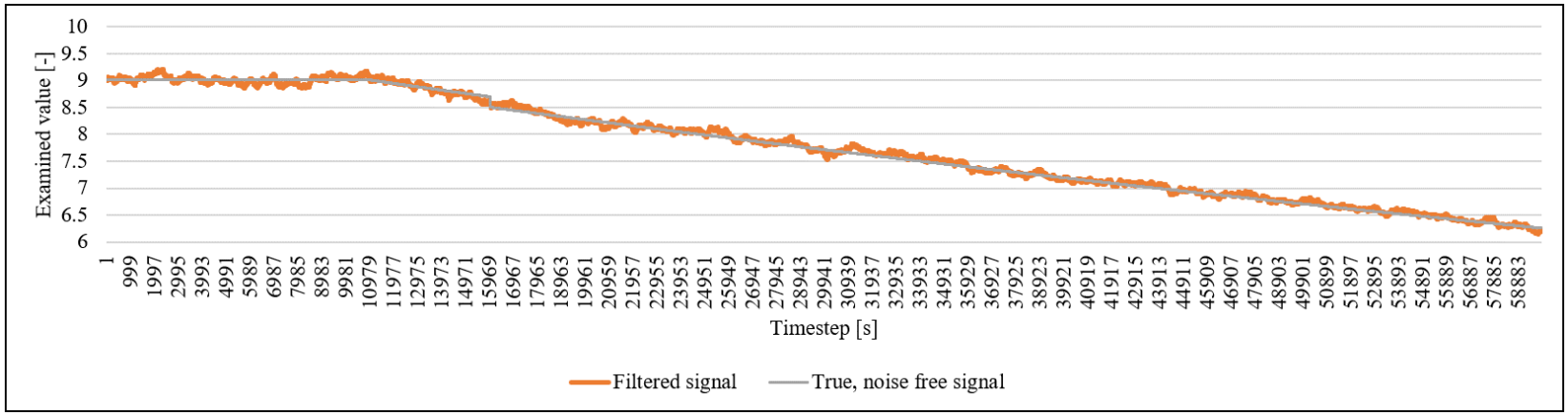

Figure 3.36: Kalman filtered signal with a SNR of 15 and a fast decrease, filter parameters as described in section 3.3.3

3.3.4 Application of the Moving Average Filter

The Moving average filter is very simple in its application. Therefore, it is very common and can even be computed manually. In the following, a weighted moving average approach is realized. Several weighting functions are tested. Furthermore, the number of values to create the moving average is part of the tuning process.

Tuning of the Moving Average Filter

The tuning of the filter includes two aspects, the number of values for creating the moving average, which varies from 40 to 180, as well as the weighting function. For the weighting function, a constant, a line through the origin and a square function is used. All of them can be seen in fig. 3.37. The higher number represent the most current measurements.

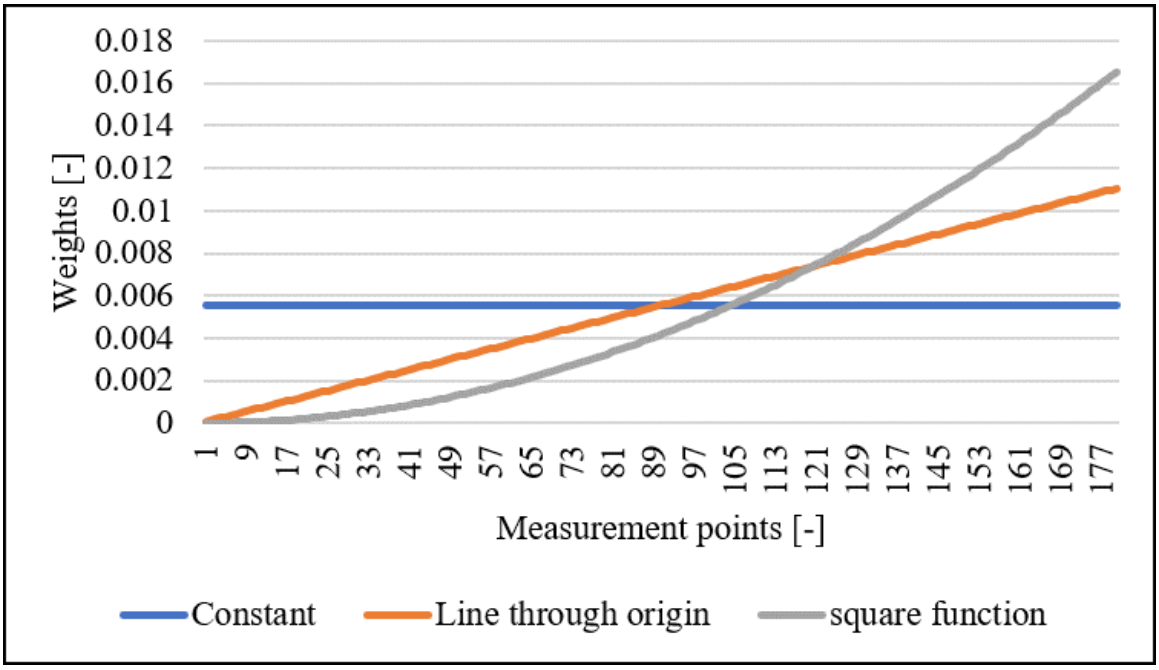

Figure 3.37: Applied weight functions for determining the moving average

The result of the tuning process can be found in figs. 3.38 to 3.40. For the line through the origin as well as for the square function, the results concerning signal error and variation

are decreasing for a larger number of measurements to create the moving average. For the constant weighting function however, it is increasing for a big number of samples. This is because historical measurements have a higher influence on the output. By this, the output is manipulated. As a result, the line through the origin is chosen with a sample number of 160 for further tests on different signals.

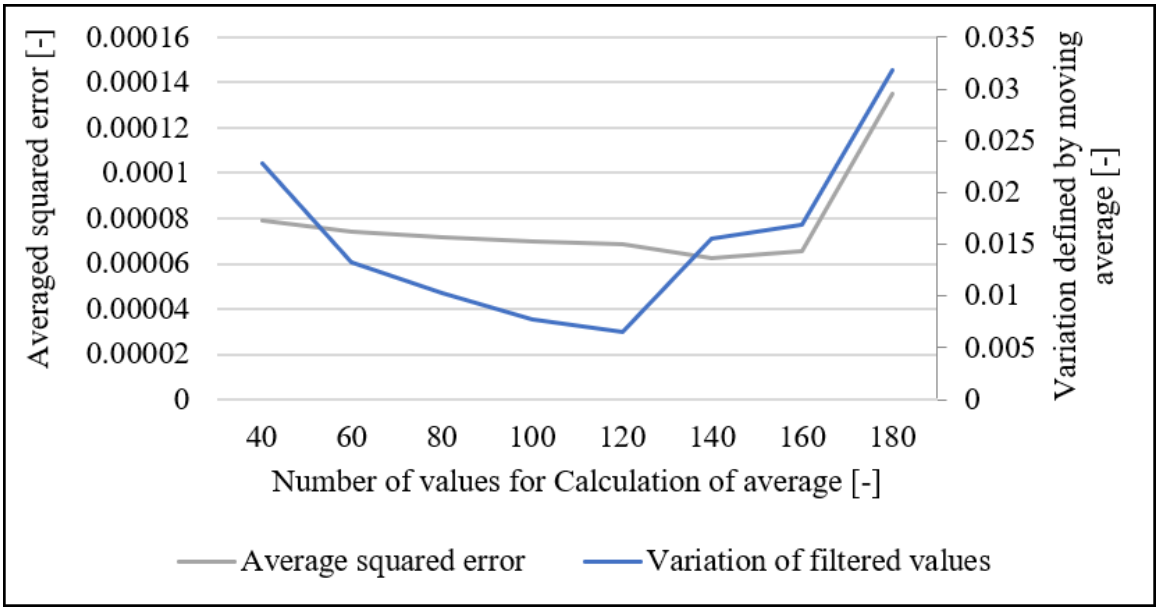

Figure 3.38: Tuning of Moving Average filter with constant weighting function

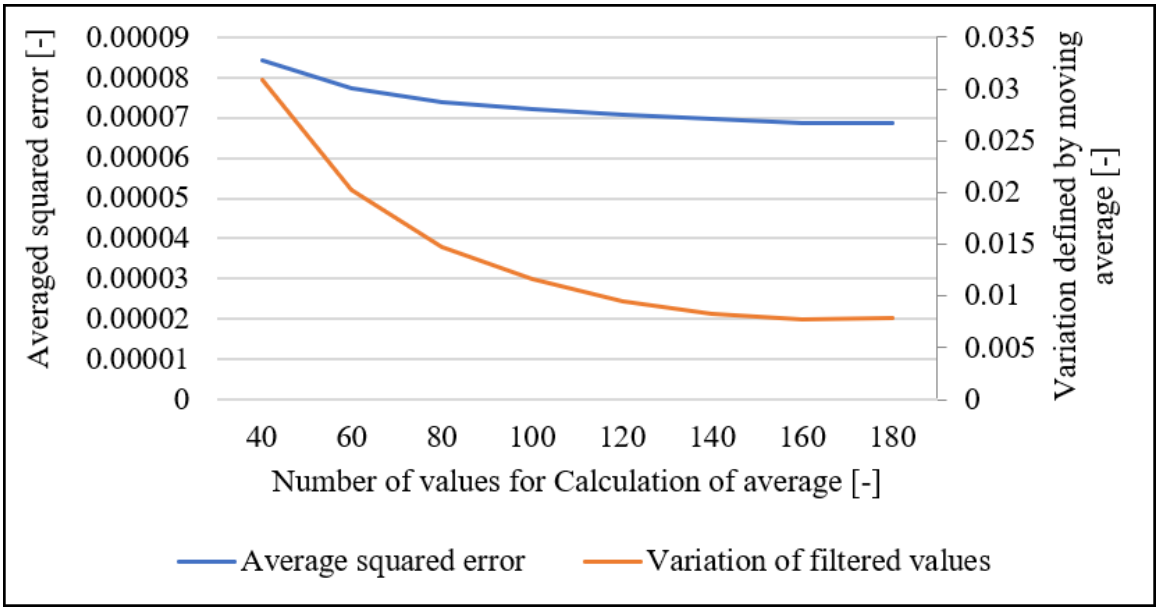

Figure 3.39: Tuning of Moving Average filter with line through origin as weighting function

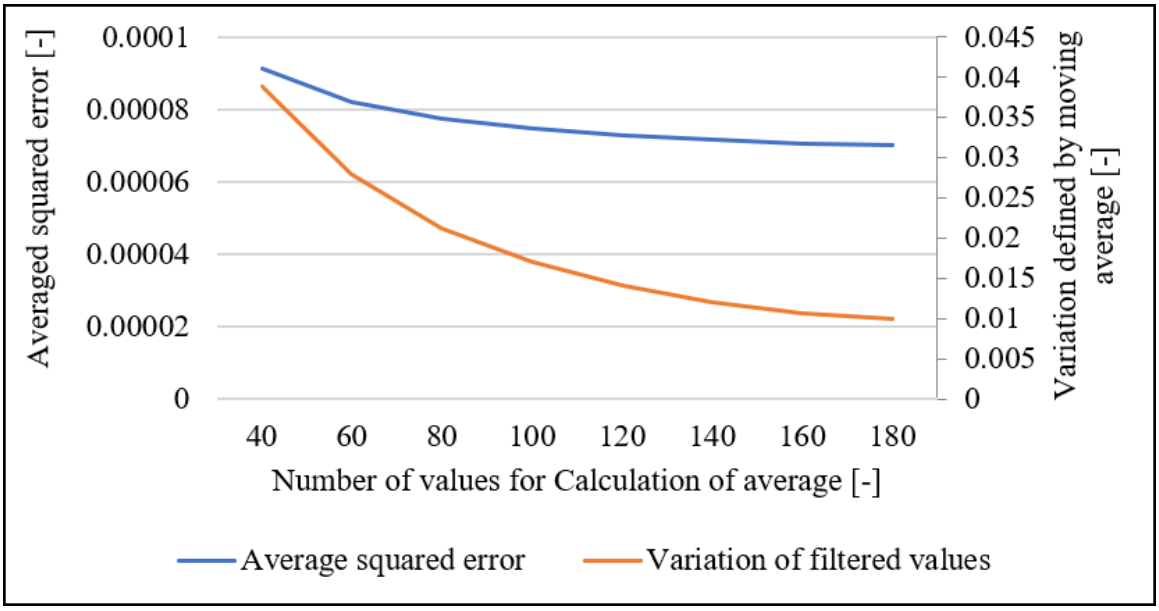

Figure 3.40: Tuning of Moving Average filter with square function as weighting function

Performance on different Signals

The performance of the Moving Average filter on signals with a low SNR is relatively bad.

The delay in the signal however is compared to the LMS filter smaller.

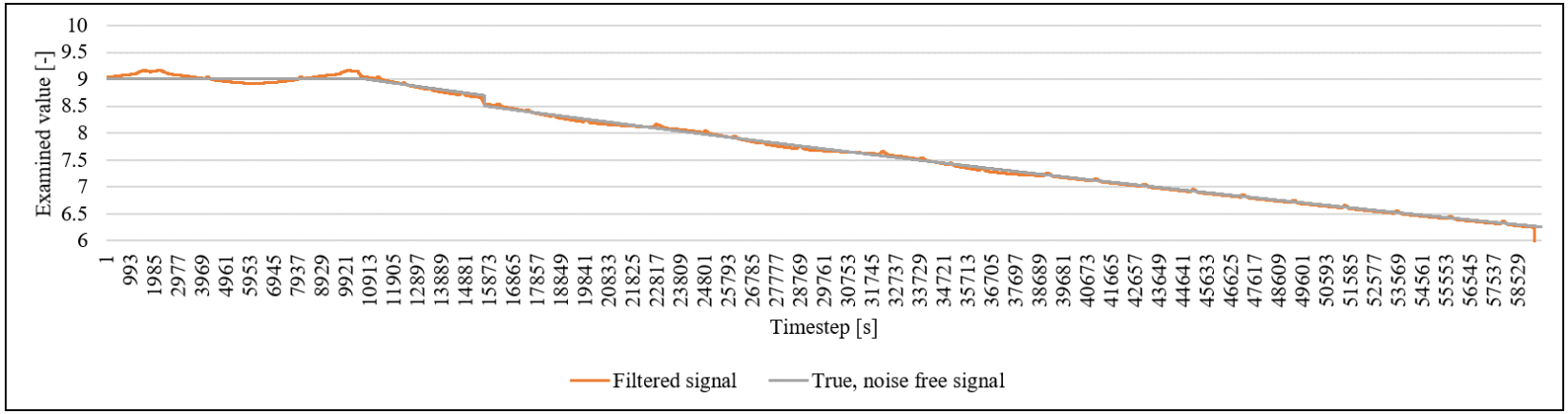

Figure 3.41: Moving Average filtered signal with a SNR of 74 and a fast decrease, filter parameters as described in section 3.3.4

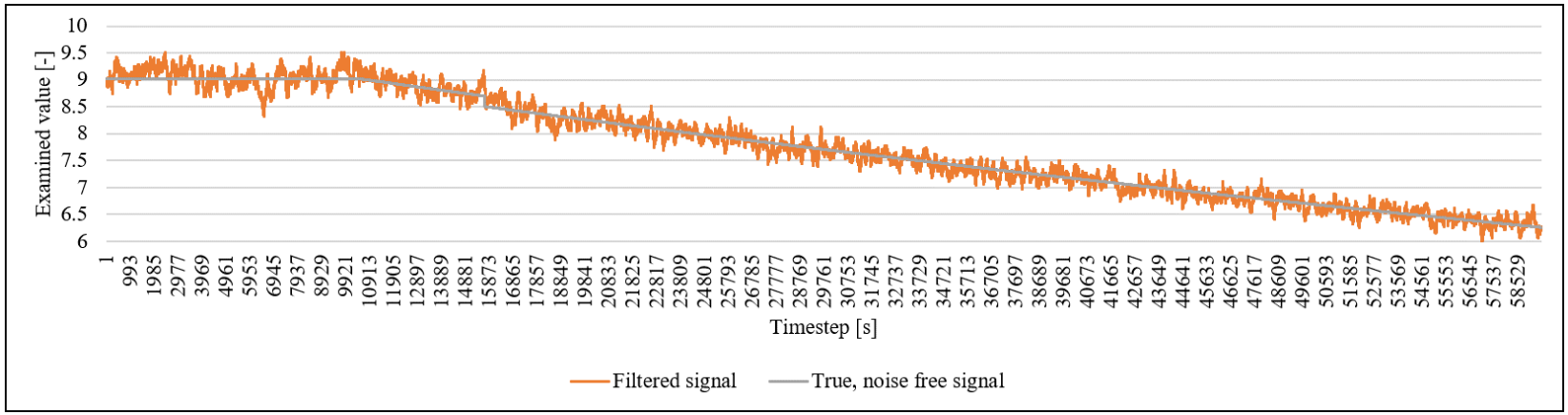

Figure 3.42: Moving Average filtered signal with a SNR of 15 and a fast decrease, filter parameters as described in section 3.3.4

3.4 Comparison of the different Filters

To compare the different signals, on the one hand the examinations made in the filter tuning chapters can be used. Furthermore, the step response is evaluated in this chapter and in particular the rise time. The rise time has two important influences on the overall performance of the filter:

- Determine the lead time (Ramp-up phase)
- Evaluate the behavior if there is an interruption in sending data for a certain amount of time

The rise time for the developed filters can be seen in table 3.4

Table 3.4: Rise time for different filters

	Moving Average	LMS	Kalman Filter
Number of measurements	93	94	735

One of the main important abilities of the filter is the achieved smoothness. This is essential since the variation in the measurement has a high influence on the calculated slope. Based on this aspect, the Kalman Filter seems to be the best choice. On the other hand, the rise time of the step response is similar for the Moving Average as well as for the LMS but eight times as much for the Kalman filter. This is due to the tuning of the filter. The most important result of the comparison of the rise time and the variation as well as the averaged square error is the dependency of the performance on the input signal. The state estimation filter has to be adapted to every signal to perform as expected.

Furthermore, it can be seen that the filter is not able to deal with the low frequency noise / pattern. It is still visible in the filtered signal. This issue has to be addressed when calculating the slope of the signal.

3.5 Slope Calculation of the Signal

The slope calculation needs to deal with the rest of the noise in the filtered signal as well as the low frequency noise which cannot be removed from the signal in the first step. The expected output of the algorithm is on the one hand the slope itself but on the other hand a warning message when a certain limit is reached. Furthermore, the time until this limit is reached under the current conditions has to be stated. For this reason, a minimum or maximum value (from now on only described as minimum) is required to make a statement about whether a system fails and/or when it fails. Furthermore, it is convenient to have an idea about the expected rate of change which should be detected. By this, the filter can be adapted to the signal. For this reason, there is an input mask for these values to be submitted:

- Minimum / Maximum Value
- Expected rate of change [change / day]
- Desired sampling rate [s]

Even the filtered signal shows a certain amount of noise. For this reason, a stepwise calculation of the slope on the filtered signal cannot be evaluated. The slope calculation would be hugely influenced by the step size and by the noise which is still in the signal. For this reason, another technique for calculating the slope has to be introduced. By including statistics into the slope calculation, an estimation can be done to determine whether a calculated slope value is due to noise or if the signal is effectively increasing.

Every consecutive slope value with the same algebraic sign as the previous one is counted and added up. By summarizing positive and negative values, a specific value is generated (same sign value). The ratio of this value (positive same sign values / negative same sign values) determines whether the slope is due to noise or due to the signal. The explained procedure is shown in fig. 3.43. For this setup, a positive same sign value of 8 and a

negative same sign value of 2 would be generated, which indicates an increasing signal (only slope values are examined). In fig. 3.44 the histogram shows the distribution of slope values of the same algebraic sign. The abscissa represents the number of values with the same algebraic sign in a row. Negative values indicate negative signs and positive values vice versa. For a decreasing signal, a shift to the left can be seen. This shift indicates a slope while the constant signal has a normal distribution with its maximum in the middle.

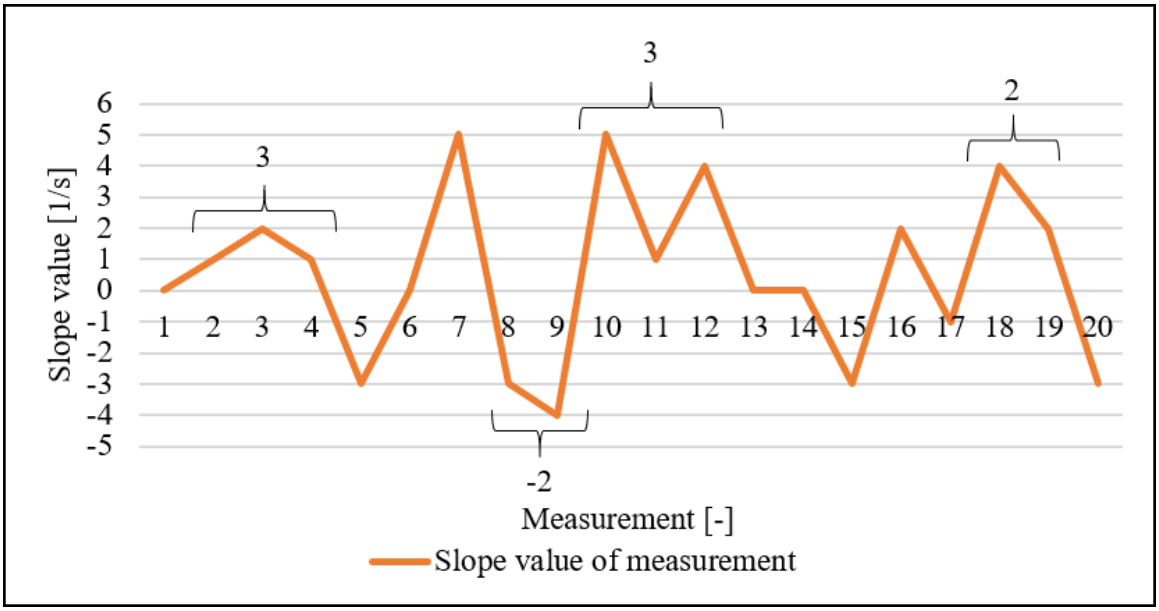

Figure 3.43: Explanation of the calculation of same sign value

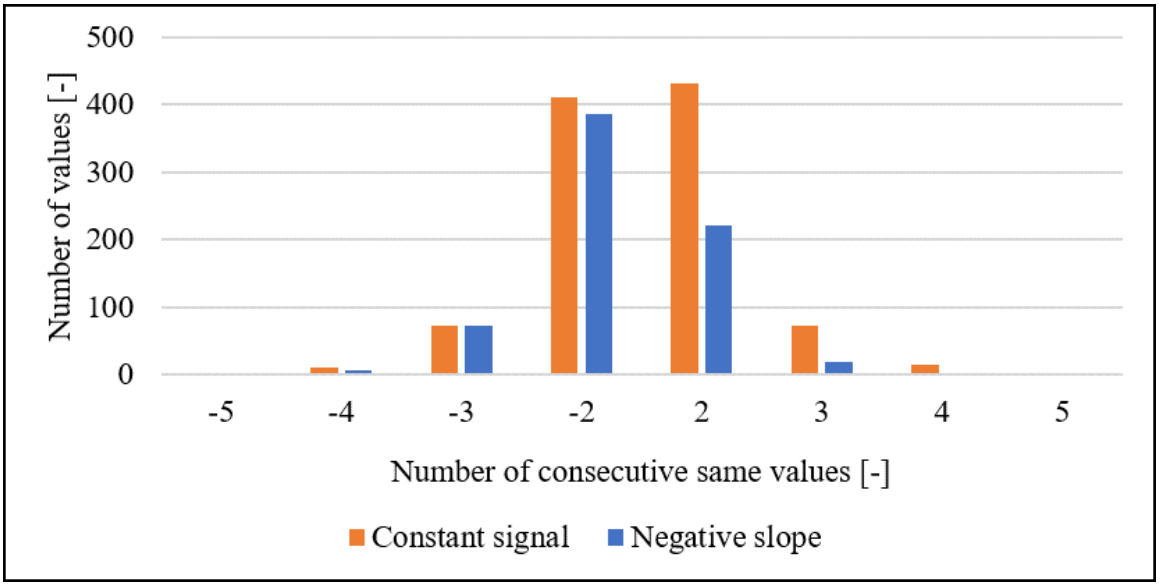

Figure 3.44: Histogram of consecutive slope values with same algebraic sign; fast decrease

However, in fig. 3.45, the same plot is shown with a slower decreasing signal (decreasing rate of 0.24 % per day). The distributions for both signals look very similar this time; a differentiation based on the plot cannot be made. For this reason, the previously mentioned minimum value where the system fails has to be included to determine whether a system fails.

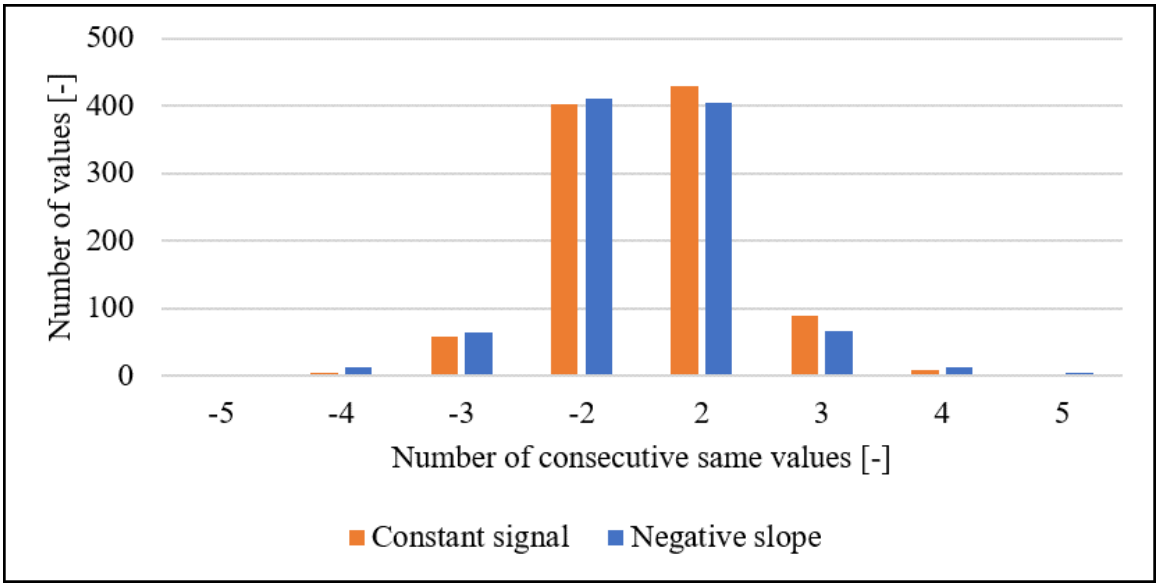

Figure 3.45: Histogram of consecutive slope values with same algebraic sign; slow decrease

The examination period for evaluating the number of consecutive values with a same algebraic sign is chosen between 200 and 500 measurements. The result based on the example signal for a SNR of 32 and a slow / fast decrease can be seen in fig. 3.46 and fig. 3.47. For this representation, the positive and negative same sign values are added up together. For a fast decrease, the signal can be evaluated very easily, since it is mostly negative. However, if the slow decrease is applied, the same sign value is not distinct enough. For this reason, it is plotted in connection with the slope value for the examination period. Only if they match and if the same sign value ratio is distinct enough, a decrease of the signal is detected.

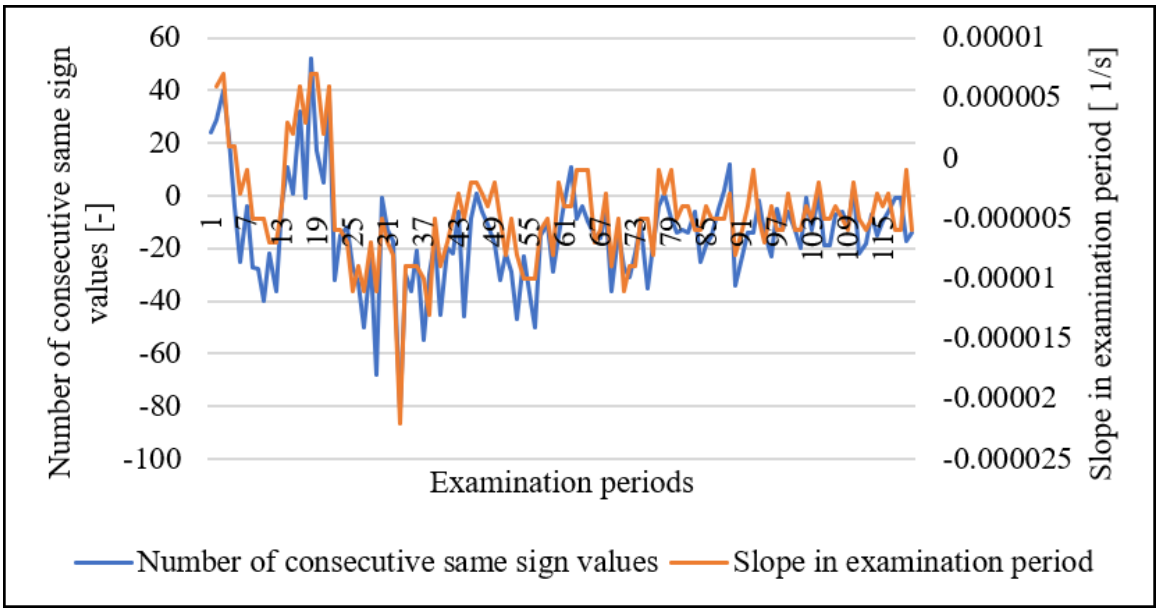

Figure 3.46: Continuously examined same sign values over filtered example signal: Kalman Filter; SNR 32; fast decrease

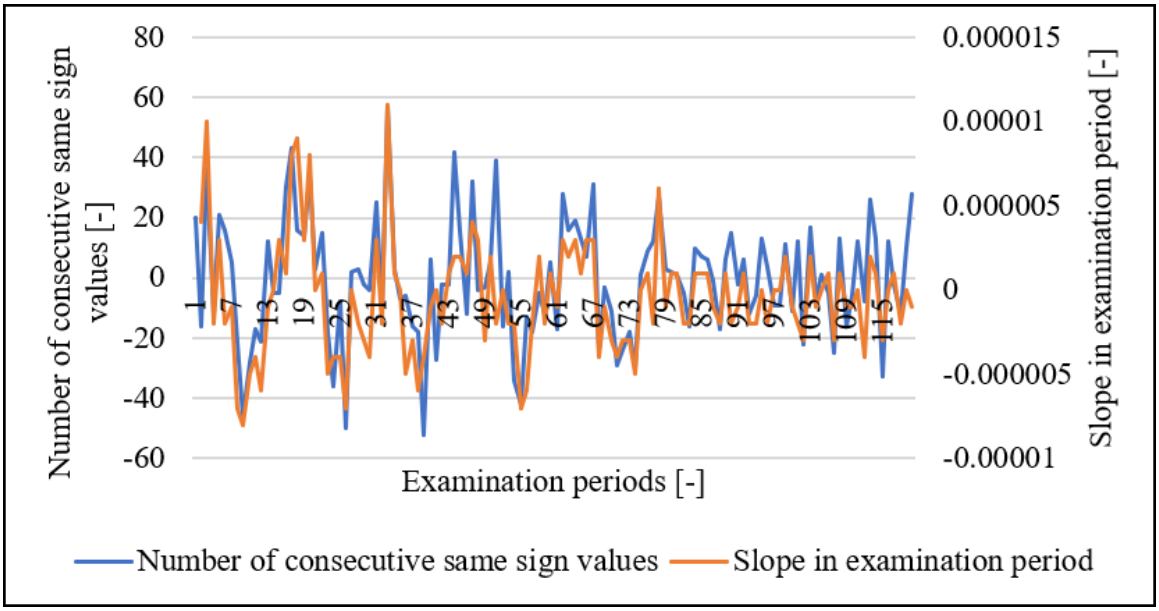

Figure 3.47: Continuously examined same sign values over filtered example signal: Kalman Filter; SNR 32; slow decrease

3.6 Validation of the Slope Estimation Module

For the validation of the slope estimation module, it is tested on several signals. An overview about the signals can be found in table 3.5. The outflow signal (last in table 3.5) represents a signal which is measured in a tank with an outflow. By including this signal, a natural signal with an obvious trend is included into the validation.

Table 3.5: Applied signals for validation of slope estimation module - selection

Signal	Decreasing / Increasing	Noise	Origin
Example signal 1	slowly decreasing	SNR of 32	developed signal
Example signal 2	quickly decreasing	SNR of 32	developed signal
Example signal 3	slowly decreasing	SNR of 15	developed signal
Example signal 4	quickly decreasing	SNR of 15	developed signal
Example signal 5	slowly decreasing	SNR of 74	developed signal
Example signal 6	quickly decreasing	SNR of 74	developed signal
Reference signal	slowly	SNR of 99	developed signal
Height measurement	stagnation	low noise	Ultrasonic sensor
pH measurement	stagnation	very low noise	pH Meter
Outflow signal	quickly increasing	medium noise	Ultrasonic sensor

To validate the algorithm, it is applied on the signals presented in table 3.5. The signals are divided into periods of 200 measurements. For each period, the algorithm detects whether the signal is increasing, decreasing or stagnating. The result is presented as a fraction of how many periods the algorithm is able to detect correctly. Furthermore, an alert is shown whenever the signal exceeds the maximum or minimum value. The overall result is shown in table 3.6. The signal is separated into a stagnation phase and a decreasing phase, see fig. 3.48.

Table 3.6: Applied signals for validation of slope estimation module - performance

Signal	Increasing	Decreasing	Alert
Ex. sign. 1 stagnation SNR 32	100 %	100 %	100 %
Ex. sign. 1 decrease SNR 32	97 %	10 %	100 %
Ex. sign. 2 stagnation SNR 32	85 %	85 %	100 %
Ex. sign. 2 decrease SNR 32	100 %	90 %	100 %
Ex. sign. 3 stagnation SNR 15	100 %	91 %	100 %
Ex. sign. 3 decrease SNR 15	100 %	17 %	100 %
Ex. sign. 4 stagnation SNR 15	100 %	88 %	100 %
Ex. sign. 4 decrease SNR 15	100 %	33 %	100 %
Ex. sign. 5 stagnation SNR 74	100 %	75 %	100 %
Ex. sign. 5 decrease SNR 74	89 %	40 %	100 %
Ex. sign. 6 stagnation SNR 74	89 %	78 %	100 %
Ex. sign. 6 decrease SNR 74	100 %	60 %	100 %
reference signal stagnation	100 %	100 %	100 %
reference signal decrease	100 %	100 %	100 %
Height measurement	100 %	95 %	100 %
pH measurement	99 %	100 %	100 %
Outflow signal	83 %	100 %	100 %

The result has to be interpreted as followed: For Ex. sign. 1 the algorithm is able to detect all increasing values correctly during its stagnation phase, which is 0 out of 0. For its decreasing phase, out of 62 periods, an increasing signal is detected 2 times. An example for such a signal with a slow decrease can be seen in fig. 3.48.

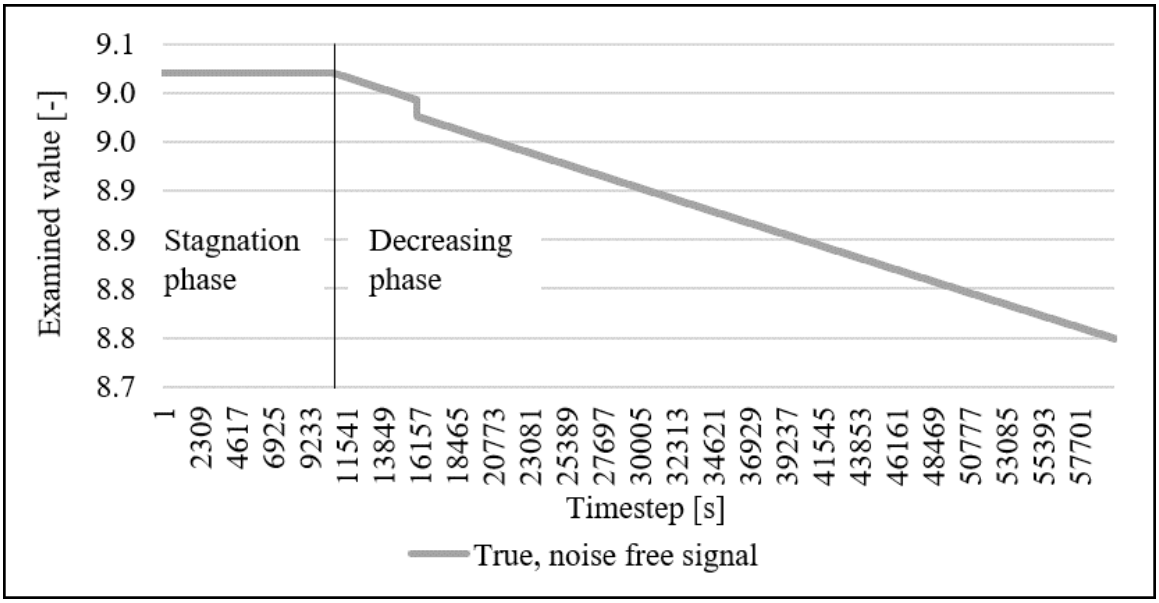

Figure 3.48: Slowly decreasing signal, separated in stagnation phase (Example signal 1 stagnation) and decreasing phase (Example signal 1 decrease)

The big difference in performance of the algorithm between example signals 1 and 2 is very obvious. The major difference is the decreasing rate. This rate is higher for example signal 2. A higher decreasing rate is generally easier to detect. Generally, a better performance can be seen for higher SNRs. This is due to the limited capabilities of the state estimate filter. It is not able to fully cancel out the noise of the signal. In comparison to the example signal, the reference signal, which has no noise in it (low or high frequency), achieves a performance of $100\ \%$ in all categories. By comparing the artificial signals with the natural ones, a better performance of the slope module can be seen for the natural ones. This indicates the challenging character of the example signal compared to real life signals.

3.7 Power Supply for Sensors and Microprocessors

As already described (see section 2.4.6), there are several possibilities of powering a sensor and microprocessor (Sensor node). Very often, the main goal is to be independent of power outlets and other power sources. For this reason, battery powered solutions are preferred.

When applying a battery powered solution, some things have to be kept in mind:

- Identify most power consuming process
- Eliminate or avoid most power consuming process
- Improve power consumption of most power consuming process

In the case of a wireless Sensor node, in general the most power consuming process is the connection with the Wi-Fi. For this reason, there are several possibilities to temporarily switch off the Wi-Fi on the Sensor node if it is not used. This can heavily improve the lifespan of a battery powered Sensor node.

Another aspect which has to be kept in mind is to improve the most power consuming process. This can be done by improving the Wi-Fi accessibility to the Sensor node. In fact, if the Wi-Fi is not accessible the reconnection after switching the Wi-Fi off for a certain amount of time can delay the program which is running on the Sensor node or even interrupt it. In this case, the power consumption increases due to the attempts to reconnect to the Wi-Fi if the connection cannot be made. This leads to a loss in data and unreliable Sensor nodes.

Due to problems with the signal strength of the Wi-Fi network at the location of employment of the Sensor node, no experimental data can be collected. In the case where the Wi-Fi on the sensor node kept running, the battery was not able to power the sensor node for more than one day. Due to this, the influence of battery powered sensor nodes on the signal as well as the lifespan of battery powered Sensor nodes cannot be investigated. Nevertheless, the importance of a good accessibility of the Wi-Fi network can be identified as a major requirement for battery powered sensor nodes in general.

CHAPTER 4

DISCUSSION

Some major topics in this thesis have to be discussed in order to evaluate in how far the goal, the development of a slope estimation algorithm, is fulfilled. For this reason, the major sections of the previous chapter, their results and the influence on the overall result have to be critically analyzed. Furthermore, the whole result of the thesis has to be investigated to determine whether all the requirements are fulfilled.

4.1 Influence of Sensors and Example Signal

The sensors have a very high influence on the designed algorithm. Based on their output, the requirements on the slope module are defined. For this reason, a greater variety of sensors would be useful to be able to take more influences into account. However, influences of both sensors are included into the example signal and can be handled by the module (SNR, wrong measurements and long term trends are based on the Ultrasonic sensor, low frequency noise as well as interruptions in reading is based on the pH meter). Nevertheless, the slope estimation module is capable of evaluating both sensor outputs with the same accuracy.

All in all, a greater variety of sensors would be helpful to improve the validation of the slope estimation, an improvement of the performance itself however is not expected.

In contrast to this, the adequacy of the example signal has to be checked in detail. One of the most critical aspects of the example signal is the low frequency noise, which can be seen in fig. 4.1. The maximum and minimum values are also shown in this figure. Especially for the stagnation part of the signal, the periodic character of the system has to be recognized

by the slope algorithm, otherwise a decrease of the signal and a future violation of the minimum value would be detected. But also the decreasing phase shows the problem of the low frequency noise: Even though the trend of the signal is decreasing, for specific periods it is increasing. This is why the overall trend of the signal has to be identified. Cases of a high amplitude of the low frequency noise or a longer period of this noise are critical. For this reason, the slope estimation module has a rather poor performance on the shown signal, see table 3.6: "Signal 1 decrease".

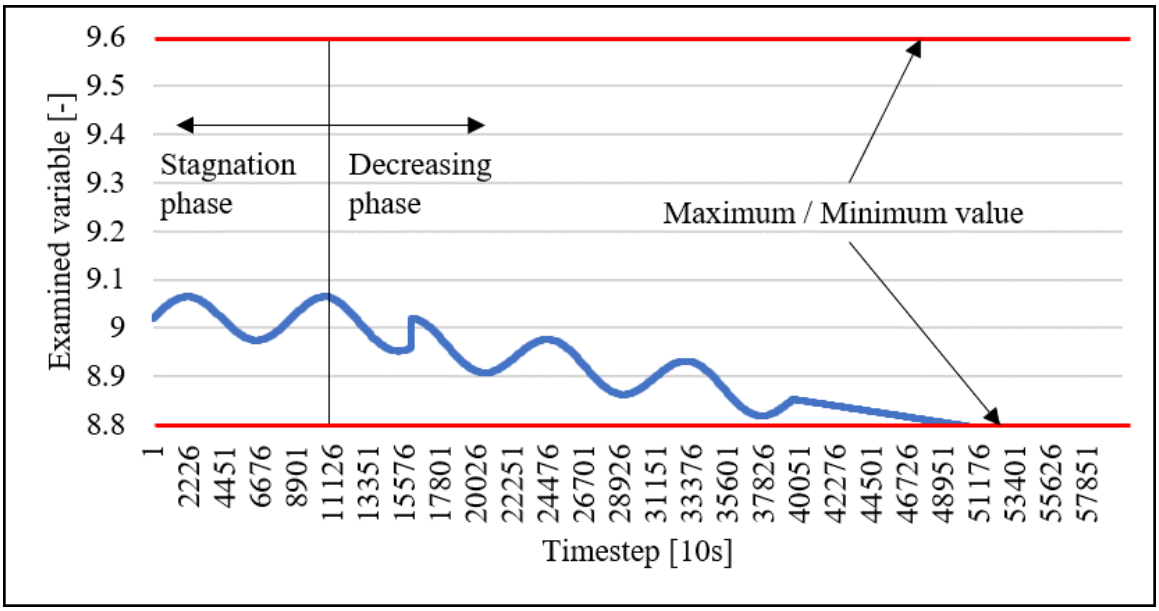

Figure 4.1: Low Frequency noise added on signal with a slow decrease, minimum and maximum values are marked

Another critical point of the example signal is the very low SNR. The measured signal of the US sensor has a very good SNR of $74\ dB$. Also, the SNR of the pH meter is well above $40\ dB$. Nevertheless, the example signal contains variations with a SNR of $15\ dB$. This is not representing the experienced reality based on the evaluated sensors. Nevertheless, it represents a possible case which has to be covered.

All in all, the example signal can be assumed to be more challenging to analyze compared to signals from the used sensors. This can also be seen by the performance of the slope

estimation module on the example signals compared to the measured signals in table 3.6.

4.2 Discussion of Filter Algorithms

The filter algorithms perform for varying signals differently. This can be seen in section 3.3 as well as section 3.4. For this reason, the state estimation filter has to be adapted to the signal. This adaption needs to be done by an input of the operator. With this information, the observation period of the slope module is adapted as well as the step response.

In this case, the small number of sensors leads to an issue since the filter can only be adapted on them. A greater variety of sensors would offer the possibility to adapt the filter to different signals. Furthermore, since the variety of signals can hardly be covered by a single value to tune the filter, several tuning values have to be applied. However, a great variety of tuning parameters confuse operators. Due to this issue, signals, which differ from the ones handled so far, have to perform test runs on the slope estimation algorithm before the optimal tuning is achieved.

4.3 Discussion of overall Slope Module

The overall slope estimation module consists of the filter part as well as the slope calculation unit. The influence of the filter on the overall result is already discussed. The slope estimation unit suffers from very similar problems. Due to different signals the requirements are manifold. One of the main problems the slope estimation unit has to deal with is the low frequency noise. This noise cannot be filtered out by the filter. Therefore, the slope calculation unit has to deal with it. Based on the current frequency (period of 1 day), this low frequency noise can be detected. If the frequency changes due to alien influences (period length of one week, one month, one year), the current module cannot distinguish it from an actual trend in the data.

All in all, the slope estimation module is able to detect slope for a great variety of signals. However, if the signal has several corrupting influences, a reliable detection cannot be made. Due to this, a test of the module on the specific signal is recommended.

CHAPTER 5

CONCLUSION

Based on the problem statement, a slope estimation module is developed which is able to handle high frequency noise, interruptions in sending data as well as wrong measurements. Depending on the frequency and the amplitude, it is also able to handle low frequency noise based on natural patterns such as day/night cycle, weekly cycle and so forth.

In the beginning, a literature research is done to show the importance of the slope as a predictive tool. Based on the slope of the pH value in a cutting fluid tank, its lifespan can be predicted. Furthermore, the used sensors as well as different state estimation approaches are presented. Afterwards, the sensors are tested and based on these results a set of example signals is created. With the help of these signals, a state estimation algorithm is developed and tuned. To calculate the effective slope of the signal, a slope estimator is created. At the end, the whole module is tested on different signals.

Based on the results of the thesis, the slope module is able to detect the slope on different types of signals. Nevertheless, the filter as well as the slope calculation unit have to be adapted to different use cases. For this adaption, test runs might be required.

The slope estimation is only one step towards a predictive maintenance of manufacturing systems. Furthermore, the digital architecture is an important part of this task. The question about where to run the calculation (locally or cloud based) and what to do with these data is very essential for the success of predictive maintenance. So far, the slope estimation is used as a warning tool whenever the variable shows a tendency towards one direction. Based on this warning signal, a maintenance action can be planned. Whereas in an integrated system, based on several variables the slope could be used draw a conclusion about changes of the

environment. To realize this, the slope estimation module has to be applied on several signals and the evaluation has to be connected in a smart way.

Appendices

APPENDIX A

EXPERIMENTAL EQUIPMENT

For the experimental setup, the described sensors (Ultrasonic sensor and pH meter) are used. Since they are both described in detail within the thesis, they are not discussed in here.

Experiments on coolant pH as well as level are realized on a Multus Millturn machine. The coolant tank for this machine is easily accessible and the machine is used regularly.

Furthermore, a combination of Microcontrollers is used to process the data. For reading data from the sensor, a particle photon is employed. For testing the whole module, the particle photon is connected to an Arduino Mega. The whole setup is shown fig. A.1. With the help of this setup, the example signal can be send to the Particle Photon on which the slope estimation module is running.

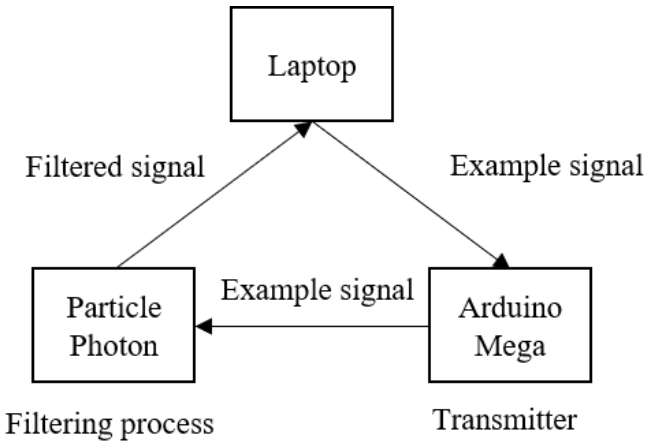

Figure A.1: Setup for testing of example signals

APPENDIX B

DATA PROCESSING

B.1 Example signals at different conditions

B.2 Least Mean Square Filter applied on varying Signals

B.3 Kalman Filter applied on varying Signals

B.4 Moving Average Filter applied on varying Signals

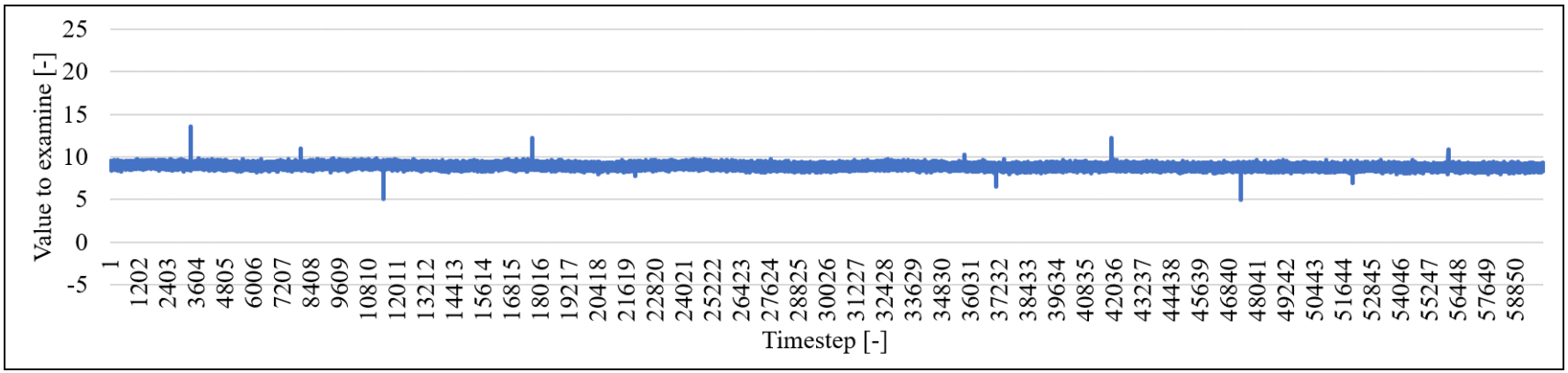

Figure B.1: Example signal 1: SNR 74; 0.24% decrease per day

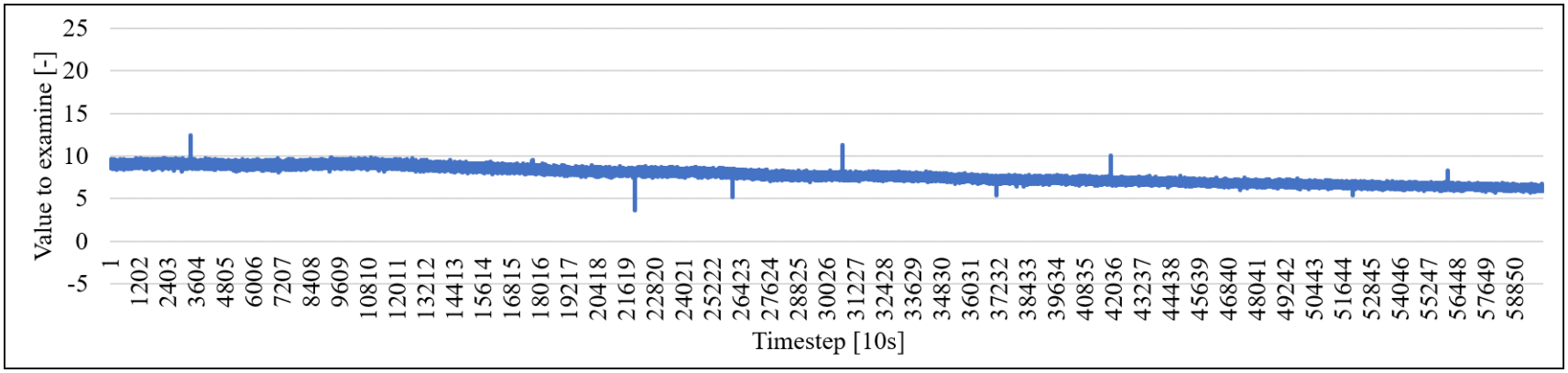

Figure B.2: Example signal 1: SNR 74; 6% decrease per day

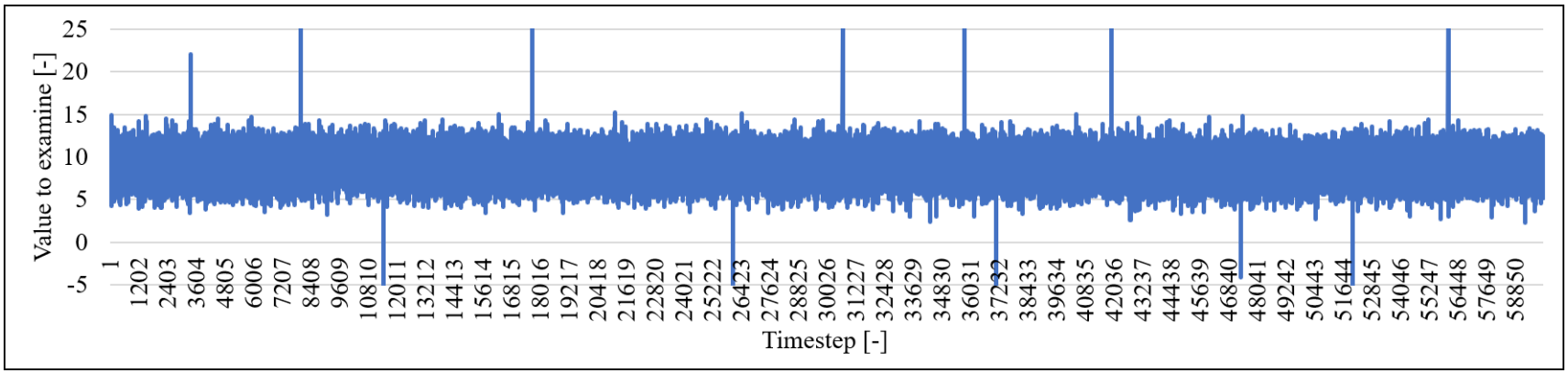

Figure B.3: Example signal 1: SNR 74; 0.24% decrease per day

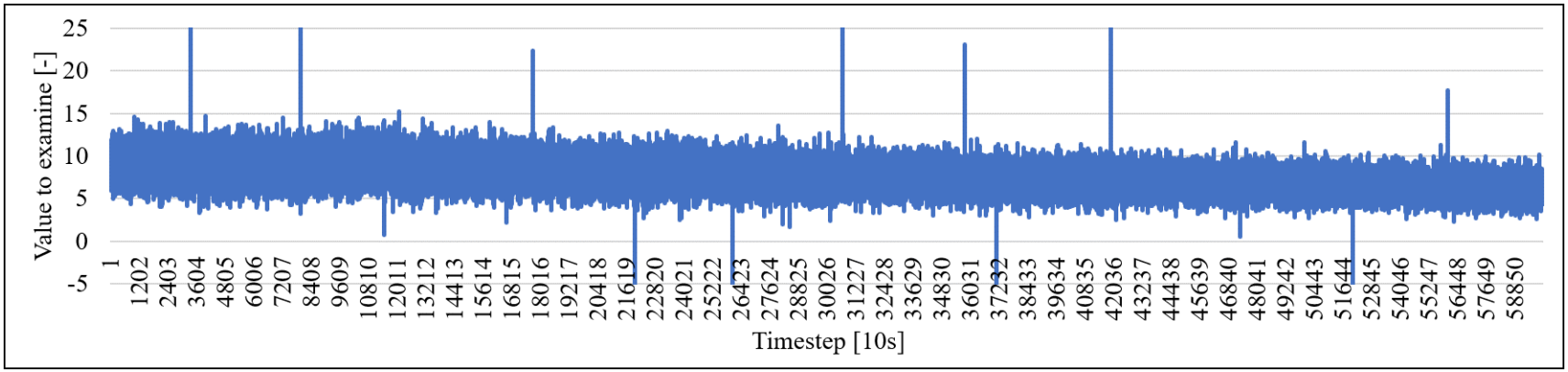

Figure B.4: Example signal 1: SNR 74; 6% decrease per day

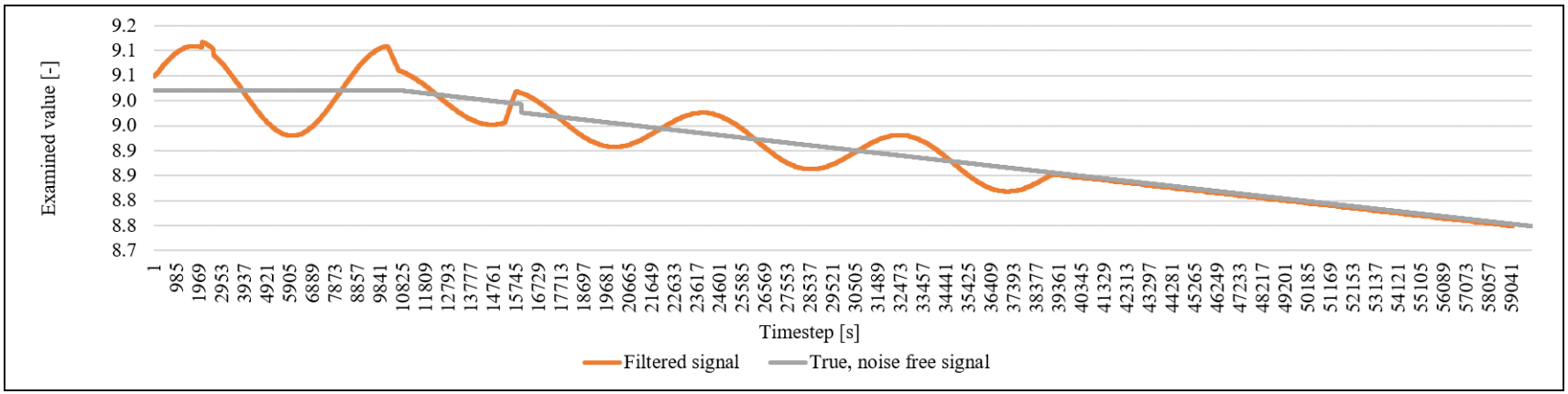

Figure B.5: LMS filtered signal with a SNR of 74 and a slow decrease, filter parameter as described in section 3.3.2

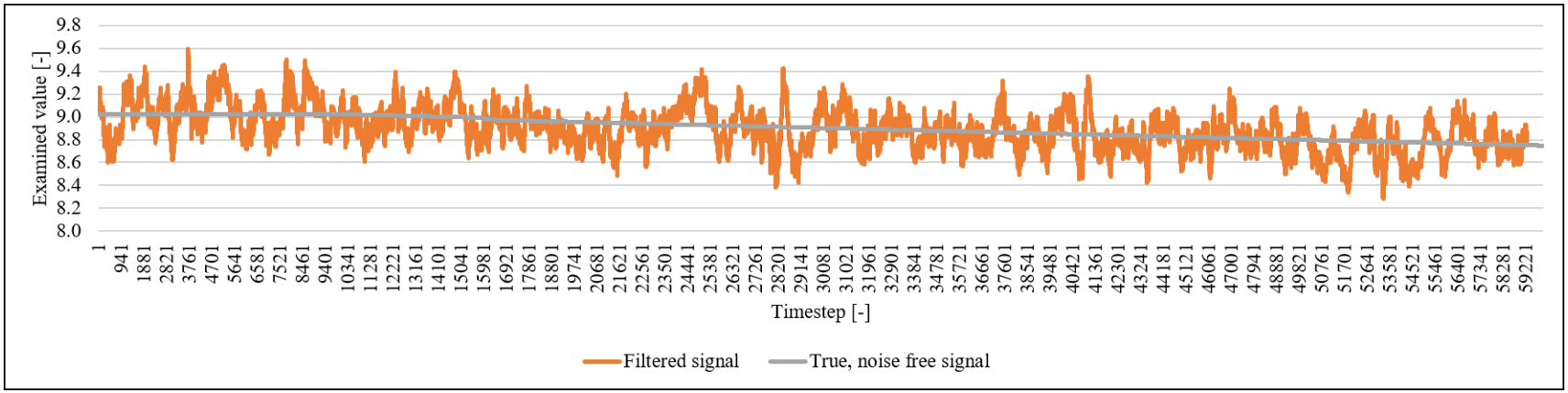

Figure B.6: LMS filtered signal with a SNR of 15 and a slow decrease, filter parameter as described in section 3.3.2

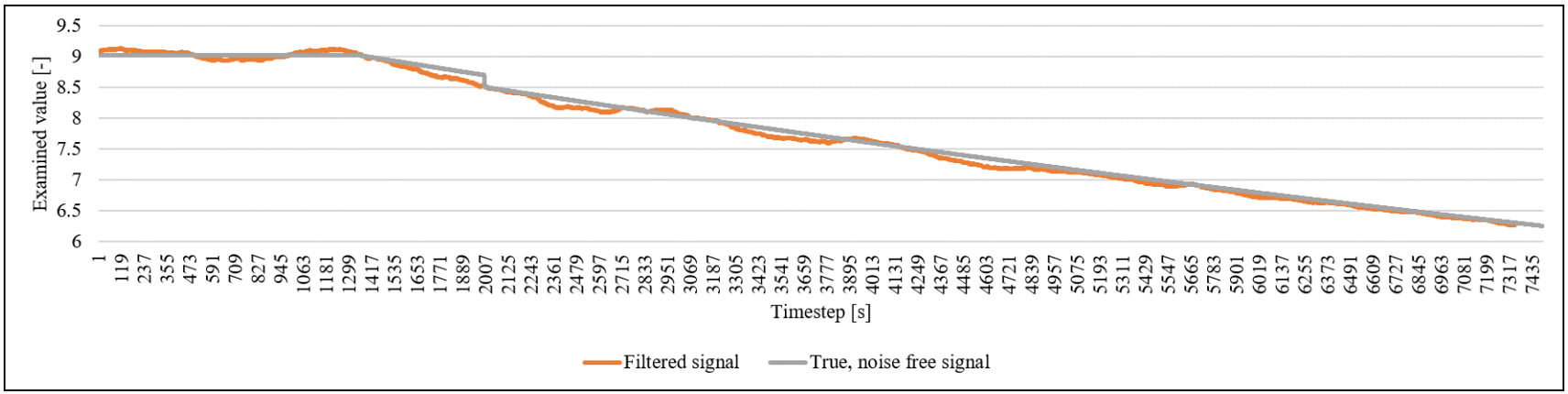

Figure B.7: LMS filtered signal with a SNR of 32 and a fast decrease, filter parameter as described in section 3.3.2

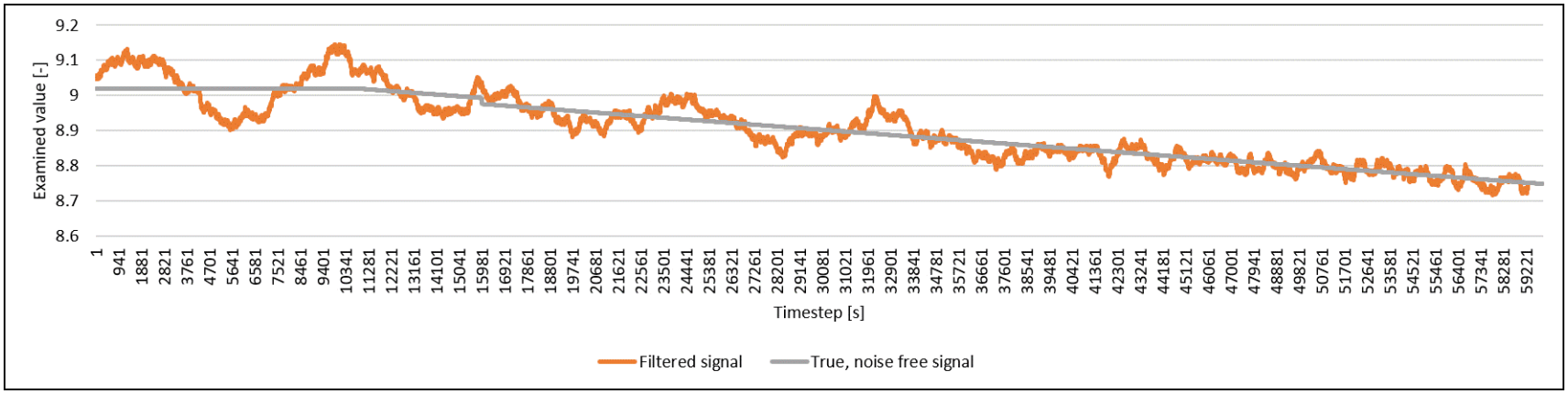

Figure B.8: LMS filtered signal with a SNR of 32 and a slow decrease, filter parameter as described in section 3.3.2

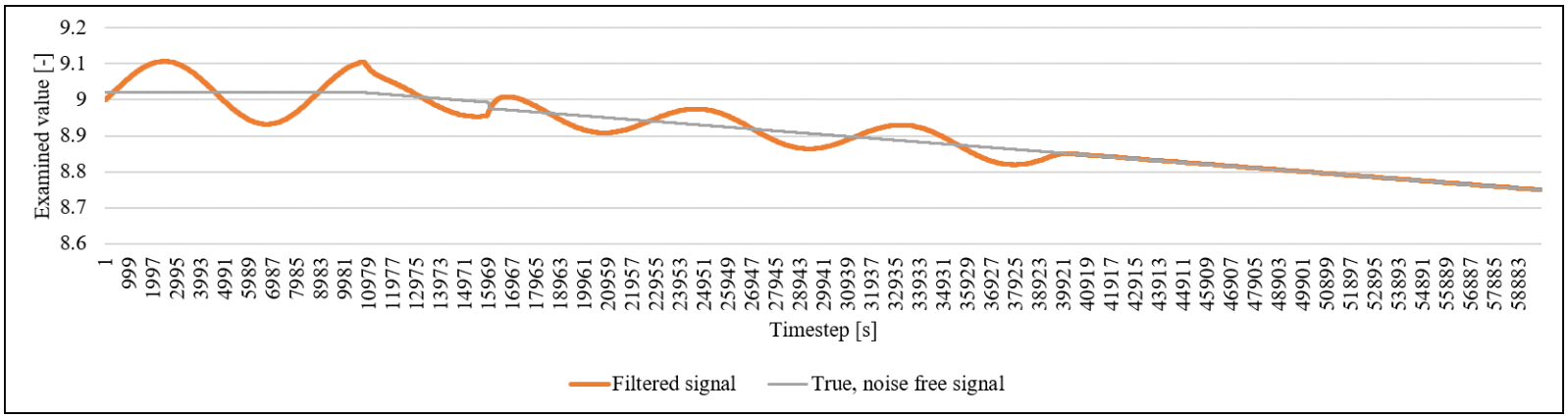

Figure B.9: Kalman filtered signal with a SNR of 74 and a slow decrease, filter parameter as described in section 3.3.3

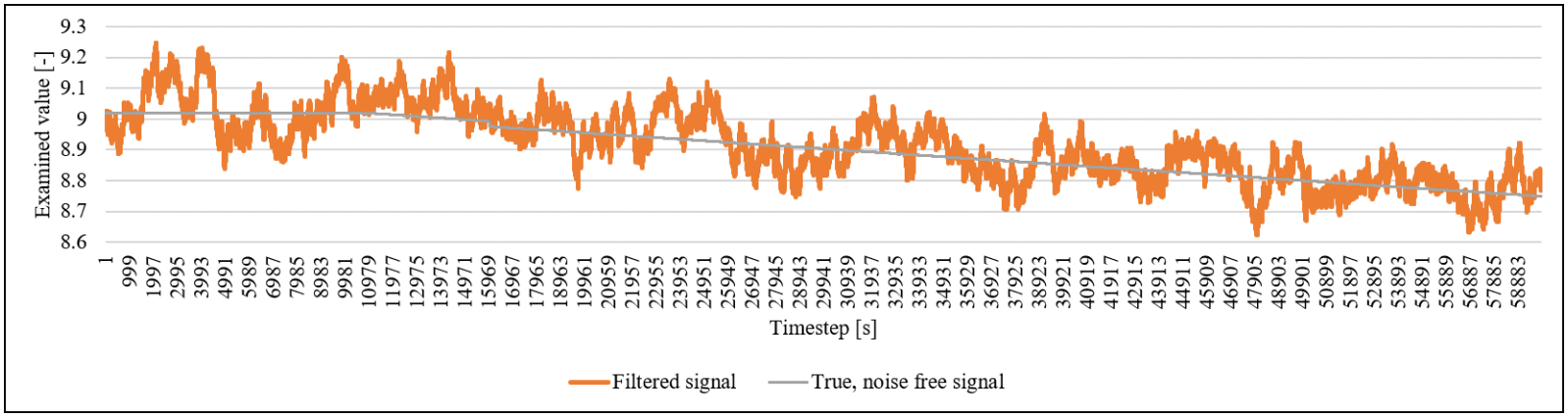

Figure B.10: Kalman filtered signal with a SNR of 15 and a slow decrease, filter parameter as described in section 3.3.3

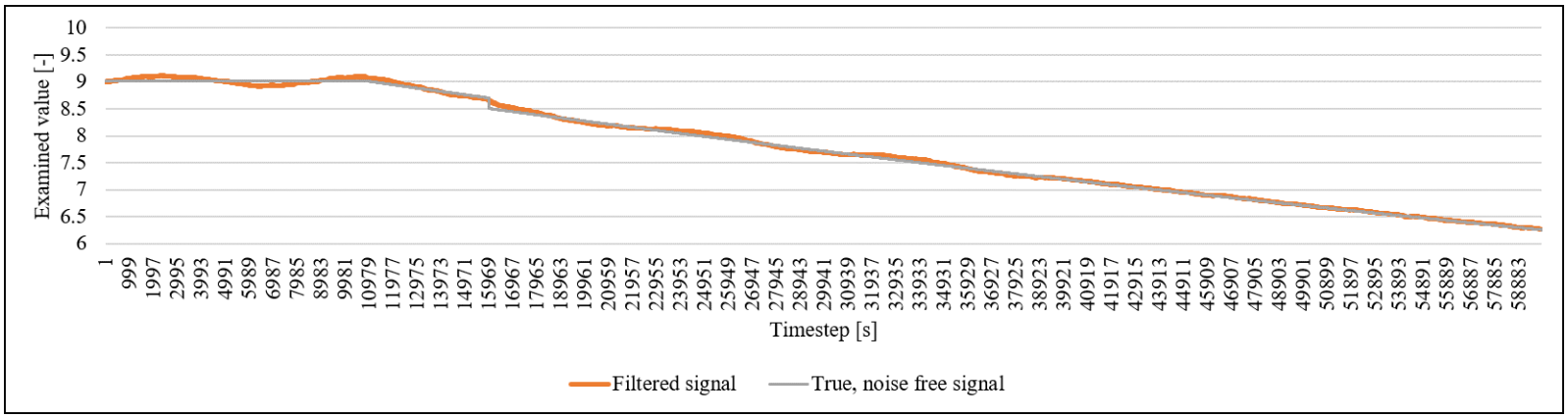

Figure B.11: Kalman filtered signal with a SNR of 32 and a fast decrease, filter parameter as described in section 3.3.3

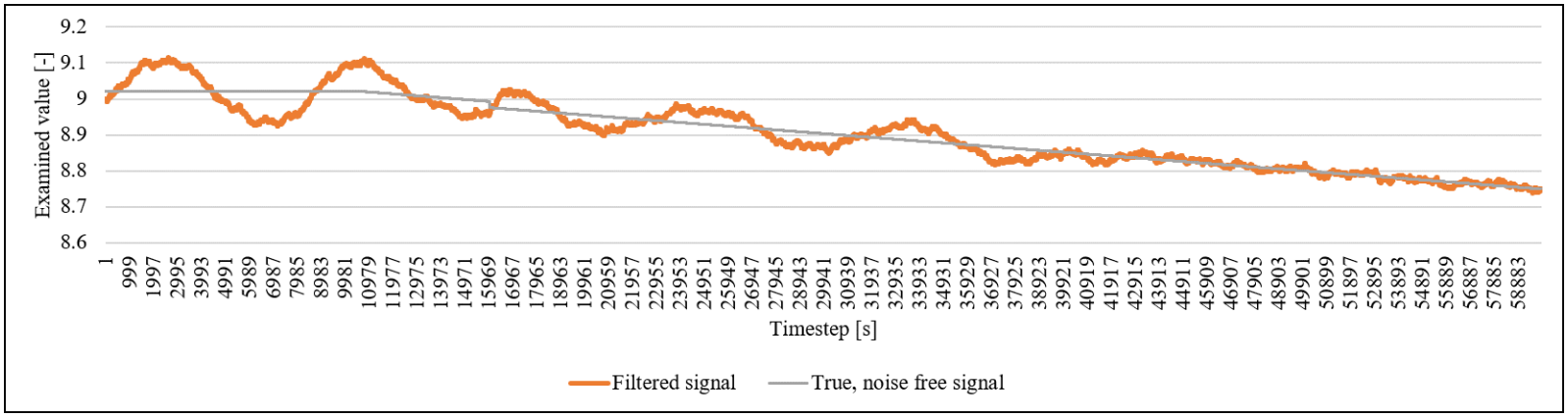

Figure B.12: Kalman filtered signal with a SNR of 32 and a slow decrease, filter parameter as described in section 3.3.3

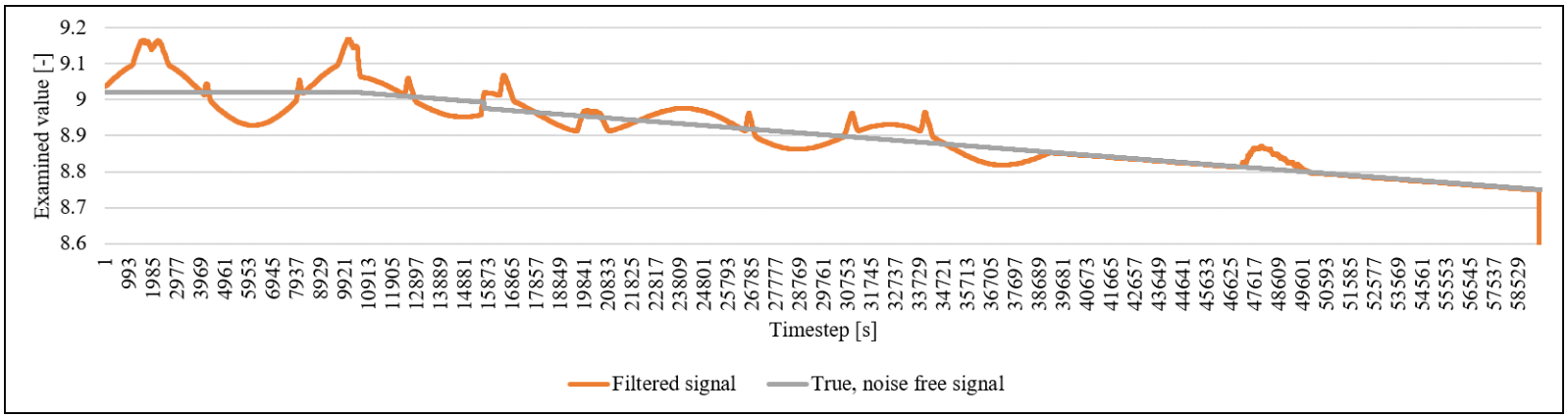

Figure B.13: Moving Average filtered signal with a SNR of 74 and a slow decrease, filter parameter as described in section 3.3.4

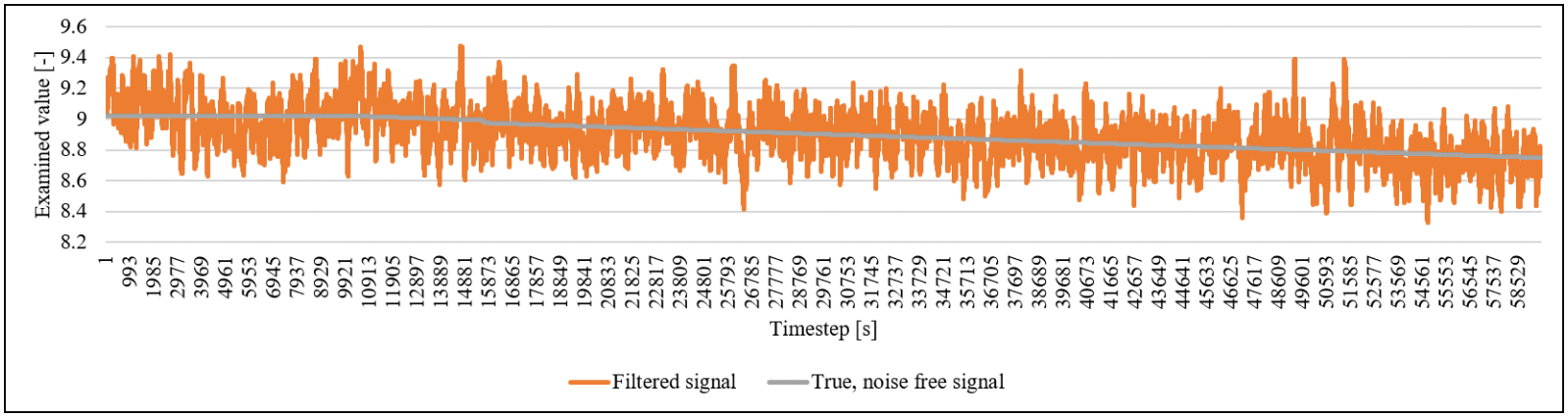

Figure B.14: Moving Average filtered signal with a SNR of 15 and a slow decrease, filter parameter as described in section 3.3.4

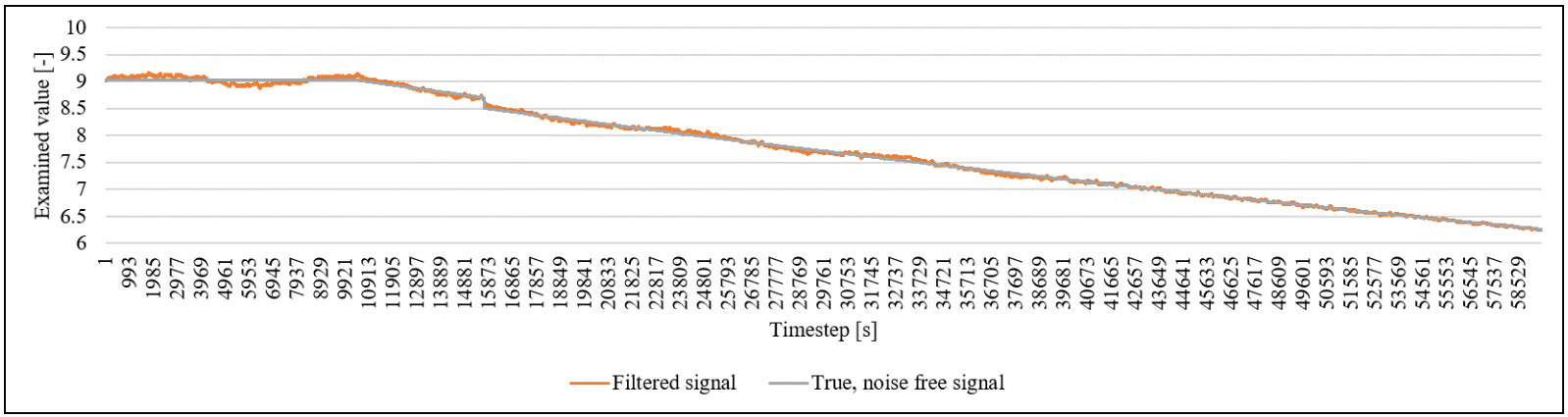

Figure B.15: Moving Average filtered signal with a SNR of 32 and a fast decrease, filter parameter as described in section 3.3.4

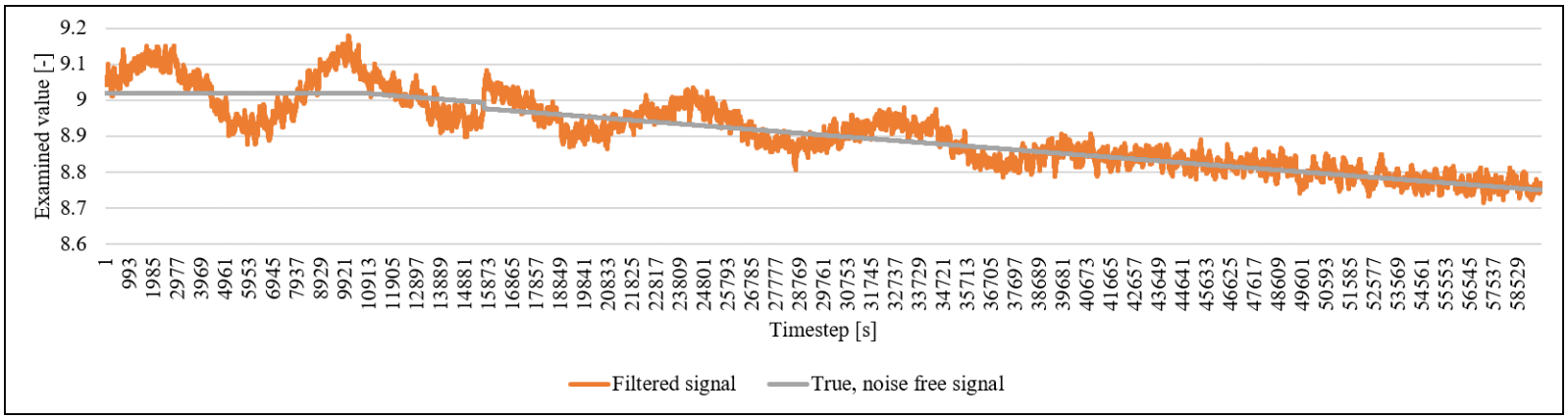

Figure B.16: Moving Average filtered signal with a SNR of 32 and a slow decrease, filter parameter as described in section 3.3.4

REFERENCES

[1] J. Wilkins, "How industry 4.0 impacts globalisation," *Global Manufacturing*, 2017.

[2] P. Mehta, "8 ways the internet of things will impact your everyday life," *Entrepreneur*, 2014.

[3] Wired Brand Lab, "People are the point of iot," *IBM Internet of Things blog*, 2017.

[4] G. Li, Y. Hou, and A. Wu, "Fourth industrial revolution: Technological drivers, impacts and coping methods," *Chinese Geographical Science*, vol. 27, no. 4, pp. 626–637, 2017.

[5] J. Manyika, J. Woetzel, and R. Dobbs, *Unlocking the potential of the internet of things*, `https://www.mckinsey.com/business-functions/digital-mckinsey/our-insights/the-internet-of-things-the-value-of-digitizing-the-physical-world`, 2015.

[6] W. Kester, *Practical Design Techniques for Sensor Signal Conditioning, ADCs for Signal Conditioning*. Analog Devices, 1999, ISBN: 0-916550-20-6.

[7] Texas Instruments, *Selecting an A/D Converter (Rev. A)*. Texas Instruments, 2015.

[8] J. Zhou, Y. Qiao, Z. Yang, Q. Cheng, Q. Wang, M. Guo, and X. Tang, "Capacity limit for faster-than-nyquist non-orthogonal frequency-division multiplexing signaling," *Scientific Reports*, vol. 7, no. 3380, 2017.

[9] A. Waters, J. Leung, and U. K. Moon, "Lsb-first sar adc with bit-repeating for reduced energy consumption," in *2014 21st IEEE International Conference on Electronics, Circuits and Systems (ICECS)*, 2014, pp. 203–206.

[10] Texas Instruments, "Choose the right a/d converter for your application."

[11] J. R. Pierce, "Physical sources of noise," *Proceedings of the IRE*, vol. 44, no. 5, pp. 601–608, 1956.

[12] W. R. Bennet, "Electrical noise," *McGraw-Hill*, pp. 101–109, 1960.

[13] R. Pettai, *Noise in Receiving Systems*. Wiley, 1984, ISBN: 9780471892359.

[14] A. Jain, *Fundamentals of Digital Image Processing*, ser. Prentice-Hall information and system sciences series. Prentice Hall, 1989, ISBN: 9780133325782.

[15] R. L. J. Easton, *Fundamentals of digital image processing*, 2010.

[16] T. Barbu, "Variational image denoising approach with diffusion porous media flow," *Abstr. Appl. Anal.*, vol. 2013, Special Issue, 8 pages, 2012.

[17] J. Davidson, *Stochastic Limit Theory: An Introduction for Econometricians*, ser. Advanced Texts in Econometrics. OUP Oxford, 1994, ISBN: 9780191525049.

[18] Q. Chaudhari, *Wireless Communications from the Ground Up: Fundamentals of Digital Communication Systems*. CreateSpace Independent Publishing Platform, 2016, ISBN: 9781539774587.

[19] H. Pham, *Springer Handbook of Engineering Statistics*, ser. Springer Handbook of Engineering Statistics. Springer, 2006, ISBN: 9781852338060.

[20] N. Achieser, *Theory of Approximation*, ser. Dover Books on Mathematics. Dover Publications, 2013, ISBN: 9780486153131.

[21] T. Namera and A. R. Stubberud, "Gaussian sum approximation for non-linear fixed-point prediction," *International Journal of Control*, vol. 38, no. 5, pp. 1047–1053, 1983.

[22] K. N. Plataniotis, D. Androutsos, and A. N. Venetsanopoulos, "Nonlinear filtering of non-gaussian noise," *Journal of Intelligent and Robotic Systems*, vol. 19, no. 2, pp. 207–231, 1997.

[23] H. Sorenson and D. Alspach, "Recursive bayesian estimation using gaussian sums," *Automatica*, vol. 7, no. 4, pp. 465 –479, 1971.

[24] D. Alspach and H. Sorenson, "Nonlinear bayesian estimation using gaussian sum approximations," *IEEE Transactions on Automatic Control*, vol. 17, no. 4, pp. 439–448, 1972.

[25] X. Liu, "Cmos image sensors dynamic range and snr enhancement via statistical signal processing," PhD thesis, Stanford University, 2002.

[26] S. Smith, *The Scientist and Engineer's Guide to Digital Signal Processing*. California Technical Pub., 1999, ISBN: 9780966017649.

[27] B. Farhang-Boroujeny, *Adaptive Filters: Theory and Applications*. Wiley, 2013, ISBN: 9781118591338.

[28] S. Haykin, *Adaptive Filter Theory*, ser. Prentice-Hall information and system sciences series. Prentice Hall, 2002, ISBN: 9780130901262.

[29] Y. Huang, J. Benesty, and J. Chen, "Optimal step size of the adaptive multichannel lms algorithm for blind simo identification," *IEEE Signal Processing Letters*, vol. 12, no. 3, pp. 173–176, 2005.

[30] R. H. Kwong and E. W. Johnston, "A variable step size lms algorithm," *IEEE Transactions on Signal Processing*, vol. 40, no. 7, pp. 1633–1642, 1992.

[31] J. Miller, *Earliest Known Uses of Some of the Words of Mathematics*, `http://jeff560.tripod.com/mathword.html`, Accessed: 2018-06-14.

[32] D. L. Chandler, *Explained: Sigma*, `http://news.mit.edu/2012/explained-sigma-0209`, Accessed: 2018-06-14, 2012.

[33] D. Simon, "Kalman filtering," *Embedded System Programming*, vol. 14, pp. 72–79, 6 2001.

[34] S. L. Lauritzen, "Time series analysis in 1880: A discussion of contributions made by t.n. thiele," *International Statistical Review*, vol. 49, pp. 319–331, 3 1981.

[35] S. M. Grewal and A. P. Andrews, "Applications of kalman filtering in aerospace 1960 to the present," *IEEE Control Systems Magazine*, vol. 30, pp. 69–78, 3 2010.

[36] R. Kalman, "A new approach to linear filtering and prediction problems," *ASME-Journal of Basic Engineering*, vol. 82, pp. 35–45, 1960.

[37] S. S. Julier and J. K. Uhlmann, "Unscented filtering and nonlinear estimation," *Proceedings of the IEEE*, pp. 401–422, 2004.

[38] E. Courses and T. Surveys, "Sigma-point filters: An overview with applications to integrated navgiation and vision assisted control," *Nonlinear Statistical Signal Processing Workshop*, vol. 47, pp. 201–202, 10 2006.

[39] G. Welch and G. Bishop, "An introduction to the kalman filter," Chapel Hill, NC, USA, Tech. Rep., 1995.

[40] P. Yan, Y. Rong, and G. Wang, "The effect of cutting fluids applied in metal cutting process," *Proceedings of the Institution of Mechanical Engineers, Part B: Journal of Engineering Manufacture*, vol. 230, no. 1, pp. 19–37, 2016. eprint: `https://doi.org/10.1177/0954405415590993`.

[41] T. Thepsonthi, M. Hamdi, and K. Mitsui, "Investigation into minimal-cutting-fluid application in high-speed milling of hardened steel using carbide mills," *Interna-*

tional Journal of Machine Tools and Manufacture, vol. 49, no. 2, pp. 156 –162, 2009.

[42] B. Reynolds and D. Fecher, *Metalworking Fluid Management and Best Practices*, https://www.productionmachining.com/articles/metalworking-fluid-management-and-best-bractices, Accessed: 2018-05-14.

[43] H. Burge, *Machining Coolants*, https://www.emlab.com/resources/education/environmental-reporter/machining-coolants-hygrocybe-species/, Accessed: 2018-05-14.

[44] E. O. Bennet, "The biology of metalworking fluid," *J. Am. Soc. Lubr. Eng.*, vol. 289, pp. 237 –247, 1972.

[45] F. Passman, "Microbial problems in metalworking fluid," vol. 27, pp. 14–17, Jun. 1988.

[46] S. T. Newman, Z. Zhu, V. Dhokia, and A. Shokrani, "Process planning for additive and subtractive manufacturing technologies," *CIRP Annals*, vol. 64, no. 1, pp. 467 –470, 2015.

[47] F. Klocke and G. Eisenblätter, "Dry cutting," *CIRP Annals*, vol. 46, no. 2, pp. 519 –526, 1997.

[48] J. Maida, *Top 3 Trends Impacting the Global Metalworking Fluid Market Through 2020: Technavio*, https://www.businesswire.com/news/home/20161004006138/en/Top-3-Trends-Impacting-Global-Metalworking-Fluid, Accessed: 2018-05-14.

[49] National Research Council, *Expanding the Vision of Sensor Materials*. Washington, DC: The National Academies Press, 1995, ISBN: 978-0-309-05175-0.

[50] R. M. White, "A sensor classification scheme," *IEEE Transactions on Ultrasonics, Ferroelectrics, and Frequency Control*, vol. 34, no. 2, pp. 124–126, 1987.

[51] T. Mohammad, "Using ultrasonic and infrared sensors for distance measurement," *World Academy of Science, Engineering and Technology*, vol. 51, pp. 293–298, 2009.

[52] A. D. Adhvaryu and et al., "Performance comparison of infrared and ultrasonic sensors for obstacles of different materials in vehicle/robot navigation applications," *IOP Conf. Ser.: Material Science and Engineering*, vol. 149, p. 841, 2016.

[53] B. Mustapha, A. Zayegh, and R. K. Begg, "Ultrasonic and infrared sensors performance in a wireless obstacle detection system," in *2013 1st International Conference on Artificial Intelligence, Modelling and Simulation*, 2013, pp. 487–492.

[54] ELEC Freaks, "Ultrasonic ranging module hc - sr04, datasheet," Accessed: 2018-04-10.

[55] EMERSON Process Management, "Theory and practice of ph measurement," vol. 44-6033, D 2010.

[56] AtlasScientific, "Industrial ph probe, datasheet," Accessed: 2018-04-10.

[57] G. Chryssolouris, D. Mavrikios, N. Papakostas, D. Mourtzis, G. Michalos, and K. Georgoulias, "Digital manufacturing: History, perspectives, and outlook," *Proceedings of the Institution of Mechanical Engineers, Part B: Journal of Engineering Manufacture*, vol. 223, no. 5, pp. 451–462, 2009. eprint: `https://doi.org/10.1243/09544054JEM1241`.

[58] D. Thangavel, X. Ma, A. C. Valera, H.-X. Tan, and C. K.-Y. Tan, "Performance evaluation of mqtt and coap via a common middleware," *2014 IEEE Ninth International Conference on Intelligent Sensors, Sensor Networks and Information Processing (ISSNIP)*, pp. 1–6, 2014.

[59] C. Daniel, *Handbook of battery materials*, 2nd, completely rev. and enlarged ed.. Weinheim: Wiley-VCH Verlag, 2011, ISBN: 3-527-63720-6.

[60] Sony, "Lithium ion rechargeable batteries - technical handbook,"

[61] M. Stern and A. L. Geary, "Electrochemical polarization: I . a theoretical analysis of the shape of polarization curves," vol. 104, no. 1, pp. 56–63, 1957.

[62] D. Linden and T. Reddy, *Handbook of batteries*, ser. McGraw-Hill handbooks. McGraw-Hill, 2002, ISBN: 9780071359788.

[63] V. Agubra and J. Fergus, "Lithium ion battery anode aging mechanisms," *Materials*, vol. 6, pp. 1310 –1325, 4 2013.

[64] S. Nikoletseas, Y. Yang, and A. Georgiadis, *Wireless Power Transfer Algorithms, Technologies and Applications in Ad Hoc Communication Networks*. Springer International Publishing, 2016, ISBN: 9783319468105.

[65] S. Epenstein, "Capability validation of wireless sensor systems for monitoring machine tools in manufacturing," 2015.

[66] Y. Malik, "Power consumption analysis of a modern smartphone," Dec. 2012.

[67] X. Liu and F. Qian, "Measuring and optimizing android smartwatch energy consumption: Poster," in *Proceedings of the 22Nd Annual International Conference on*

Mobile Computing and Networking, ser. MobiCom '16, New York City, New York: ACM, 2016, pp. 421–423, ISBN: 978-1-4503-4226-1.

[68] A. Frye, "Energy efficiency's role in a zero energy building: Simulating energy efficient upgrades in a residential test home to reduce energy consumption," 2011.

[69] C. Press, *Wireless Sensor Networks: Current Status and Future Trends*. CRC Press, 2016, ISBN: 9781466506084.

[70] A. Wang and A. Chandrakasan, "Energy-efficient dsps for wireless sensor networks," *IEEE Signal Processing Magazine*, vol. 19, no. 4, pp. 68–78, 2002.

[71] C. Im, H. Kim, and S. Ha, "Dynamic voltage scheduling technique for low-power multimedia applications using buffers," in *Low Power Electronics and Design, International Symposium on, 2001.*, 2001, pp. 34–39.

[72] R. M. Passos, C. J. N. Coelho, A. A. F. Loureiro, and R. A. F. Mini, "Dynamic power management in wireless sensor networks: An application-driven approach," in *Second Annual Conference on Wireless On-demand Network Systems and Services*, 2005, pp. 109–118.

[73] I. Neri and A. Moschitta, "Power consumption assessment in wireless sensor networks," in *ICT - Energy - Concepts Towards Zero*, G. Fagas, Ed., Rijeka: InTech, 2014, ch. 9.

[74] E. Shih, S.-H. Cho, N. Ickes, R. Min, A. Sinha, A. Wang, and A. Chandrakasan, "Physical layer driven protocol and algorithm design for energy-efficient wireless sensor networks," in *Proceedings of the 7th Annual International Conference on Mobile Computing and Networking*, ser. MobiCom '01, Rome, Italy: ACM, 2001, pp. 272–287, ISBN: 1-58113-422-3.

[75] Environmental Technology Best Practice Programme, *Benchmarking the consumption of metal cutting fluids*, 1999.

[76] R. L. Smith, "Predicting evaporation rates and times for spills of chemical mixtures," *Ann. occup. Hyg.*, vol. 45, no. 6, pp. 437 –445, 2001.

[77] A V. Voloshin, E F. Dolzhenkova, L. Lytvynov, A A. Petukhov, and E V. Slyunin, "The influence of coolant ph on efficiency of machining sapphire," vol. 35, Mar. 2013.

[78] R. Labbe, *Kalman and bayesian filters in python*, `https://github.com/rlabbe/Kalman-and-Bayesian-Filters-in-Python`, 2014.